

**MODELLING AND MONITORING OF A
HERHOF BIO-DEGRADATION SYSTEM**

A Thesis

Presented to

The Faculty of Graduate Studies

of

The University of Guelph

by

CATHERINE LINDSAY DENNISON

In partial fulfilment of the requirements

for the degree of

Master of Science

August, 1998

© Catherine Lindsay Dennison, 1998



**National Library
of Canada**

**Acquisitions and
Bibliographic Services**

**395 Wellington Street
Ottawa ON K1A 0N4
Canada**

**Bibliothèque nationale
du Canada**

**Acquisitions et
services bibliographiques**

**395, rue Wellington
Ottawa ON K1A 0N4
Canada**

Your file Votre référence

Our file Notre référence

The author has granted a non-exclusive licence allowing the National Library of Canada to reproduce, loan, distribute or sell copies of this thesis in microform, paper or electronic formats.

The author retains ownership of the copyright in this thesis. Neither the thesis nor substantial extracts from it may be printed or otherwise reproduced without the author's permission.

L'auteur a accordé une licence non exclusive permettant à la Bibliothèque nationale du Canada de reproduire, prêter, distribuer ou vendre des copies de cette thèse sous la forme de microfiche/film, de reproduction sur papier ou sur format électronique.

L'auteur conserve la propriété du droit d'auteur qui protège cette thèse. Ni la thèse ni des extraits substantiels de celle-ci ne doivent être imprimés ou autrement reproduits sans son autorisation.

0-612-33218-7

Abstract

Modelling and Monitoring of a Herhof™ Bio-Degradation System

C. Lindsay Dennison
University of Guelph, 1998

Supervisor:
Professor L. Otten

The primary goal of this research was two-fold. The first objective was to develop a mathematical model of the Herhof™ Bio-degradation system and to test the ability of such a model to predict responses in the physical system. The second objective was to analytically determine the risk of off-site odour problems, and to meet the facility requirements for a Certificate of Approval from the Ministry of the Environment and Energy.

Results indicate that the model is capable of predicting the general trends and responses similar to those observed in the physical system. With inclusion of additional reaction rate correction factors and the use of multiple substrates, it could potentially be a very useful tool for determining system response to various conditions and inputs.

The odour emissions study concluded that there is unlikely to be off-site odour problems due to the Herhof System. On the occasion that odour panel tests were completed, the results were in general agreement with analytical results, indicating that on-line monitoring could be considered as an preventative measure.

Acknowledgments

I wish to express my gratitude to Dr. Lambert Otten, my thesis advisor, for his guidance and patience through this research. I would also like to thank Dr. Warren Stiver for his invaluable consultation and assistance. As well, this research would not have been possible without the assistance of Sandra Ausma in the laboratory, Paul Della Bianca at the Caledon Sanitary Landfill site and Mike Gibson as a general sounding board.

I would also like to thank my fellow students, the faculty and staff who made my time at Guelph, both undergraduate and graduate, some of the greatest times of my life. In particular, thank you to Dave Arsenault, Jeff Kemp and Tanya Smyth for all the great times at graduate school and for being such great friends. Special thanks to my mother, my late father and my brother for their encouragement and support. Finally I would like to thank my husband, Chris Anderson, for his confidence, encouragement and for our future together.

TABLE OF CONTENTS

Abstract	
Acknowledgments	i
List of Figures	iv
List of Tables	v
Nomenclature	vi
1.0 INTRODUCTION	1
1.1 Research Objectives	2
2.0 LITERATURE REVIEW	4
2.1 The Composting Process	4
2.1.1 The Phases of Composting	5
2.2 Process Configurations	7
2.3 Process Control Parameters	9
2.3.1 Temperature	9
2.3.2 Aeration	10
2.3.3 Moisture Content	11
2.3.4 Nutrient Availability	12
2.3.5 Retention Time	12
2.5 Mathematical Models of the Composting Process	13
2.4 Odour Generation in Composting	16
2.4.1 Odour Compounds	17
2.4.2 Measurement of Odours	17
2.4.3 Reduction of Odours	21
2.4.4 Atmospheric Dispersion of Odours	23
3.0 MODELLING THE HERHOF PROCESS	25
3.1 Mathematical Model Development	25
3.1.1 Stoichiometry	25
3.1.2 Kinetics	27
3.1.3 Energy and Mass Balances	28
3.1.4 Finite Difference Equations	32
3.1.5 Model Stability	33
3.2 Model Verification	35
3.2.1 Data Collection	35
3.2.2 Model Calibration	36

3.2.3	Measuring Model Performance	39
3.3	Modelling Results	40
3.3.1	Selection of the Calibrated Model	41
3.3.2	Model Verification	51
3.3.3	Simulations of Extreme Conditions	57
3.4	Discussion of Modelling Results	60
3.4.1	Temperature Profile	60
3.4.2	Comparison of Dry Mass Reduction	63
3.4.3	Comparison of Final Moisture Content	64
3.4.4	Comparison of Process Duration	65
3.5	Extreme Condition Simulations	67
3.5.1	High Ambient Temperature (305 K)	67
3.5.2	Low Ambient Temperature (270 K)	68
3.5.3	High Levels of Fast-Degrading Volatiles (100%)	69
3.5.4	Low Levels of Fast-Degrading Volatiles (100%)	69
4.0	COMPOST QUALITY	71
5.0	EMISSIONS MONITORING	75
5.1	Methodology	76
5.1.1	Sampling Protocol	76
5.1.2	Sample Collection	76
5.1.3	Sample Analysis	77
5.1.4	Limits of Detection/Limits of Quantification	79
5.1.5	Additional Analyses	80
5.2	Emissions Monitoring Results	81
5.2.1	Phase 4 Odour Sampling	82
5.2.2	Distributed Sampling	83
5.2.3	Mass Spectral Analysis	83
5.2.4	Desiccant Test	83
5.3	Discussion of Emissions Monitoring Results	84
6.0	CONCLUSIONS AND RECOMMENDATIONS	87
6.1	System Modelling Study	87
6.2	Odour Emissions Study	88
7.0	REFERENCES	90
	APPENDIX A - Schematic of a Herhof Biocell	94
	APPENDIX B - Sample Calculations: Degradation Model	96
	APPENDIX C - Degradation Model Computer Code	107
	APPENDIX D - Sample Calculations - Odour Emissions Study	117
	APPENDIX E - Graphical Results - Odour Emissions Study	122

List of Figures

Figure 1 - Typical Temperature Profile of a Composting Process	5
Figure 2 - Dilution Characteristics of Pervasive and Non-Pervasive Odours	20
Figure 3 - A Conceptual Diagram of Mass and Energy Flows in a Herhof Biocell	26
Figure 4 - Flowchart of the Simulation Model	34
Figure 5 - Temperature Profile Comparison, Theoretical	42
Figure 6 - Temperature Profile Comparison, Adjusted Model 1	42
Figure 7 - Temperature Profile Comparison, Adjusted Model 2	43
Figure 8 - Temperature Profile Comparison, Adjusted Model 3	43
Figure 9 - Temperature Profile Comparison, Adjusted Model 4	44
Figure 10 - Temperature Profile Comparison, Adjusted Model 5	44
Figure 11 - Temperature Profile Comparison, Adjusted Model 6	45
Figure 12 - Temperature Profile Comparison, Adjusted Model 7	45
Figure 13 - Temperature Profile Comparison, Adjusted Model 8	46
Figure 14 - Temperature Profile Comparison, Adjusted Model 9	46
Figure 15 - Temperature Profile Comparison, Adjusted Model 10	47
Figure 16 - Temperature Profile Comparison, Adjusted Model 11	47
Figure 17 - Temperature Profile Comparison, Adjusted Model 12	49
Figure 18 - Comparison of Overall Duration	49
Figure 19 - Comparison of Dry Mass Reduction	50
Figure 20 - Temperature Profile Comparison, Batch 1	54
Figure 21 - Temperature Profile Comparison, Batch 3	54
Figure 22 - Temperature Profile Comparison, Batch 27	55
Figure 23 - Temperature Profile Comparison, Batch 38	55
Figure 24 - Temperature Profile Comparison, Batch 47	56
Figure 25 - Temperature Profile Comparison, Batch 54	56
Figure 26 - Reactor Environment Profiles - High Ambient Temperature	58
Figure 27 - Reactor Environment Profiles - Low Ambient Temperature	58
Figure 28 - Reactor Environment Profiles - High Fast Degradable Content	59
Figure 29 - Reactor Environment Profiles - High Slow Degradable Content	59
Figure 30 - Sample Calibration Lines	78

List of Tables

Table 1 - Stages of the Herhof Composting Process	2
Table 2 - Classifications of Composting Systems'	8
Table 3 - Suspected Odour Compounds from Composting Facilities	18
Table 4 - Recommended Design and Operating Parameters for Biofilters	23
Table 5 - Compost and System Data	35
Table 6 - Field Batches	36
Table 7 - Summary Adjusted Model Parameters	37
Table 8 - Parameters for Extreme-Condition Runs	40
Table 9 - Comparison of Model Results	41
Table 11 - MAPE Calculation for Selection of Calibrated Model	51
Table 12 - Ambient Input Temperatures	52
Table 13 - Comparison of Predicted to Observed Batches	53
Table 14 - MAPE Comparison of Simulated Batches	53
Table 15 - Calculated MAEs for Temperature Profiles	57
Table 16a - Statistical Summary of all samples submitted for analysis	72
Table 16b - Statistical Summary of all samples submitted for analysis (cont.)	73
Table 17 - GC-PID Settings	77
Table 18 - Analytical Limits	82
Table 19 - Phase 4 Sampling Results	82
Table 20 - Distributed Sampling Results	83
Table 21 - Results of Desiccant Tests	84

Nomenclature

Symbol	Definition	Units
C	specific heat	kcal/kg-K
G	generation factor	kg/kg _{vs}
h	enthalpy	kcal/kg
H	henry's law constant	kPa ⁻¹
k	rate constant	h ⁻¹
m	mass flow rate	kg/h
M	mass	kg
MM	molar mass	kmol/kg
PP	partial pressure	kPa
q	energy	kcal
Q	flow rate of fluid	kg/h
t	time	h
T	temperature	K
V	volume	m ³
Y	absolute humidity	kg _w /kg _{air}
λ	heat of vapourization	kcal/kg

subscripts

a	dry air
acc	accumulation of heat/mass
ai	dry air in
ao	dry air out
adj	adjusted (for temperature and/or other conditions)
aq	aqueous phase
avg	average
c	combustion
g	dry gas
i	inlet or initial condition
o	outlet
rw	reactor walls
s	dry solids
vs	volatile solids
w	water

1.0 INTRODUCTION

The Herhof Bio-degradation System is used extensively in Germany, and to a lesser extent in other parts of Europe and North America. The Herhof company, which had been a road construction company since 1968, conceived of the modular compost container system in 1980. It's first installation was in 1987 at Aßlar in Germany. This site uses eighteen single boxes and one double box to process 27,000 tonnes of compost per year. Herhof currently has eight plants in Austria, one in Canada, one in Luxembourg, one in Belgium and thirty-four in Germany, making a total forty-five installations.

The Canadian installation of the Herhof Biocell™ is located in the Regional Municipality of Peel, at the Caledon Sanitary Landfill. This site currently disposes of the organic wastes from approximately 4500 homes in two Herhof Biocells™. The system, which was pre-fabricated and imported from Germany, has the capacity to process 50 tonnes of waste per week. The system is a completely automated in-vessel, static pile system that produces commercial-quality compost which is sold for \$30/tonne. A schematic of a single Herhof Biocell™ is provided in Appendix A.

The waste is shredded, using a Danner™ model AZ50 slow-speed shredder, to a particle size < 75mm and mixed before being placed in the reactor. The cell is completely sealed and the substrate proceeds through the four stage process described in Table 1 before being removed from the reactor and placed in windrows for curing. While in the reactors, airflow is forced

through the pile from below. This airflow is recycled continually until the CO₂ concentration in the reactor reaches 5% by mass, at which time the reactor air is exhausted and fresh air is taken in. The solids retention time, usually approximately seven to ten days, is determined by the length of the phases.

Table 1 - Stages of the Herhof Composting Process

Stage	Description
Stage 1	Stage 1 is an initial warming stage. The reactor remains in stage 1 until the temperature inside reaches 40°C.
Stage 2	Stage 2 is an additional warming stage. Requirements of this phase are a minimum of 48 hours at 45°C, followed by a warm up to the set-point of 60 °C.
Stage 3	Stage three is a high-rate phase 72 hours in duration, beginning when the reactor temperature reaches 60°C.
Stage 4	Stage 4 is a 36 hour cooling/drying stage. During stage 4, the reactor is continually flushed with ambient air.

Any gases exiting the reactors are vented through a biofiltration system. Each of the biocells has a three-level biofilter. The biofilters are 1 m by 1.2 m in cross-section, and each level is 0.66 m high. The three sections of the filter contain 0.3 m of cured compost, 0.3 m of wood chips and 0.3 m of bark, respectively. The purpose of the biofilters is to sorb the odorous compounds and maintain an active microbial population which will degrade them.

1.1 Research Objectives

The Caledon System is the first Herhof unit in Canada and the process is a significant departure from other composting facilities. As such, it was considered useful to examine its operations over sufficient time to account for seasonal effects. The results of the study would be of interest to other municipalities.

The Herhof Biocell™ is a closed, automatically controlled, fully-instrumented system which makes it particularly useful for research and especially for model development. To have a suitable model that simulates the process under different operating conditions would obviously be beneficial for waste-management planners and operators. Furthermore, the Certificate of Approval issued by the Ontario Ministry of the Environment and Energy (MOEE) for the Caledon facility required monitoring of odour emissions and compost quality.

Therefore, the specific objectives of this research are to:

1. Develop a mathematical model of the Herhof System to predict mass reduction, temperature profile and process duration based on inputs and conditions
2. Compare the observed field performance to that predicted by the model
3. Monitor the Herhof installation at Caledon Sanitary Landfill for odour emissions

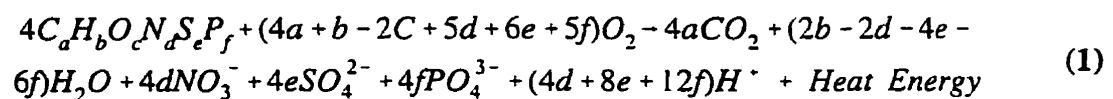
2.0 LITERATURE REVIEW

The following review of relevant literature provides background regarding composting systems, the problems associated with them and the process models that are available.

2.1 The Composting Process

In recent decades, the composting process has received renewed interest as an alternative to landfilling and incineration of all types of organic wastes including sludges, yard wastes, food wastes and agricultural wastes. The composting process in the context of this study is the biological degradation of organic material under controlled aerobic conditions. The desired product of this process is compost of sufficient stability for use as a soil amendment without adverse environmental and plant growth effects.

In order for composting to be considered an acceptable and efficient method of organic waste disposal, the rate of the degradation process must be optimized. This is generally achieved through careful control of the process parameters including temperature, moisture, oxygen availability and the presence of desirable microbial populations whose metabolism achieves degradation of the wastes (Jeris & Regan, 1973b; MOEE, 1990). Theoretically, complete breakdown of municipal solid wastes can be described by the following stoichiometric equation;



Where $C_aH_bO_cN_dS_eP_f$ is an elemental description of the substrate with the value of the subscripts attained from an ultimate analysis of representative substrate samples. Based on this stoichiometric relationship, knowledge of the fractional components of the organic material (a through f, in Equation 1) allows calculation of the quantity of O_2 consumed during degradation and the quantity produced of each of the products of the reaction.

2.1.1 The Phases of Composting

The characteristic temperature profile of the composting process is shown in Figure 1.

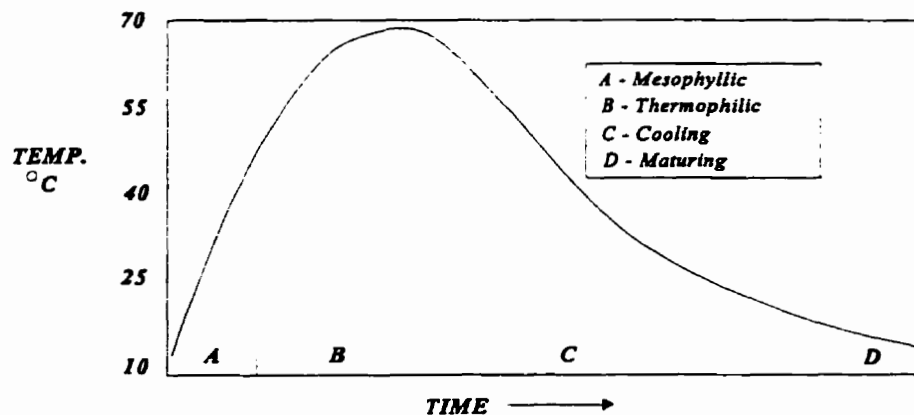


Figure 1 - Typical Temperature Profile of a Composting Process
(Adapted from Wong, 1991)

This profile illustrates the four distinct phases of the process; the mesophilic stage, the thermophilic or high rate phase, the cool down phase and the maturing phase. Typically, the first three phases are completed within a few days to weeks, depending on the substrate characteristics and process parameters. The fourth phase, known as the maturing phase, can

take months to reach completion.

The mesophilic stage is the first stage in the process, characterized by a rapid increase in substrate temperature from ambient. During this phase, mesophilic organisms begin to break down the organic matter in the waste to simple organic acids and a substantial amount of energy is released in the form of heat. Because of the low thermal conductivity of the organic material, heat accumulates within the pile until the pile temperature reaches approximately 40°C. This temperature is limiting to the mesophilic organisms, and they begin to die off.

The second stage in the process is called the thermophilic, or high-rate, phase. This stage is characterized by the presence of facultative nitrogen-fixing microbes. These organisms operate in the 40-60°C range, and cause a rise in pH to alkaline levels. Heat continues to accumulate in the pile, and if excessive quantities of nitrogen are present, ammonia will also be volatilized (Jiménez & García, 1991; Wong, 1991). Once the temperature within the pile reaches 55-60°C, the thermophilic fungi will begin to die off, and spore-forming bacteria and actinomycetes take over. The thermophilic phase comes to an end when most of the easily-degradable organics are broken down. At this time, biological activity will decrease, and the pile temperature will begin to fall.

The third phase of the composting cycle begins when the pile temperature falls below 60°C. At this time, the thermophilic fungi will become active once again. Since the majority of the

easily degradable organics have been broken down, the fungi will begin to break down the more resistant cellulosic materials. Since these materials are much more resistant to degradation, the reactions are much slower, and the heat generation is not rapid. Therefore the compost pile will continue to cool. As the pile reaches 40°C, the mesophilic microbes take over, accompanied by a small drop in pH (Wong, 1991).

The final phase of the composting process is a longer-term maturing phase, beginning when pile temperature approaches ambient. During this phase the mesophilic organisms remain relatively active, and microfauna begin to appear. It is during the maturing cycle that complex humification processes occur, and humus is produced.

2.2 Process Configurations

Although composting is a natural process, in order to make it a feasible waste-management alternative, the rate of degradation must be increased. In order to achieve this, numerous different process configurations have been developed, each attempting to maximize process efficiency. These processes can be characterized into non-reactor systems, vertical flow reactor systems, horizontal and inclined flow reactor systems, and non-flow reactor systems. General system descriptions are provided in Table 2 (Haug, 1993).

Table 2 - Classifications of Composting Systems*

(Adapted from Haug, 1993)

CLASSIFICATIONS	GENERAL DESCRIPTION
Non-Reactor Systems	
Agitated Solids Bed	Windrows are the most common of the agitated solids bed system. Usually on open ground, with haystack cross section, turned periodically. May be forced or conventionally aerated.
Static Solids Bed	Waste may be placed in piles or compressed into solid blocks for degradation and curing. Aeration is by natural diffusion. Wide applications for sludge cake in the US. Installations in Germany and Switzerland.
Vertical Flow Reactor Systems	
Moving Agitated Bed	Probably the oldest reactor system - numerous versions, but the basic configurations include vertically stacked decks, the compost is dropped from deck to deck, to provide aeration. There are many modifications to this system, installations have been reported in Korea Italy, Switzerland, Thailand and Japan. Residence times range from 2 days to 8 weeks.
Moving Packed Bed	Reactor consists of a cylindrical tower with no interior floors or other mechanisms. Waste moves gradually downward as the bottom layers are removed by scraping. There are at least 3 variations of the systems, with residence times ranging from 4-12 days. Curing is required post-reactor. In 1993, over 25 installations were reported to be operating in Germany and France.
Horizontal and Inclined Flow Reactor Systems	
Rotary (rotating) drums	Typically a cylindrical or hexagonal shaped screen drum, compost is aerated by rotation of the drum. May be a single drum or drums in series. Some are inclined, and screens may be covered for a portion of the degradation process. Drums may also be divided into compartments to avoid short-circuiting. Typically curing is required after removal from the reactor. Probably the most popular reactor system for MSW.
Agitated Bins	Rectangular or circular tank, with mechanical agitation and/or forced aeration. Substrates include MSW, yard wastes and industrial and municipal sludges. Past installations include Canada, United States, Spain, Indonesia.
Static Bed Bins	A horizontal, static bed reactor developed in 1979 as an adaptation of the vertical silo systems. A plug-flow, tubular reactor of rectangular cross-section, with volumes ranging from 10-500m ³ . Gases may be exchanged along the length of the reactor, and new material is added by either a 'pusher-plate' or a 'walking floor' mechanism, which forces the matured compost to the other end.
Non-Flow Reactor Systems	A number of 'box-type' reactor processes have been developed recently. Substrate is placed in the box at the start of the cycle, which may be 7-14 days in duration, controlled aeration Windrow curing is typically required for several months after removal from the reactor.

*More detailed information is provided by Haug (1993)

2.3 Process Control Parameters

In order to produce good quality compost product in a reasonable amount of time, process parameters must be maintained at optimum levels. The most significant parameters that can be controlled and directly affect the composting process are temperature, oxygen availability, moisture content, nutrient availability and retention time.

2.3.1 Temperature

As previously mentioned a major by-product of microbial degradation is heat energy which accumulates within the pile. Heat generation from pulverized refuse is estimated to be 7 MJ/kg of initial dry volatile solids (as cited by Wong, 1991). The evolution of heat within the pile is an indication that the compost substrate is being degraded and is important for pathogen destruction, but can also be self-limiting. If temperature is uncontrolled, it can reach 75-80°C, which will result in the death of almost all active bacteria and therefore a slowing of the composting process (Finstein *et al.*, 1987b; Strom 1985a).

Strom (1985a) found that microbial species diversity decreased sharply above 60°C, and recommended that the maximum allowable temperature for MSW composting be maintained at that level. Additional studies by Finstein *et al.* (1980), McGregor *et al.* (1981) and Jeris and Regan (1973a), as cited in Wong (1991), illustrate that at temperatures below 60°C, the microbial population is active and diverse, with biodegradation and heat and water production proceeding efficiently. At temperatures greater than 60°C, all of these processes are retarded. Based on the results of these studies, Finstein (1980) concluded that the

optimum temperature for the thermophilic stage of degradation is 55°C. These results were also supported by Hamamoto *et al.* (1979), who determined that the degradation rate constant was maximized at 60°C, based on a mathematical model of MSW composting process.

In order to ensure that the pile temperature does not exceed 60°C, a method of heat removal is usually required. The three main methods of heat removal in composting are the result of vaporization of water, heating of ventilation air and conduction. As mentioned previously, the compost matrix has low conductivity, thereby eliminating conduction as a significant mode of heat removal. Typically, approximately 90% of heat removal from a composting pile is as the result of evaporative cooling (water vaporization), while the remaining 10% is due to sensible heating of ventilation air (convection) (MacGregor *et al.*, 1981; Finstein *et al.*, 1980; Wong, 1991).

2.3.2 Aeration

Aeration is required in composting for three main functions; to meet the biological oxygen demand of the organic matter, for heat removal and for vaporization of water from the pile (Diaz *et al.*, 1994; Wong, 1991). Aeration mechanisms are divided into two main groups; agitation and forced aeration. Agitation is achieved by tumbling, stirring and/or mixing of the composting mass. In forced aeration, air is either forced through the mass under pressure, or pulled through the mass by suction (Diaz *et al.*, 1994). Typically, aeration of in-vessel systems is achieved by one or a combination of these methods. Although aeration by natural diffusion has been used in the past, it is generally considered inadequate to meet oxygen

demand and cooling or drying requirements (Diaz *et al.*, 1994; Wong, 1991; Gray *et al.*, 1973).

The maintenance of aerobic conditions in the compost pile is important in encouraging rapid degradation and minimizing odours, but maintenance of oxygen concentrations within the pile is not the only goal of aeration (Hay *et al.*, 1990). In fact, studies by Finstein (1992), Gray *et al.* (1973) and Cardenas & Wang (1979) have all found that the aeration required for maintenance of aerobic conditions is insufficient for cooling and drying of the compost mass. Instead, each of these authors recommends that the aeration/agitation system be designed to maintain optimum temperatures and moisture content. This level of aeration will ensure sufficient oxygen to meet the demand of degradation reactions.

2.3.3 Moisture Content

Moisture is essential for the biological reactions that result in humification of organic matter. However, if the moisture content of the waste is too high, the interstitial spaces of the waste may become filled with liquid, thereby limiting the availability of oxygen within the pile. Therefore the moisture content required for efficient and complete aerobic digestion of municipal solid wastes is a balance between the microbial requirement for moisture and the maintenance of free air space (FAS) for movement of gases.

Free air space is also a function of the waste material itself, so the critical moisture content will vary based on the type of substrate, particle size and particle size distribution. Even

within the category of MSW composting, optimum moisture contents have been quoted that range between 25% and 80% (Jeris & Regan, 1973). This large variability of moisture content is a function of the MSW composition and particle size. Waste with larger particle size will maintain a greater air/solid ratio in the matrix, providing more efficient movement of gases. Therefore the critical value for moisture content will depend on the degree of grinding and screening prior to composting, as well as the fraction of porous materials such as wood chips, paper and yard wastes (Haug, 1993; Jeris & Regan, 1971).

2.3.4 Nutrient Availability

Nutrients are required in biological processes for formation of microbial cell mass and enzyme production, and for process energy (Golueke, 1979). For these function, almost all elements are utilized to some extent by the microbes in a compost pile. The most significant elements are divided into two categories; macronutrients which are required in the greatest quantities, and micronutrients which are required in small quantities. Macronutrients are; Carbon (C), Nitrogen (N), Phosphorous (P) and Potassium (K) while the micronutrient category includes Cobalt (Co), Manganese (Mn), Magnesium (Mg), Copper (Cu) and Calcium (Ca) (Golueke, 1979; Gray *et al.*, 1971; Diaz *et al.*, 1994).

2.3.5 Retention Time

The solids retention time required for complete stabilization of wastes depends on the type of system, maintenance of optimum conditions and the degree of stabilization required. Even under optimum conditions, the rate of degradation is still subject to genetic limitations of

microbial growth and degradation. Due to these limitations, even under optimum conditions, stabilization of MSW should take at least one month (Wong, 1991).

The solids retention times quoted for the in-vessel systems described in Table 2 are much shorter than a month. This is because most of the in-vessel systems are used only for the rapid decay stages, and the product must then be placed in windrows for curing and maturation before a useful soil amendment is obtained.

2.5 Mathematical Models of the Composting Process

There have been many attempts to model the composting process. Different types of mathematical models range from entirely empirical to purely theoretical, although many are a hybrid of these two extremes. The particular models discussed here are hybrid models developed by Haug (1980), Nagasaki *et al.* (1987) and MacDonald (1995).

Haug (1980) developed two commercially available computer models, CMSYS41B and CMSYS52B, to simulate the composting process. The former is used to simulate systems in which all feed components, or substrates are homogeneously mixed and flow through the process without subsequent separation. The second model, CMSYS52B, is used to simulate systems in which bulking agents are used and are then screened at some point in the process for recycle to the first stage. Both model types allow simulation of recycle of the feed mixture to the first stage.

The Haug models are based on energy and mass balances around the composting system and its stages. It is a hybrid between theoretical and empirical relationships in that the model is based on fundamental mass and energy balances, while some peripheral relationships, including reaction rate constants and temperature corrections, are empirical in nature.

For the purpose of the simulation, the composting process is divided into a number of stages. Up to ten different substrates may be fed into stage one, and the output from stage 1 becomes the input to stage 2, etc. Each of these stages is modelled as a continuous flow, completely mixed reactor and the solution is based on energy and mass balances performed around the entire system and each of the stages individually.

Model inputs include the substrate components, temperature, heating value, water content, degradability coefficient, volatile solids content and degradation rate of the substrates as well as the hydraulic residence time (HRT), water addition, airflow rate, air temperature and humidity, solids content setpoints and temperature setpoints for each of the stages.

Nakasaki *et al.* (1987) developed a model based on mass and energy balances on a laboratory scale reactor. The model predicted percent dry solids, moisture content and temperature with time, by using an empirical reaction rate. The empirical reaction rate relates temperature, percent conversion of volatile solids and rate of CO₂ generation.

The mathematical model developed by MacDonald (1995) is based on a stoichiometric

relationship for the reaction, a kinetic rate equation and a heat and mass balance of the system. The stoichiometry was based on rabbit chow as a volatile solids source and the common kinetic rate equation, shown in Equation 2, was used:

$$\frac{dM_{vs}}{dt} = -kM_{vs} \quad (2)$$

Because temperature is considered the key factor affecting biological activity, it was assumed that the rate constant is a function of temperature only.

MacDonald (1995) also cited the following relationship between temperature and rate constant from Haug (1993):

$$k_T = 0.000525(1.066^{(T-20)} - 1.21^{(T-60)}) \quad (3)$$

but adjusted the optimum temperature range to suit MSW composting, which has a range approximately 13°C lower than that used for sludge composting by Haug (1993). This results in the following temperature dependance equation:

$$k_T = 0.000525(1.066^{(T-7)} - 1.21^{(T-37)}) \quad (4)$$

MacDonald (1995) also incorporated a lag phase into his model. This was meant to account for the delay before the advent of microbial growth, which is often attributed to microbial acclimation. The lag factor is described by:

$$t_{lag} = 1 - e^{-\left(\frac{t}{\lambda}\right)} \quad (5)$$

This is incorporated into the model by multiplying the temperature adjusted rate constant (k_T) by t_{lag} before applying the kinetic equation.

Mass, energy and water balances are then performed over the system. These balances are solved using a finite different approach over each time-step. The resulting model has some difficulty predicting the behaviour of the laboratory-scale reactor and would not be applicable to a full-scale system.

There are many other composting models available but those described here are representative of mathematical models that, with some modifications, could be used to model a highly-controlled process such as the Herhof Biocell.

2.4 Odour Generation in Composting

One of the greatest challenges faced by large-scale composting facilities is odour control. Regardless of the practicality of composting as a method of solid waste management, if a facility produces excessive odours that are a nuisance to the surrounding community the end result is likely to be the shut-down of the facility.

2.4.1 Odour Compounds

Historically, it was believed that odours from composting were only the result of anaerobic conditions in composting piles (Haug, 1993), however, it is now known that odorous compounds are natural by-products of both aerobic and anaerobic degradation. The organic material that is the input to composting processes contains a number of components that are precursors to odour formation, including proteins, amino acids and carbohydrates (Walker, 1993). In the composting cycle, odorous compounds that can be formed include ammonia (NH_3), hydrogen sulphide (H_2S), organic sulfur compounds, aliphatic (fatty) acids, amines and aromatics (Haug, 1993; Miller, 1993; Walker, 1993). However, the most predominant odours associated with composting of municipal wastes are ammonia (NH_3) and the organic sulphur compounds dimethyl sulphide (DMS) and dimethyl disulphide (DMDS). Table 3 is a more exhaustive list of compounds that have been implicated in causing odours in composting and their threshold detection levels.

2.4.2 Measurement of Odours

Knowing that odour compounds are present leads to the need for a method of characterization and comparison of odours. Odour compounds are characterized by emission rate, intensity and persistence which cause differences in when and where they are detected, if at all. For example, ammonia is extremely intense, but is easily diluted. Therefore, the smell of ammonia may be very strong on-site and may mask other odours, but it is rarely an odour problem any distance off-site. Conversely, organic sulfur compounds, such as methyl sulphides, are very pervasive meaning that they may be detected easily even when highly

Table 3 - Suspected Odour Compounds from Composting Facilities

Name	Formula	M.W.	B.P °C	Odour	Odour Threshold (µg/m ³)		
					Low	High	ADL [†]
sulfur compounds							
Hydrogen Sulphide	H ₂ S	34.1	-60.7	rotten egg	0.7	14	6.7
Carbon oxysulphide	COS	60.1	-50.2	pungent	n/a	n/a	n/a
Carbon Disulphide	CS ₂	76.1	46.3	disagreeable, sweet	24.3	2.3e04	665
Dimethyl Sulphide	(CH ₃) ₂ S	62.1	37.3	rotten cabbage	2.5	50.8	2.5
Dimethyl Disulphide	(CH ₃) ₂ S ₂	94.2	109.7	sulphide	0.1	346	-
Dimethyl Trisulphide	(CH ₃) ₂ S ₃	126.2	165	sulphide	6.2	6.2	-
Methane thiol	CH ₃ SH	48.1	6.2	sulphide, pungent	0.04	82	4.2
Ethanthiol	CH ₃ CH ₂ SH	62.1	35	sulphide, earthy	0.032	92	2.6
ammonia and nitrogen containing compounds							
Ammonia	NH ₃	17	-33.4	pungent, sharp	26.6	3.96e04	3.3e04
Amino methane	(CH ₃)NH ₂	31.6	-6.3	fishy, pungent	25.5	1.2e04	-
Dimethylamine	(CH ₃) ₂ NH	45.1	7.4	fishy, amine	84.6	84.6	88.1
Trimethylamine	(CH ₃) ₃ N	59.1	2.9	fishy, pungent	0.8	0.8	0.52
3-methylindole (skatole)	C ₆ H ₅ C(CH ₃)CHNH						
volatile fatty acids							
Methanoic (formic)	HCOOH	46	100.5	biting	45	3.78e04	-
Ethanoic (acetic)	CH ₃ COOH	60.1	118	vinegar	2500	2.5e05	2500
Propanoic (propionic)	CH ₃ CH ₂ COOH	74.1	141	rancid, pungent	84	6e04	-
Butanoic (butyric)	CH ₃ (CH ₂) ₂ COOH	102.1	187	rancid	1	9e03	3.7
Pentanoic (valeric)	CH ₃ (CH ₂) ₃ COOH	102.1	187	unpleasant	2.6	2.6	-
ketones							
Propanone (acetone)	CH ₃ COCH ₃	58.1	56.2	sweet, minty	47500	1.61e06	2.4e05
Butanone (MEK)	CH ₃ COCH ₂ CH ₃	72.1	79.6	sweet, acetone	737	1.47e05	3e04
2-Pentanone (MPK)	CH ₃ COCH ₂ CH ₂ CH ₃	86.1	102	sweet	28000	4.5e04	-
other compounds							
Benzothiozole	C ₆ H ₄ SCHN	135.2	231	penetrating	442	2210	-
Ethanal (acetylaldehyde)	CH ₃ CHO	44.1	20.8	green sweet	0.2	4140	385
Phenol	C ₆ H ₅ OH	94.1	181.8	medicinal	178	2240	184

†Analytical Detection Limit (ADL)

(Williams & Miller, 1993)

diluted. As a result these odours may not be apparent on-site due to masking by other compounds, but are often the source of complaints from neighboring communities (Walker, 1993).

Odour *quantity* is generally determined by the human nose, typically using odour panel tests. It is expressed in terms of the number of effective dilutions required for the odour to be detected by 50% of the participants in the odour panel. This value is known as the ED₅₀ level (Haug, 1993; Walker, 1993).

Odour *intensity* is the measure of the strength of the scent, compared to a standard compound such as n-butanol. The intensity is matched by the odour panel to a concentration of the standard that gives an equivalent intensity to the compound being tested, and is then expressed on an equivalence basis as milligrams/litre of the standard compound (Haug, 1993; Walker, 1993).

The *pervasiveness* of an odour is determined by its intensity. A high intensity compound can be detected at very low concentrations and is considered to be pervasive. A quantitative measure of pervasiveness is determined by plotting the intensity measured at various dilutions, as shown in Figure 2. The slope of the relationship is then calculated by regression analysis. As illustrated here, a flatter slope would indicate a highly pervasive compound, where the intensity of the odour does not vary considerably over a range of dilutions.

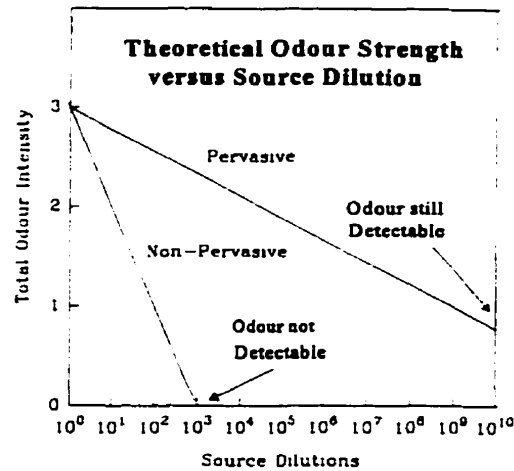


Figure 2 - Dilution Characteristics of Pervasive and Non-Pervasive Odours (Walker, 1993)

Also important in characterizing an odour problem is the mass of odour produced per unit time, or the rate of emission. Even intense, pervasive odours may not cause a problem if the production rate is low.

As previously mentioned, the accepted method of measurement of composting off-gas samples is an odour panel. The panel is usually comprised of 8-10 people, who are asked to smell a series of dilutions of the sample, ranging from highest dilution (lowest concentration) to lowest dilution (highest concentration). Determination of the odour by this method examines the off-gases as a mixture, accounting for synergistic and antagonistic effects of different compounds in the gas. However, because odour panels identify overall odour strength, the potential for causing odour nuisance is not addressed directly. Furthermore, the

collection and preparation of the off-gas samples for analysis by odour panels is time consuming and expensive. It is therefore of little value for process control.

Since the major odour-causing compounds from the composting process have been identified, it may also be possible to determine the risk of causing nuisance odours analytically. Mass spectral or gas chromatographic analysis of off-gas samples could determine the presence of the offensive odour compounds, and measure their concentration. If such an analysis could be performed on-line, remedial action could be taken before the concentrations/amounts reach a nuisance level.

2.4.3 Reduction of Odours

Minimization of odour emitted from a composting facility may be achieved by one or a combination of physical, chemical or biological methods. Historically, the most common methods for odour control include dilution, masking, sorption, condensation, oxidization by combustion, chemical scrubbing, and more recently, by microbes in biofiltration (Balling & Reynolds, 1980; Gibson, 1995; Van Durme *et al.*, 1992, Wilson *et al.*, 1980).

The popularity of biofiltration for odour reduction has increased tremendously in recent years. The basis of the technique is the use of a biologically active, solid media bed to sorb compounds from the air stream and retain them for oxidation by the microbial population in the media. Early 'biofilters' used soil as a filter media, but recent trends use compost or peat due to their higher microbial activity and specific surface area. The most desirable

characteristics of biofilter media include high specific surface area, air and water permeability, water holding capacity, active microbial population and relatively low cost. Table 4 outlines the basic design and operating parameters as described by Haug (1993).

The usefulness of biofilters for treatment of odorous composting gases has been subject to some controversy. Haug (1993) cites studies on a number of European installations that have observed 99% removal efficiencies on gases where inlet concentrations have been as high as 25,000 to 50,000 ED₅₀. A study by Hartestein and Allen (1990), reported high removal efficiencies for some of the most important compounds in compost odours, including H₂S (>99%), methyl mercaptan, DMS and DMDS (>90%) and various terpenes (>98%). But, these studies are contradicted by other results that have reported insignificant removal of both organic and inorganic sulfur compounds when highly loaded (Haug, 1993).

However, bench-scale studies by Gibson (1995) and Cho *et al* (1991a) also support the positive results obtained with biofilters for odour removal, and it is generally believed that if designed and operated properly, biofilters are an extremely effective method of reducing odour problems in composting (Gibson, 1995; Haug, 1993). The use of biofilters at the Guelph Wet/Dry Facility, as well as other full-scale plants, has also clearly demonstrated over the past few years that odour control is readily achievable.

Table 4 - Recommended Design and Operating Parameters for Biofilters (Haug, 1993)

Filter Media	Biologically active, but reasonably stable Organic Content >60% Porous and friable with 75-90% void volume Resistant to water logging and compaction Relatively low fines content to reduce gas head loss Relatively free of residual odour Specifically designed mixtures of material may be desirable to achieve the above characteristics
Moisture Content	50-70% by weight Provisions must be made to add water and remove bed drainage
Nutrients	Must be adequate to avoid rate limitations Usually not a problem with composting gases because of the high NH ₄ content
pH	7 to 8.5
Temperature	Near ambient, 15-35 or 45°C
Gas Pretreatment	Humification as necessary to achieve near 100% inlet gas humidity. Dusts and aerosols should be removed to avoid media plugging
Gas Loading Rate	<100m ³ /h-m ² , unless pilot testing supports higher loads
Gas Residence Time	30-60 sec, unless pilot testing supports a shorter residence time
Media Depth	> 1m or 3 ft.
Elimination Capacity	Depend on media and compound (about 2.2 mg/H ₂ S/kg media VS per min for H ₂ S)
Gas Distribution	The manifold must be properly designed to provide a uniform gas flow to the filter media

2.4.4 Atmospheric Dispersion of Odours

Once odours are released from the facility, they will be dispersed within the atmospheric sublayer, which typically extends approximately 18 m above ground level (Wilson *et al.*, 1980). The distance travelled and how quickly they become diluted are a function of both the source and the atmospheric conditions, including heat flux, sublayer temperature, lapse rate and wind speed (Wilson *et al.*, 1980).

The source may be considered either a point source or an area source, depending on the individual facility. Release from a scrubber or stack is considered to be a point source, while odours originating from an open compost pile, or a biofilter bed are considered to be area sources (Walker, 1993). Typically, area sources result in greater numbers of odour complaints from surrounding communities than point sources. Although point source odours are generally more concentrated than area source odours, they are usually released at a higher elevation, resulting in greater mixing and dilution of the odours. Area sources released lower to the ground will travel across the ground surface, thereby increasing the risk of detection by receptors (Walker, 1993, Wilson *et al.*, 1980).

There are numerous mathematical and/or computer models available to predict atmospheric dispersion. These can be used with appropriate caution to estimate odour transport from an existing facility, assess odour dilution techniques or assist in plant siting and design (Haug, 1993; Wilson *et al.*, 1980).

3.0 MODELLING THE HERHOF PROCESS

The purpose of modelling the Herhof process is to determine if system performance can be reproduced mathematically. If this is possible, a computer model of the system could be used to predict the response of the physical system to changes in conditions and substrates. The original intent was to modify the models developed by Haug (1993), but the nature of the highly-controlled Herhof System would require significant modifications to the Haug models. It was therefore decided that the best approach was to develop a new model specifically for this application. A conceptual diagram of the flows in the Herhof Process is given in Figure 3.

3.1 Mathematical Model Development

The model development involved the stoichiometric relationship for the process, estimation of degradation rates in the kinetic equation, mass and energy balances, and verification using observed operating data and results.

3.1.1 Stoichiometry

The equations required to describe the bio-degradation of volatile solids are readily available in literature. The simplified stoichiometric equation used by Haug (1993) and MacDonald (1995) to describe the relationship between the substrate and the products of the oxidation process is given by;

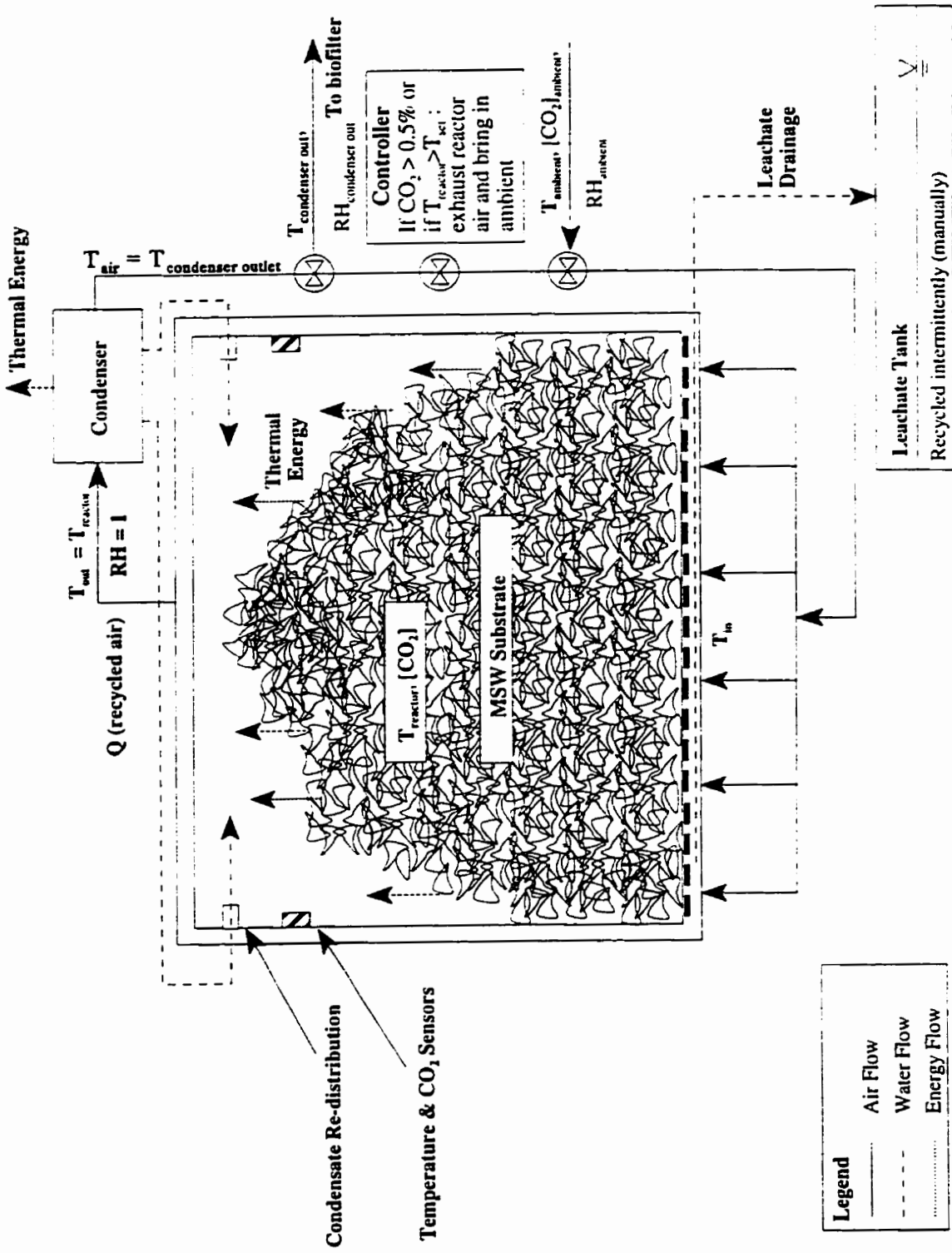
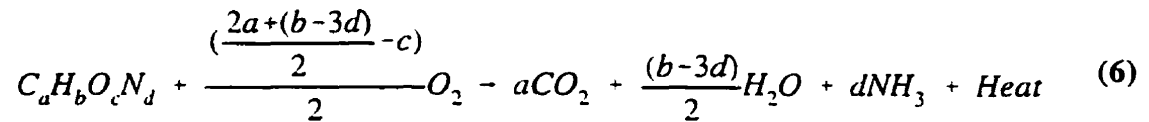
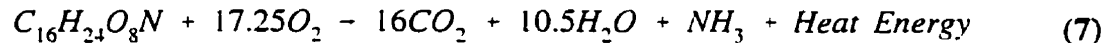


Figure 3 - A Conceptual Diagram of Mass and Energy Flows in a Herthof Biocell



For the development of the model, the volatile solid source used for the first substrate is food waste. Based on the approximate composition for food waste, the stoichiometric relationship becomes:



The model allows the input of multiple substrates for the purpose of simulating systems which combine distinct types of wastes and/or bulking agents. With the stoichiometric composition of the substrate, equation 6 is then used to determine the mass of carbon dioxide, water and ammonia produced and the mass of oxygen consumed by each substrate per unit mass of volatile solids degraded.

3.1.2 Kinetics

In order to determine the mass of volatile solids degraded over time, a kinetic relationship is used. It is commonly assumed that, for most batch reactions, the relationship between the mass of volatile solids consumed and the concentration of volatile solids is a first-order relationship described by (MacDonald, 1995; Roels, 1983):

$$\frac{dM_{vs}}{dt} = -kM_{vs} \quad (8)$$

*Nomenclature is provided at the beginning of this document

The reaction rate, k , which is determined by the substrate characteristics, is also variable with changes in oxygen availability, moisture content and most significantly, temperature. For convenience, the rate constant is commonly considered as a function of temperature only (MacDonald, 1995; Stuparyk, 1993). For the development of this model, the relationship used by Haug (1993) in the CMSYS models is shifted 13°C and applied, as previously discussed. The relation used for the model is shown in equation 4.

3.1.3 Energy and Mass Balances

The model equations are developed by performing mass and energy balances on the reactor. The reactor is treated as a Continuous Stirred-Tank Reactor (CSTR) wherein spatial variations are ignored. Materials are considered to be instantly and uniformly mixed, and all materials within the reactor are assumed to be at the same average temperature.

The energy balance around the reactor is based on the fundamental equation;

$$\text{Rate of Energy Accumulation} = \text{Rate of Energy Input} - \text{Rate of Energy Output} \quad (9)$$

The accumulated energy in the energy balance is seen as temperature increases of all materials in the system. Therefore, the rate of energy accumulated in the reactor is described

by:

$$q_{acc} = (M_s C_s + M_w C_w + M_{rw} C_{rw}) \frac{dT_{avg}}{dt} \quad (10)$$

Losses of thermal energy from the reactor occur by three primary mechanisms, heating of the reactor exhaust gases, vaporization and removal of water vapour from the reactor and losses in the condenser. The losses in the condenser include the change in enthalpy of the dry air stream and the removal of liquid condensate from the system. It is assumed that the heat loss through the insulated reactor walls is much less significant and is ignored. Therefore, the rate of energy loss from the reactor can be described by:

$$q_{losses} = \dot{m}_a [C_g (T_o - T_i) + \lambda_w (Y_o - Y_i) + (h_{ao} - h_{ai}) + h_w (Y_o - Y_i)] \quad (11)$$

Another source of thermal energy is heat produced by microorganisms in the degradation of volatile solids. There are a number of methods to calculate energy production, but for this model, the heat of combustion of volatile solids degraded is used as an estimate (Haug, 1993).

$$q_{generated} = h_c \left(\frac{dM_{vs}}{dt} \right) \quad (12)$$

Combining equations 10, 11 and 12 gives the overall enthalpy balance for the model:

$$\frac{dT_{avg}}{dt}(C_s M_s + C_w M_w + C_{rw} M_{rw}) = \dot{m}_a [C_g (T_i - T_o) + \lambda_w (Y_i - Y_o) - (h_{ao} - h_{ai}) - h_w (Y_o - Y_i)] + h_c \frac{dM_{vs}}{dt} \quad (13)$$

The mass balance for water and dry solids are performed over the system. The water generated by the degradation process may be calculated from the stoichiometry shown in Equation 6, which is also used to calculate generation factors for each product. Leachate is added directly back into the system, so the only losses of water from the system are considered to be water vapour removed in the condenser when the airstream is recycled, and water vapour removed in the exhaust gases when the air is exhausted. The overall water balance is:

$$\frac{dM_w}{dt} = \dot{m}_a (Y_i - Y_o) + G_w \frac{dM_{vs}}{dt} \quad (14)$$

The mass balance of dry solids is governed by the kinetic rate constant as previously discussed. For clarity, the relationship is shown in Equation 15.

$$\frac{dM_{vs}}{dt} = -k_{adj} M_{vs} \quad (15)$$

In order to be able to estimate the concentration of CO₂ in the headspace gases, a balance must be performed for CO₂ as well. This balance is based on a number of assumptions, most

significantly that the CO₂ reaches instantaneous equilibrium between the headspace gas and the aqueous phase in the substrate. Like water production, the generation factor for CO₂ is estimated from the stoichiometric equation for the volatile solids degradation.

$$\frac{dM_{CO_2}}{dt} = G_{CO_2} \frac{dM_{vs}}{dt} \quad (16)$$

Henry's Law is applied to estimate CO₂ "losses" to the aqueous phase. The relationship used to calculate aqueous phase concentration is described by:

$$[CO_2]_{aq} = H_{CO_2}(PP_{CO_2,air})(MM_{CO_2})(55.56 \frac{kmol_w}{m^3}) \quad (17)$$

where H_{CO_2} is Henry's Law constant for CO₂ (kPa⁻¹).

While air is recycled, there are no inputs or losses of CO₂ attributed to aeration air. When ambient air is used for aeration, CO₂ inputs and losses are calculated using:

$$\frac{dM_{CO_2,air}}{dt} = G_{CO_2} \frac{dM_{vs}}{dt} - \frac{dM_{CO_2(aq)}}{dt} - Q_{air}([CO_2]_{headspace} - [CO_2]_{ambient}) \quad (18)$$

When the aeration air is recycled, there is no gain or loss of CO₂ associated with the exhaust gases. In this case, the last term of Equation 18 becomes zero. For completeness, a similar balance for oxygen is included in the model. This balance is described below by Equation 19:

$$\frac{dM_{O_2,air}}{dt} = Q_{air}([O_2]_{ambient} - [O_2]_{headspace}) - G_{O_2} \frac{dM_{vs}}{dt} \quad (19)$$

3.1.4 Finite Difference Equations

The differential equations used to describe this system are solved using a simple forward-difference approach. The numerical approximation of the primary equations of the model are given below.

$$M_{vs}^{(t+1)} - M_{vs}^{(t)} = -k_{adj} M_{vs}^{(t)} * \Delta t \quad (20)$$

$$M_w^{(t+1)} - M_w^{(t)} = \dot{m}_a(\Delta t)(Y_i - Y_o) + G_w(M_{vs}^{(t+1)} - M_{vs}^{(t)}) \quad (21)$$

$$T_{avg}^{(t+1)} - T_{avg}^{(t)} = \left(\frac{\Delta t}{C_s M_s + C_w M_w + C_{rw} M_{rw}} \right) [\dot{m}_a (C_g (T_i - T_{avg}^{(t)}) + \lambda_w (Y_i^{(t)} - Y_o^{(t+1)})) - (h_{ao}^{(t+1)} - h_{ai}^{(t)}) - h_w (Y_o^{(t-1)} + Y_i^{(t+1)})] + h_c (M_{vs}^{(t+1)} - M_{vs}^{(t)}) \quad (22)$$

$$M_{CO_2,air}^{(t+1)} - M_{CO_2,air}^{(t)} = G_{CO_2} (M_{vs}^{(t+1)} - M_{vs}^{(t)}) - V_w ([CO_2, aq]^{(t+1)} - [CO_2, aq]^{(t)}) - Q_{air} * \Delta t ([CO_2, air]^{(t)} - [CO_2, ambient]^{(t)}) \quad (23)$$

$$M_{O_2,air}^{(t+1)} - M_{O_2,air}^{(t)} = Q_a ([O_2]_{ambient} - [O_2]_{headspace}) \Delta t + G_{O_2} (M_{vs}^{(t+1)} - M_{vs}^{(t)}) \quad (24)$$

These equations predict average values for temperature, CO₂ concentration and degradation of volatile solids in the reactor for each time step. When multiple substrates are used, the kinetic equations for degradation and production are applied to each substrate over each time step. The energy balance is then performed over the entire system of combined substrates for the same time step. A flow diagram of the computer model is given in Figure 4.

3.1.5 Model Stability

The use of a forward finite-difference solution includes the selection of a time-step for calculation. In this case, a time-step of thirty minutes was selected. The thirty minute time-step is acceptable for biological degradation reactions that proceed slowly and some commercially available models use time-steps of the range of one hour. The reasons for the selection of this time-step is a balance of computational efficiency and model stability. The use of a finite-difference model for these differential equations could result in instability and/or error-accumulation if the time-step selected were too long.

Input Parameters
Substrate Characteristics*

- Mass of Substrate
- Moisture content of Substrate
- Solids content of Substrate
- Volatile solids fraction of substrate
- Fraction of Fast Degrading solids
- Molar Carbon content
- Molar Hydrogen content
- Molar Nitrogen content
- Molar Oxygen content
- Degradation Rate (29WK)
- Ambient Conditions
- Peak Daily Temperature
- Relative Humidity
- Air Pressure

*(for each substrate)

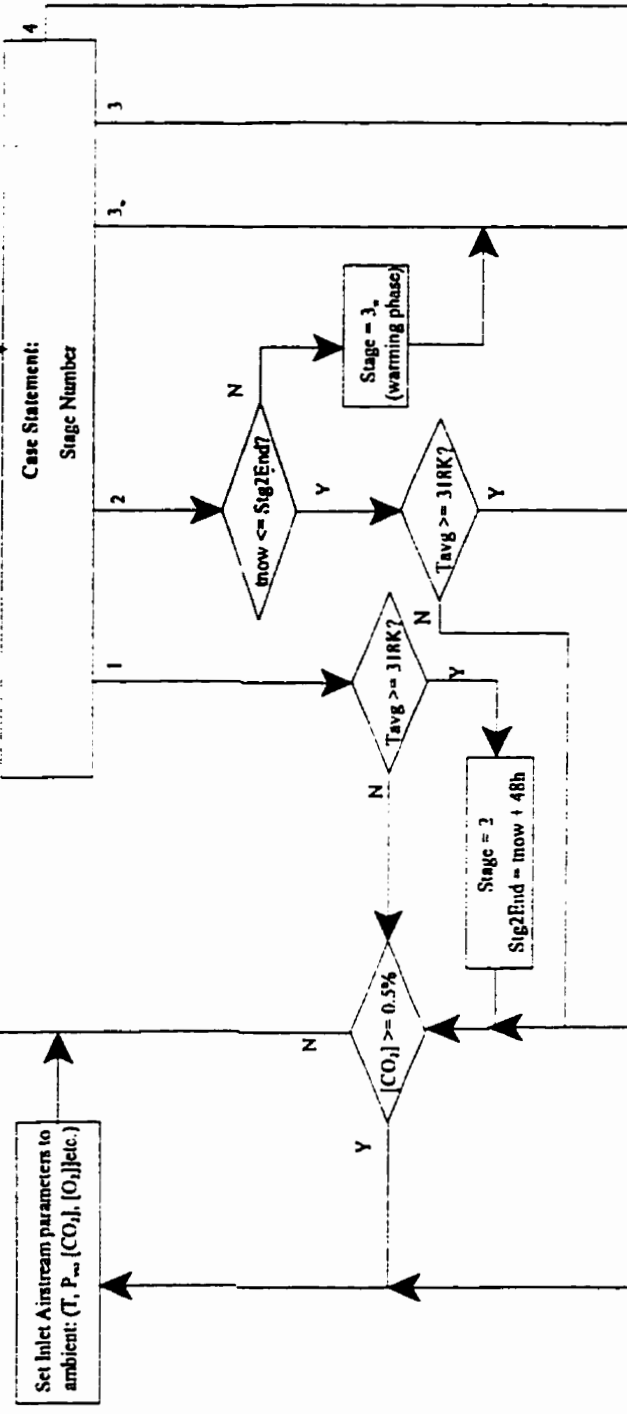
Initial Calculations
 Calculate:

- Dry Mass Substrate*
- Adjusted Rate constant*
- Generation Factors for Water, CO_2 , O_2 , NH_3 *
- Initial Ambient Temperature
- Molar Mass of Ambient air
- Vapour Pressure of Moisture in Ambient air
- Absolute humidity of Ambient air
- Flow rate of ambient air
- Flow rate of water vapour in ambient air
- Set Stage = 1

Time step Calculations*:

- Degradation rates based on reactor temperature
- Change in Volatile solids
- Water generation
- Temperature change
- CO_2 generation
- O_2 consumption
- NH_3 generation
- Overall mass of dry gases generated
- CO_2 absorbed into aqueous phase
- Mass flow of dry air and water vapour into the reactor
- Mass flow of dry air and water vapour exiting the reactor
- Percent CO_2 by mass in headspace
- Percent O_2 by mass in headspace

*Executed each timestep





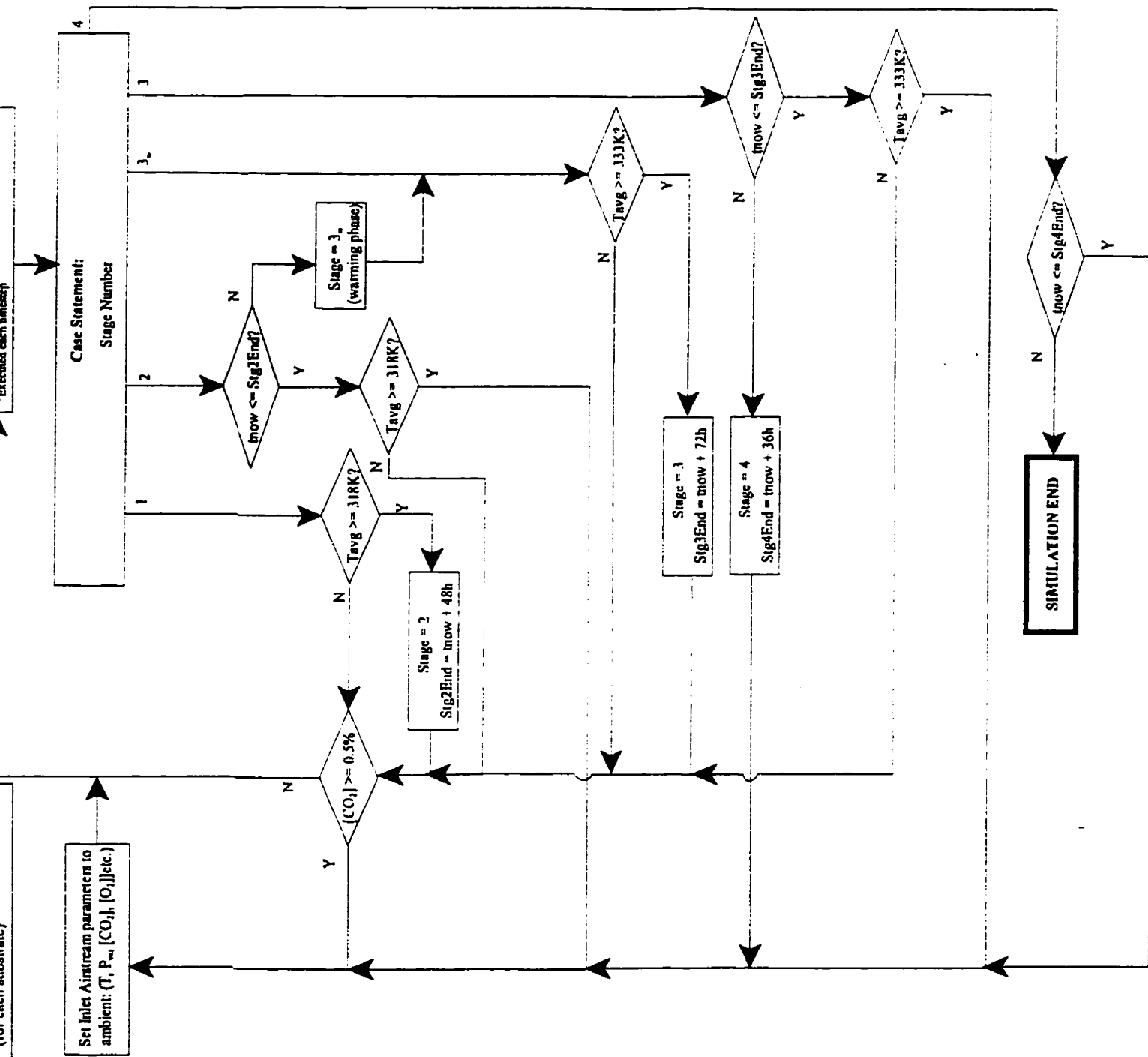


Figure 4 - Flowchart of Simulation Model

3.2 Model Verification

Once the model was developed, the results predicted must be compared to those results observed in the field. This will provide an indication of the ability of the model to predict the behaviour of the physical system.

3.2.1 Data Collection

Field data was collected for those batches processed between October 1995 and December 1996. The data collected included information about the characteristics of input substrate, output from the system, as well as process parameters. The information collected for each of these runs is outlined below in Table 5.

Table 5 - Compost and System Data

Substrate Characteristics*	Product Characteristics*	Process Parameters
Ash content	Ash content	Volume of water added*
Carbon content	Carbon content	Temperature profile
Heating value	Heating value	Duration of phases 1, 2, 3, 4
Mass	Mass	Airflow rates
Moisture content	Moisture content	Oxygen levels
Nitrogen content	Nitrogen content	Carbon dioxide levels

*This information was not available for *all* batches

This data was to used for two purposes:

- (1) calibration of the model
- (2) testing the calibrated model performance against batches processed in the field

The batches for which data was collected are summarized in Table 6.

Table 6 - Field Batches

Batch Number	Start Date ^c	Finish Date ^c
Calibration batch	03-10-95	16-10-95
1	05-10-95	17-10-95
3	04-11-95	14-11-95
27	12-06-96	19-09-96
38	09-08-96	20-08-96
47	16-10-96	22-10-96
54	12-11-96	20-11-96

^c(dd-mm-yy)

3.2.2 Model Calibration

Before using the model to simulate field batches and comparing the observed to predicted performance, it was necessary to calibrate the model to sample data.

The theoretical model is the one that was developed as described previously, using accepted literature values for rate kinetics and other operational parameters. Some of these parameters were then adjusted to better describe the actual performance of the system, resulting in an *adjusted model*.

The model parameters in which there is the least confidence are the overall degradation rate and the fraction of fast-degrading and slow-degrading substrates. These two parameters can be highly variable even between batches of MSW collected from the same area. For this reason, it was determined that these parameters would be varied to try to improve the 'fit'

of the model to the field data.

In all, eleven adjusted models were produced, based on variations of these parameters to varying degrees. The primary characteristics of the theoretical and adjusted models are illustrated in Table 7.

Table 7 - Summary Adjusted Model Parameters

Model	Degradation Rate ^o	Fast-degrading (fraction)	Slow-degrading (fraction)
Theoretical	0.0063	0.3	0.7
Adjusted 1	0.00063	0.3	0.7
Adjusted 2	0.001	0.3	0.7
Adjusted 3	0.002	0.3	0.7
Adjusted 4	0.0063	0.4	0.6
Adjusted 5	0.00063	0.4	0.6
Adjusted 6	0.001	0.4	0.6
Adjusted 7	0.002	0.4	0.6
Adjusted 8	0.0063	0.5	0.5
Adjusted 9	0.00063	0.5	0.5
Adjusted 10	0.001	0.5	0.5
Adjusted 11	0.002	0.5	0.5

^oDegradation rate shown for fast-degrading fraction. Slow degradation rate is 10% of rate shown.

Each of these models were then used to simulate the batch processed October 3-16, 1995 and the adjusted model that was shown to be most similar (based on MAPE) to the observed results was selected for further simulations of the system. This batch was selected for calibration because it is the first batch that followed the required operational profile without

interruption, and for which there was a complete data set.

In comparing the model results to the field data, the following parameters were selected:

- (1) temperature profile
- (2) mass reduction, and
- (3) overall process duration

These parameters were selected because they are the most significant operating and performance parameters, and field values were available for other batches which were subsequently used in the simulation study.

The comparison between the predicted and observed data values of the calibration batch is based on the Mean Absolute Percentage Error (MAPE). This is an average of the absolute difference between the observed and the predicted values for all data-points, calculated by:

$$MAPE = \frac{\sum_{i=1}^n \left| \frac{[\text{observed value}]_i - [\text{predicted value}]_i}{[\text{predicted value}]_i} \right|}{n} \times 100\% \quad (25)$$

where n = the number of data points

Although there are many statistical measures of fit available, the use of MAPE provides a simple quantitative measure of error, accounting for both positive and negative differences

through the use of absolute values and is not limited by the non-linearity of the model.

Field temperature data is provided at 2-hour intervals, so the MAPE is calculated at this interval. The MAPE values for all data points are then averaged over the entire duration to give a quantitative measure of the closeness of fit between the predicted and observed data.

The field data only provides mass and moisture content values for the input and output samples, so there is only a single value for calculation of the MAPE for dry mass reduction. The overall duration MAPE is also necessarily based on one value for each calibration simulation.

3.2.3 Measuring Model Performance

The purpose of developing this model was two-fold. First, to determine if a theoretically-based model would produce similar performance as the reactor system in operation, and second to use the model to determine if variable conditions can be accounted for by the model. In order to achieve these goals, the *theoretical model* was first compared to the actual operation of the reactors, and then the model was calibrated with field data from the October 3rd to 16th batch, to match the actual performance of the system as closely as possible. This *adjusted model* could then be used to simulate six field batches to test its ability to simulate other batches. The field batches selected, although not ideal, were the best of the available field data.

Once verified, the calibrated model was used to simulate operation of the Herhof Process under conditions other than those observed during the experiments, including extreme ambient temperatures, abnormally high degradation rates (very high volatile organic content) and abnormally low degradation rates (high lignin content). To test each of these conditions, a test batch was created whose parameters could be adjusted to create these scenarios. The batch parameters are summarized in Table 8.

Table 8 - Parameters for Extreme-Condition Runs

Condition	Batch and Process Parameters				Situation
	Ambient (K)	Degradation rate (h ⁻¹)	Fast degrading volatiles (%)	Slow degrading volatiles (%)	
High ambient temperature	305	0.001	30	70	seasonal
Low ambient temperature	270	0.001	30	70	seasonal
High organic content	288	0.001	100	0	100% leaves, grass clippings
Low organic content	288	0.001	0	100	2nd-run compost

The ability of the model to perform as expected under these condition will be a good indicator of its flexibility.

3.3 Modelling Results

The results of the testing and simulations are summarized below.

3.3.1 Selection of the Calibrated Model

As mentioned previously, the performance of each of the adjusted models was determined by its ability to predict the behavior of the actual system. The basis of comparison between the predicted and observed results were temperature profile, mass reduction and duration. In order to illustrate the comparison of temperature profiles, the temperatures predicted by the adjusted models are plotted against the observed temperatures for the calibration batch in Figures 5 through 16. A summary of the other parameters are shown outlined in Table 9.

Table 9 - Comparison of Model Results

Model	Mass Reduction (kg _{dry})	Process Duration (h)	Final Moisture content (%)
Observed (Oct. 3 rd batch)	4358	192	59%
Theoretical	5634	170.5	76%
Adjusted 1	3043	205	66%
Adjusted 2	4014	207	69%
Adjusted 3	4833	181	72%
Adjusted 4	4358	169	76%
Adjusted 5	5634	204	67%
Adjusted 6	3043	210.5	70%
Adjusted 7	4014	180	73%
Adjusted 8	4833	168	76%
Adjusted 9	5650	206	68%
Adjusted 10	4543	212.5	71%
Adjusted 11	5018	179	73%

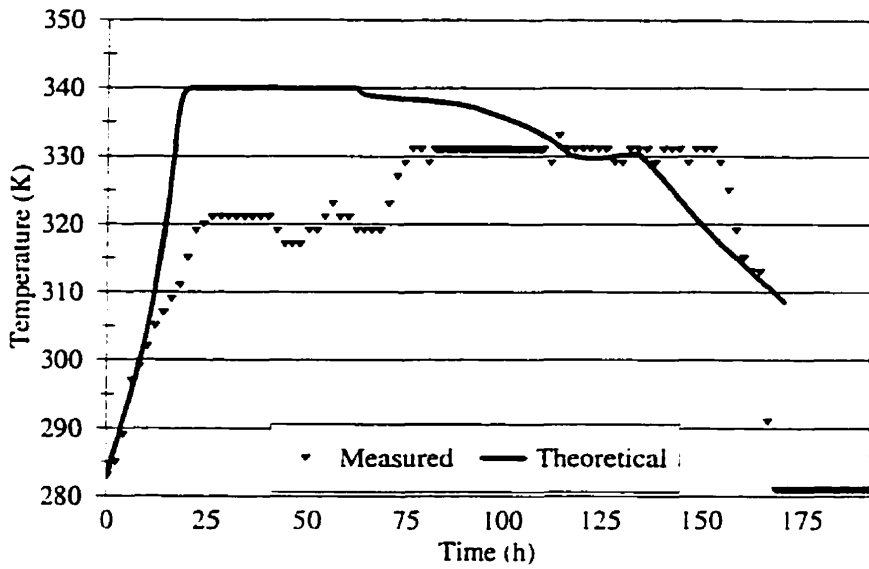


Figure 5 - Temperature Profile Comparison, Theoretical

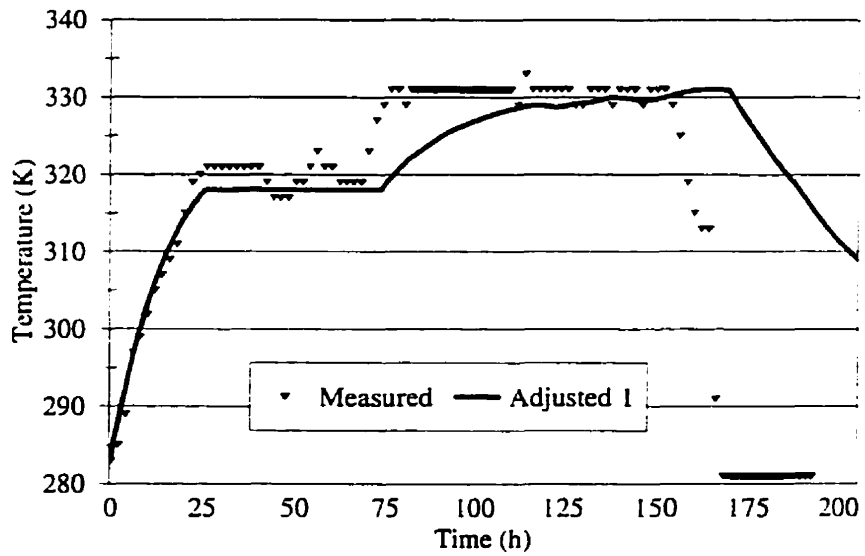


Figure 6 - Temperature Profile Comparison, Adjusted Model 1

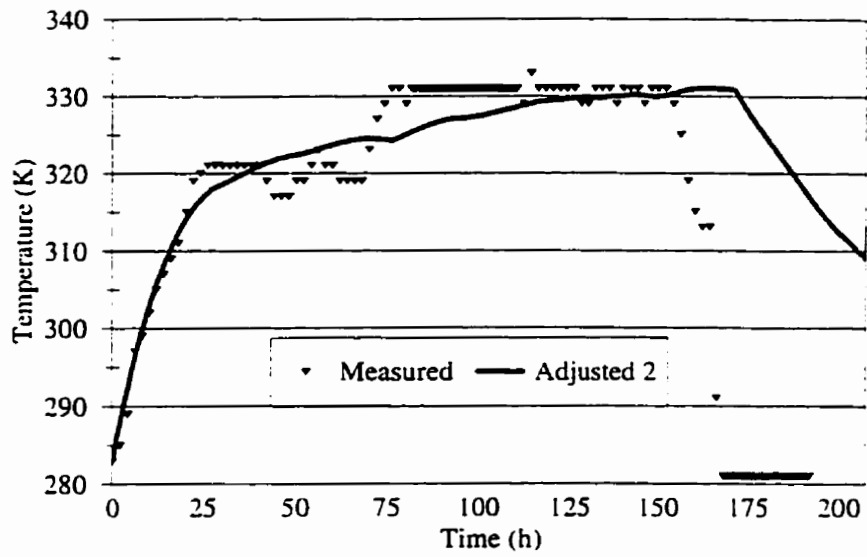


Figure 7 - Temperature Profile Comparison, Adjusted 2

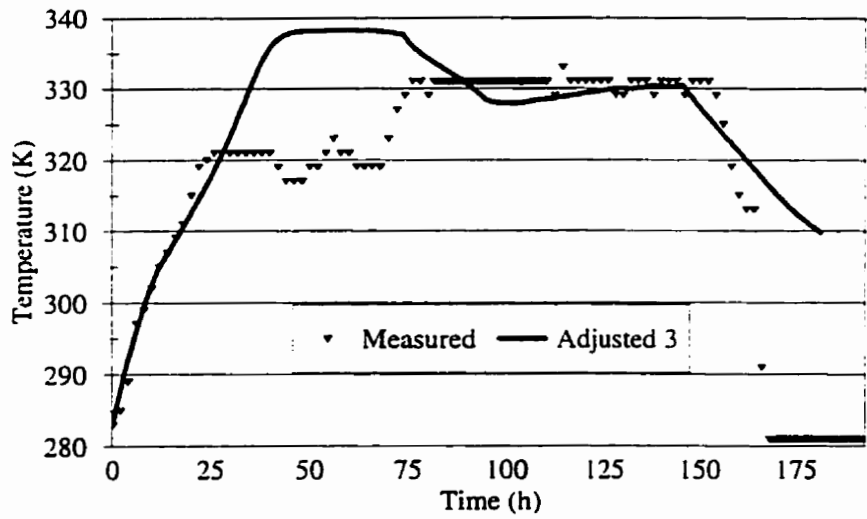


Figure 8 - Temperature Profile Comparison, Adjusted 3

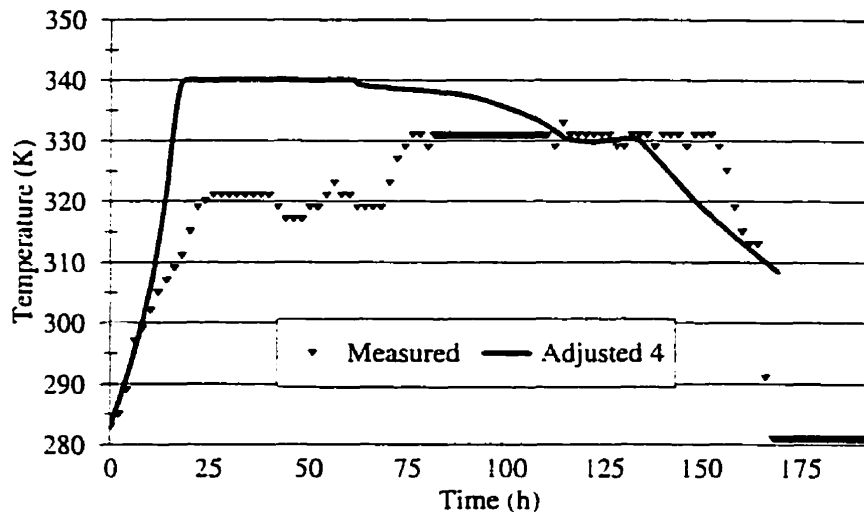


Figure 9 - Temperature Profile Comparison, Adjusted 4

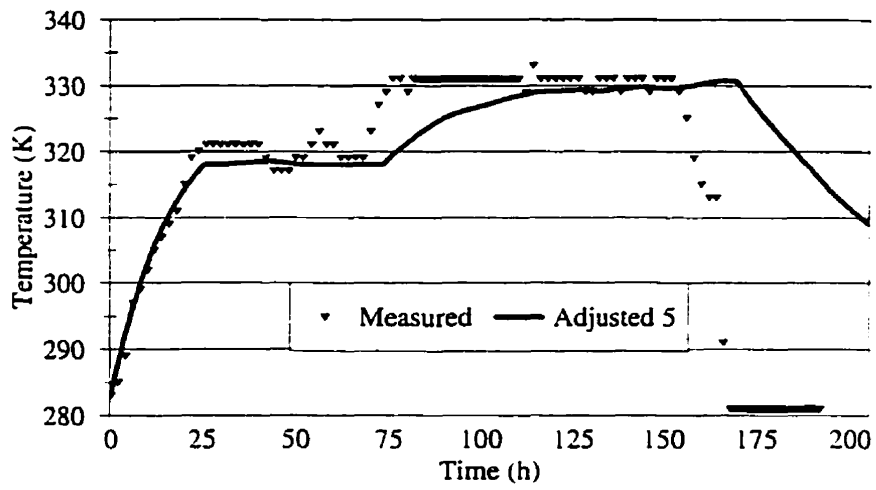


Figure 10 - Temperature Profile Comparison, Adjusted 5

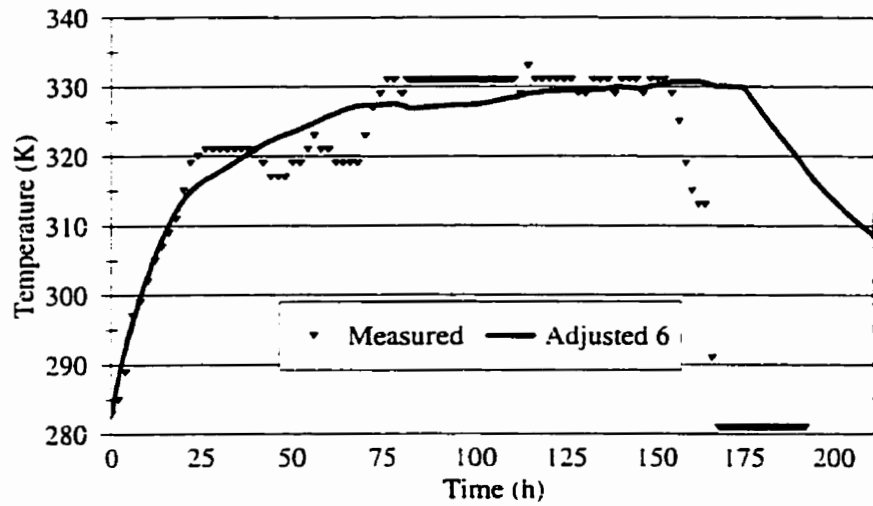


Figure 11 - Temperature Profile Comparison, Measured vs. Adjusted 6

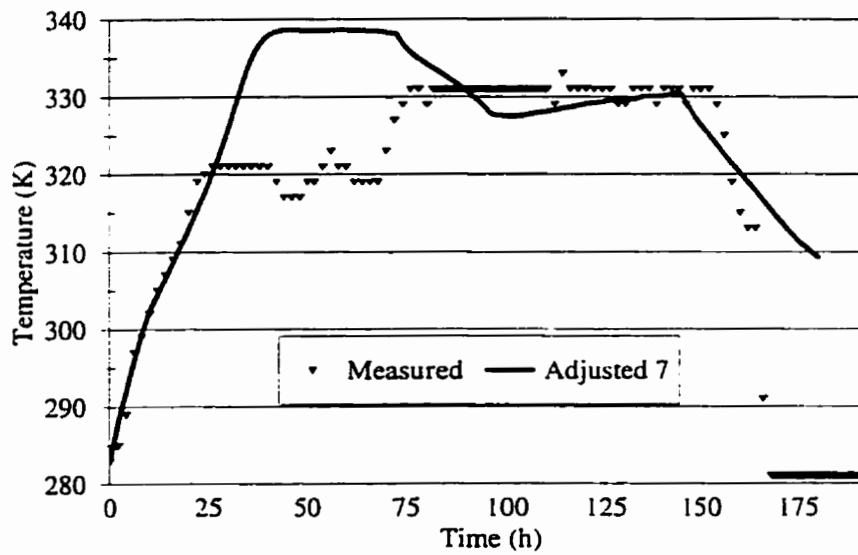


Figure 12 - Temperature Profile Comparison, Measured vs. Adjusted 7

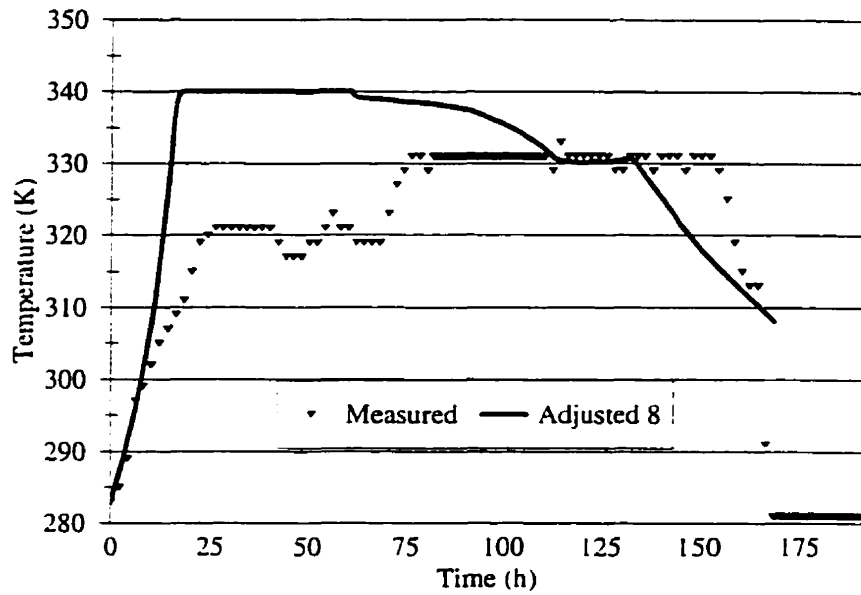


Figure 13 - Temperature Profile Comparison, Adjusted 8

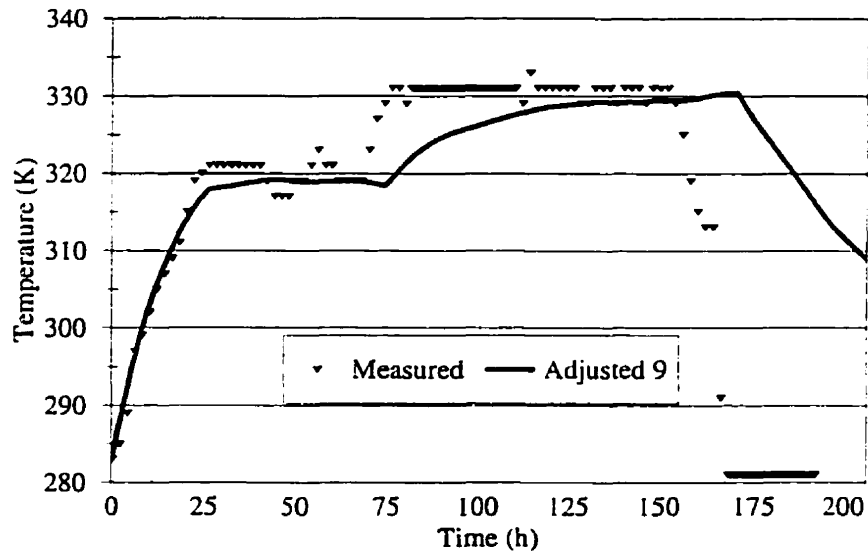


Figure 14 - Temperature Profile Comparison, Adjusted 9

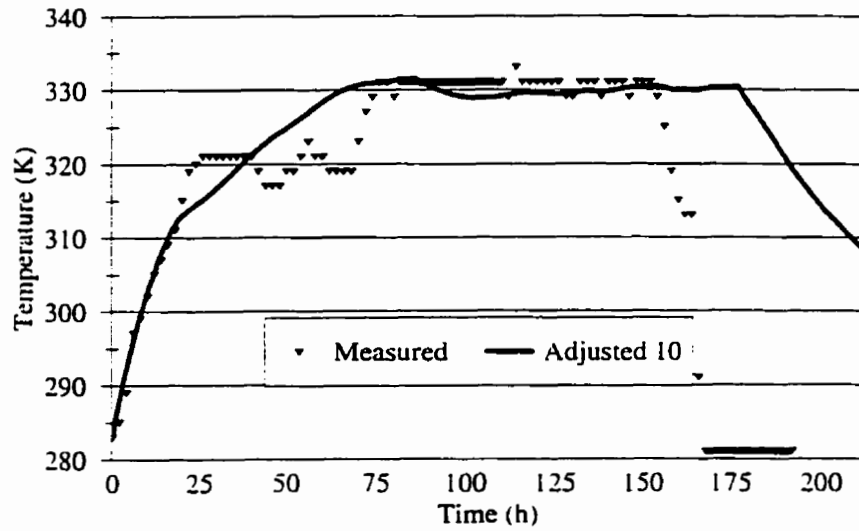


Figure 15 - Temperature Profile Comparison, Adjusted 10

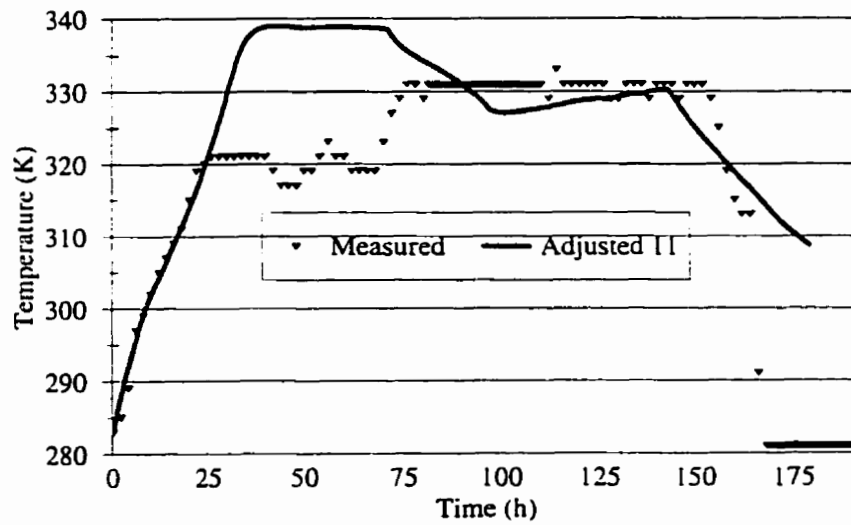


Figure 16 - Temperature Profile Comparison, Adjusted 11

In these models, acclimation of biomass is not taken into account. Adjusted model 12 was developed to simulate this type of system. The parameters used for Adjusted model 12 are given in Table 10. The acclimation was simulated by removing the distinction between fast- and slow-degrading feedstock in Phase 3. Essentially, in Phase 3 all of the remaining volatile solids became fast degraders. The temperature profile for this simulation are shown in Figure 17. Comparisons of overall duration and dry mass reduction are shown in Figures 18 and 19, respectively.

Table 10 - Adjusted Model 12 Parameters

Parameter	Value	Units
Degradation Rate (Fast)	0.001	h ⁻¹
Degradation Rate (slow)	0.0001	h ⁻¹
Phase 3 Degradation Rate*	0.001	h ⁻¹
Fast-Degrading Fraction	0.3	-
Slow-Degrading Fraction	0.7	-

*All fractions

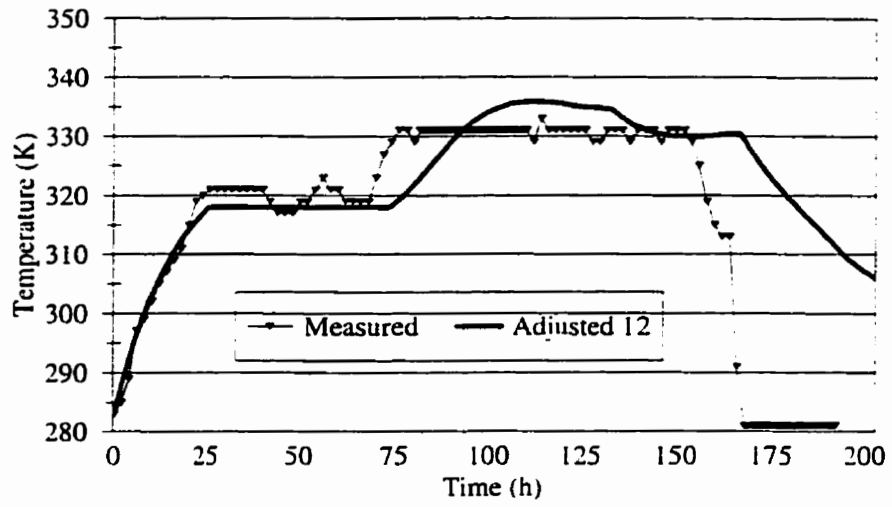


Figure 17 - Temperature Profile Comparison, Adjusted 12

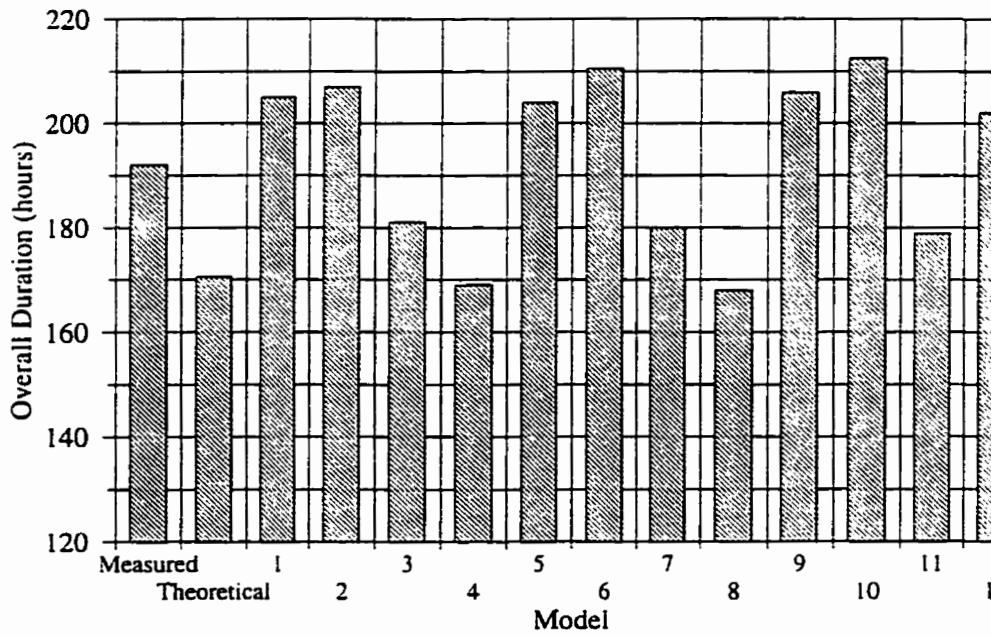


Figure 18 - Comparison of Overall Duration

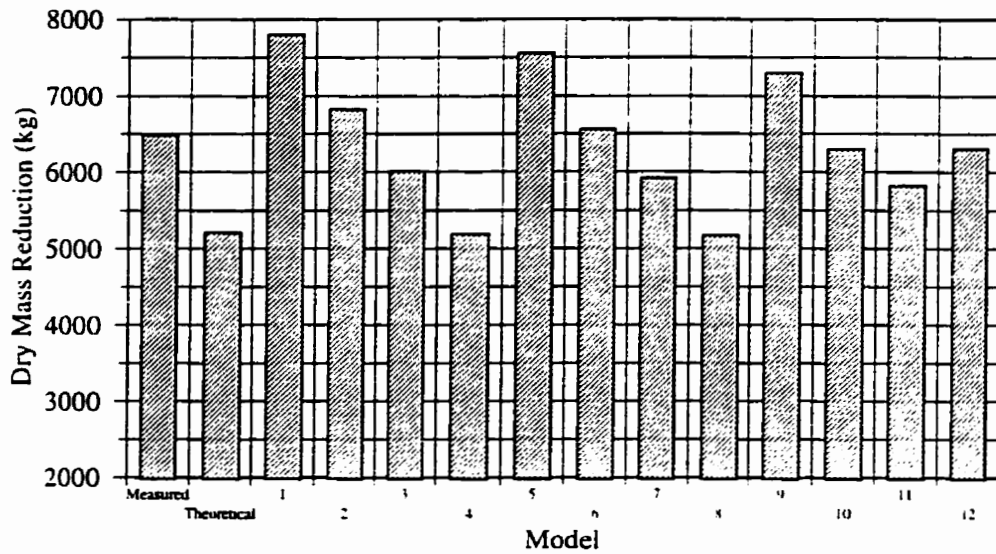


Figure 19 - Comparison of Dry Mass Reduction

A quantitative comparison of the parameters predicted by the adjusted models to those observed in the field are provided by the Mean Absolute Percentage Error (MAPE) calculation discussed previously. The MAPEs for each of the adjusted models are provided in Table 11.

For reasons provided in the discussion of the results, adjusted model 12 was chosen to be used in further simulations, and will be referred to as the “*calibrated model*” in all further discussions.

Table 11 - MAPE Calculation for Selection of Calibrated Model

Model	MAPE (%)			
	Duration	Dry Mass Reduction	Temperature	Mean
Theoretical	12.61	22.65	3.11	12.79
Adjusted 1	6.34	43.22	2.83	17.46
Adjusted 2	7.24	8.56	2.77	6.19
Adjusted 3	6.07	9.82	2.46	6.12
Adjusted 4	13.61	22.86	3.13	13.2
Adjusted 5	5.88	32.57	2.82	13.76
Adjusted 6	8.78	1.75	2.84	4.57
Adjusted 7	6.67	11.4	2.53	6.87
Adjusted 8	14.29	23.13	3.22	13.54
Adjusted 9	6.79	23.10	2.82	10.90
Adjusted 10	9.65	4.08	2.87	5.53
Adjusted 11	7.26	13.16	2.52	7.65
Adjusted 12	4.95	3.89	2.71	3.85

3.3.2 Model Verification

To verify that the calibrated model was able to simulate other batches, it was tested with data from the remaining batches that were processed between October 1995 and December 1996. Input parameters were used from the field data where available. A summary of model inputs and sample calculations are provided in Appendix B.

The ambient temperature is important in these simulations because of its influence on cooling efficiency. The ambient temperature is not recorded by the reactor control system, therefore when setting up the input parameters for each of the runs, an ambient temperature

consistent with seasonal expectations was selected.

The model accounts for daily temperature variations by a sinusoidal ambient temperature profile. The ambient temperature which is input to the model is the peak temperature of the daily profile. Peak daily temperatures were based on seasonal approximations for Southern Ontario. The ambient temperatures used for each batch are outlined in Table 12.

Table 12 - Ambient Input Temperatures

Batch ID	Start Date [‡]	Ambient Temperature (K)
1	05-10-95	288
3	04-11-95	280
27	12-06-96	298
38	09-08-96	303
47	16-10-96	288
54	12-11-96	280

[‡] (dd-mm-yy)

The comparative results of each of these simulated batches are outlined in Table 13. Figures 20 to 25 compare the observed and predicted temperature profiles for the simulations.

Quantitative comparison of the observed versus predicted temperature profile, dry mass reduction and overall duration for each simulated batch are provided in the form of Mean Absolute Percentage Error (MAPE) in Table 14. Table 15 contains Mean Absolute Error (MAE) of the temperature data for each of the process stages and for the entire simulation

Table 13 - Comparison of Predicted to Observed Batches

Batch ID	Observed			Predicted		
	Mass Reduction (kg _{dry})	Duration (h)	Final Water content (%)	Mass Reduction (kg _{dry})	Duration (h)	Final Water content (%)
1	2661	242	44	4199	195	66
3	1561	268	48.5	3097	210	74
27	-	168	-	4883	180	61
38	-	175	-	3741	168	61
47	-	138	-	6079	223	79
54	-	182	-	4187	197	79

Table 14 - MAPE Comparison of Simulated Batches

Batch Number	MAPE (%)			
	Dry Mass Reduction	Final Moisture Content	Process Duration	Temperature Profile
1	36.6	50	24.10	2.16
3	49.8	34.5	21.64	2.25
27	-	-	6.67	3.1
38	-	-	4.17	1.84
47	-	-	38.12	2.16
54	-	-	7.61	1.31

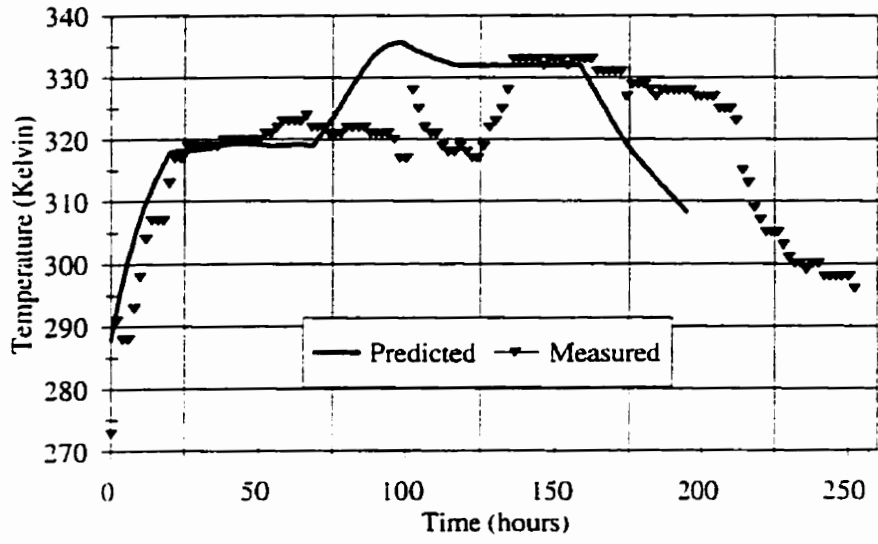


Figure 20 - Temperature Profile Comparison, Batch 1

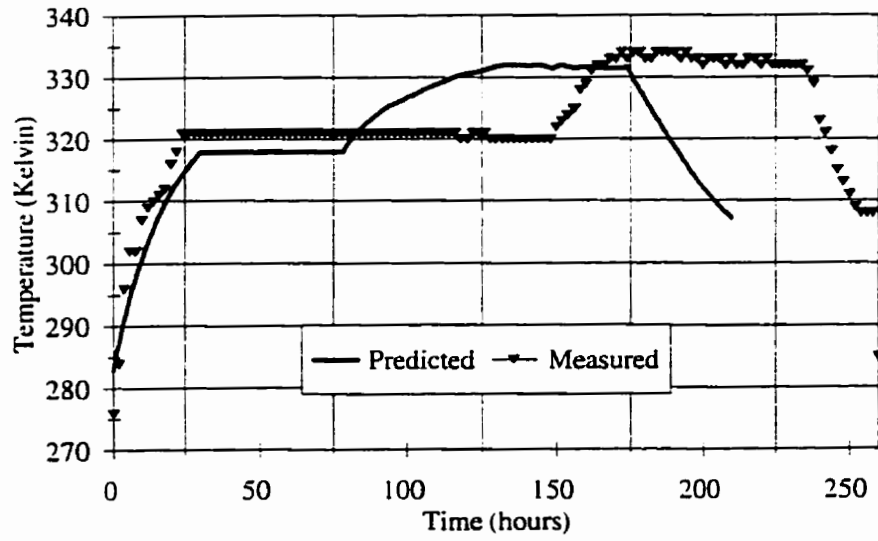


Figure 21 - Temperature Profile Comparison, Batch 3

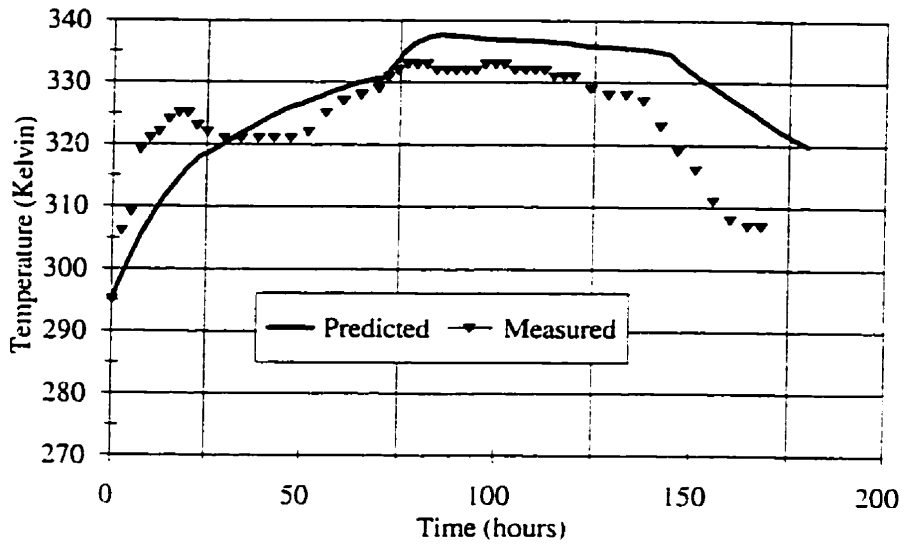


Figure 22 - Temperature Profile Comparison, Batch 27

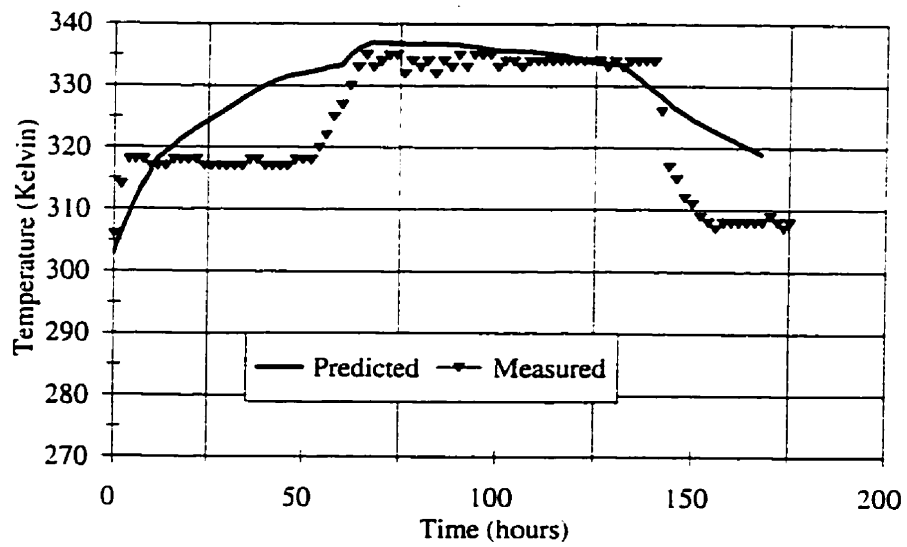


Figure 23 - Temperature Profile Comparison, Batch 38

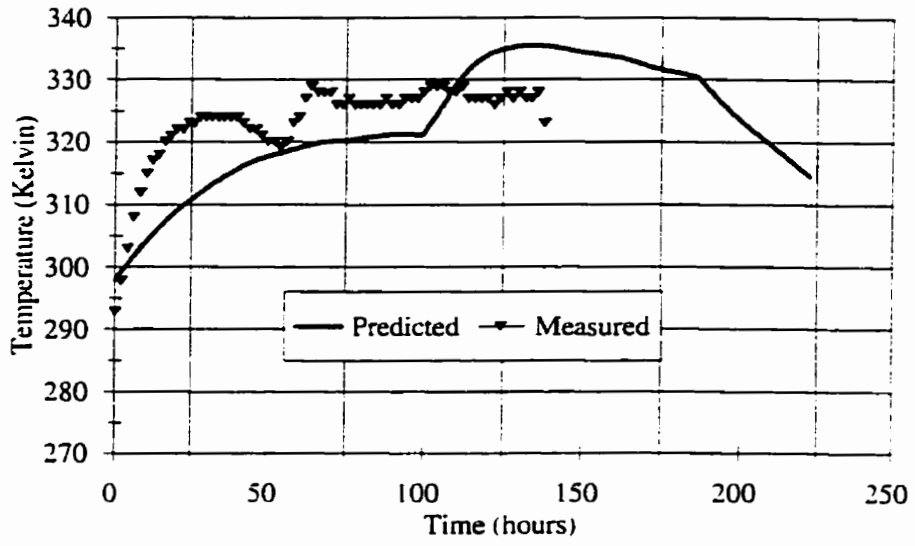


Figure 24 - Temperature Profile Comparison, Batch 47

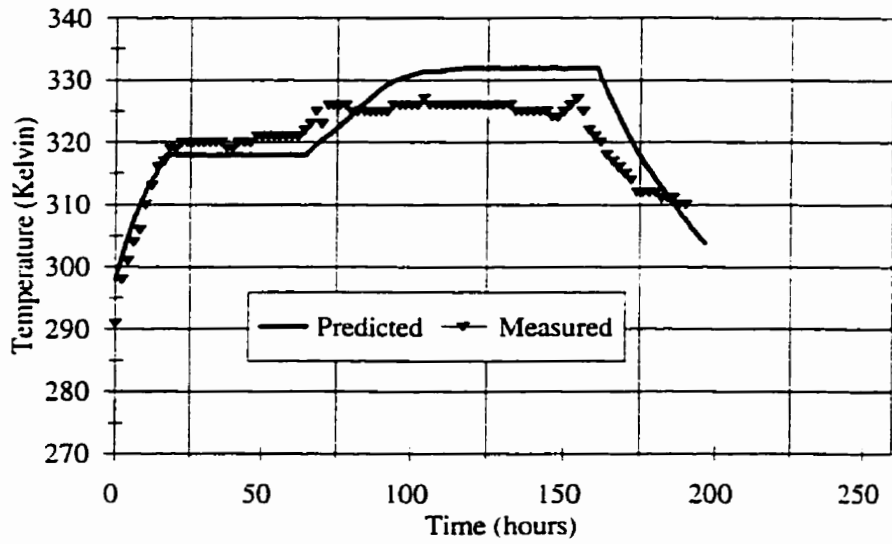


Figure 25 - Temperature Profile Comparison, Batch 54

Table 15 - Calculated MAEs for Temperature Profiles

Batch	Mean Average Error (K)				Batch Mean
	Stage 1	Stage 2	Stage 3	Stage 4	
1	8.3	1.7	7.8	11.1	7.2
1 (shifted)*	8.3	1.7	7.2	4.3	5.4
3	4.9	3.0	6.8	16	7.7
3 (shifted)*	4.9	3.0	5.2	10.1	5.8
27	9.0	2.8	5.2	17.2	8.6
38	5.1	9.3	2.2	9.7	6.6
47	8.7	5.5	6.2	n/a	6.8
54	2.8	2.2	5.3	5.1	3.9

*shifted temperature profiles are examined in the discussion of results section.

3.3.3 Simulations of Extreme Conditions

Another measure of the usefulness of a model is its ability to perform as expected under conditions that vary from those that it was originally designed to operate under. In order to test this aspect of the model, four scenarios were selected:

- extreme ambient conditions (high and low)
- very high volatile organic content
- very low volatile organic content

The parameters used in creating these scenarios were outlined in Table 8. The results of these simulations cannot be compared quantitatively since there is no available field data for these 'batches'. However, based on knowledge of the composting process, the results of the simulations can be compared conceptually to what behavior would be expected in the physical system under these conditions. The simulated temperature, CO₂, and O₂ concentration, and mass reduction profiles are illustrated in Figures 26 through 29.

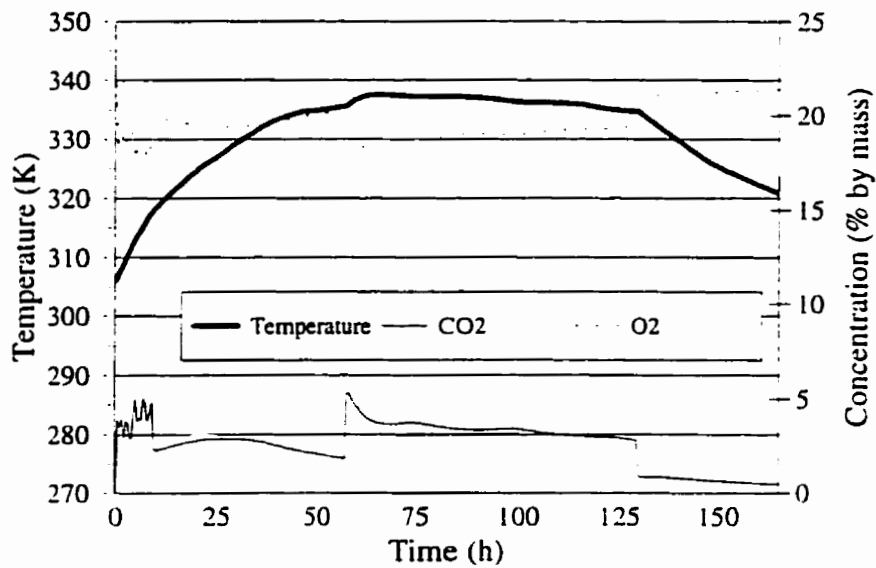


Figure 26 - Reactor Environment Profiles, High Ambient Temperature

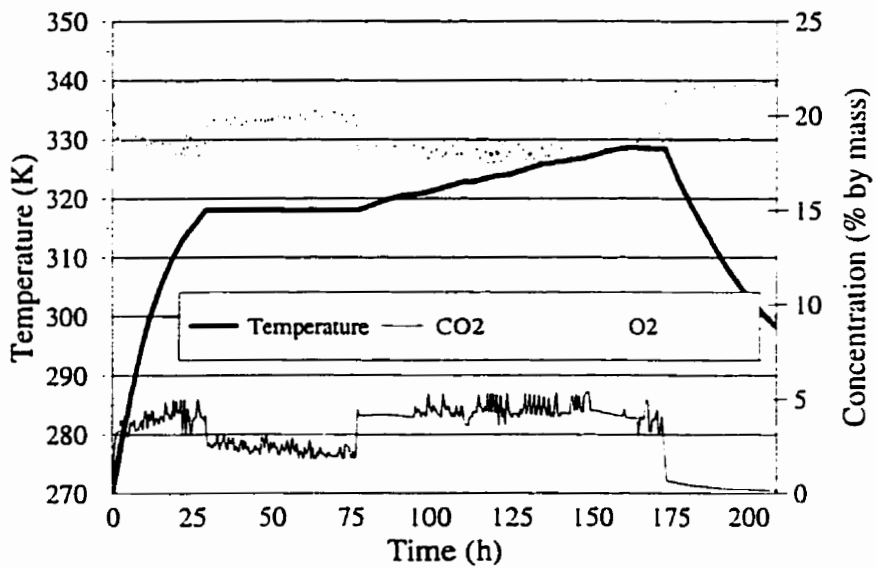


Figure 27 - Reactor Environment Profiles, Low Ambient Temperature

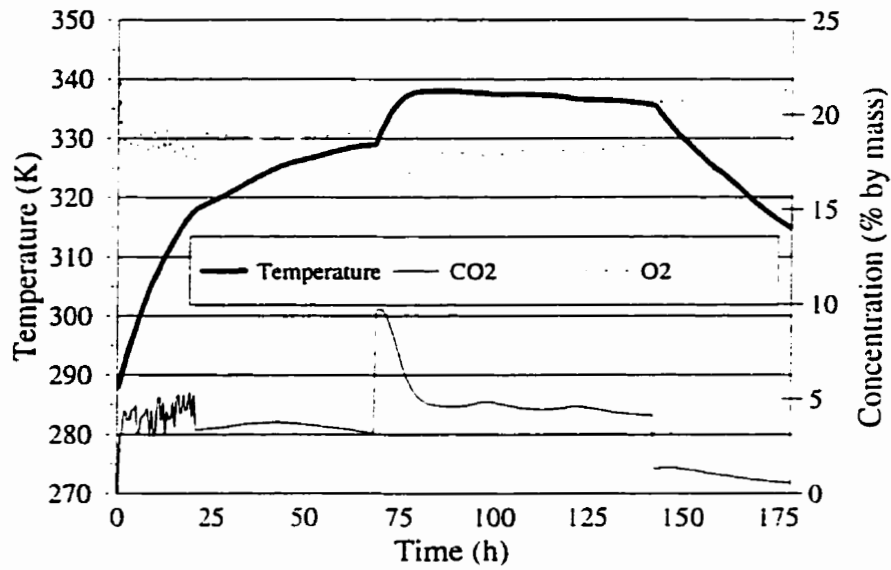


Figure 28 - Reactor Environment Profiles, High Fast Degradable Content

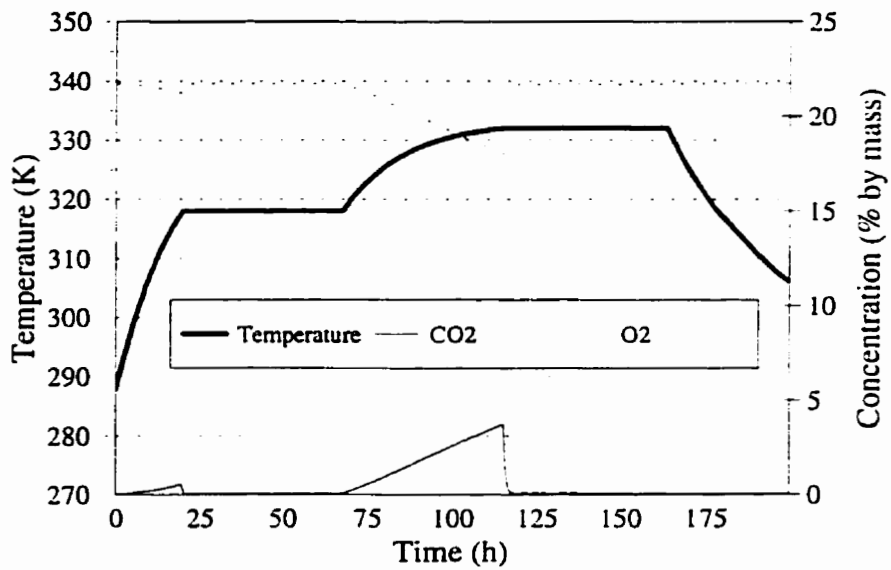


Figure 29 - Reactor Environment Profiles, High Slow Degradable Content

3.4 Discussion of Modelling Results

In order to select a calibrated model, each of the 12 adjusted models were compared based on their ability to approximate the observed data. Indicators that were the basis of comparison between the predicted and measured results were temperature profile, mass reduction and phase duration. Temperature profile comparisons were shown in Figures 5 through 17, mass reduction was compared in Figure 19 and an overall duration comparison was shown in Figure 18.

To provide an overall quantitative measure of the ability of each of the adjusted models to predict these parameters, the Mean Average Percentage Error values are compared in Table 11. It can be seen in Table 11 that Adjusted Model 12 provides the most acceptable overall fit between predicted and observed data. Based on this, Adjusted model 12 was selected as the calibrated model and used in all further simulations .

In order to compare the performance of the calibrated model to the results observed for the remaining batches, each of the 'performance parameters' is discussed individually.

3.4.1 Temperature Profile

Heat generation is a key indicator of biological activity that can be related to rate of degradation. As well, the ability to model the highly controlled aeration system is strongly indicated by the predicted and observed temperature profiles. Based on this, the closeness

of the fit between the predicted and observed temperature profiles are perhaps the best indicator of the ability of the model to simulate the physical system.

A quantitative measure of fit between the observed and predicted data is the Mean Absolute Error (MAE), given in Table 15. The ability of the model to predict the observed data can also be examined qualitatively by comparison of the predicted and observed temperature profiles. Examination of the Figures 20 through 25 provide a good illustration of this comparison.

The MAE values for each Phase give the average error, in absolute terms, between the observed and predicted temperature at each point. The absolute error was then averaged over the Phase, allowing determination of which batches, and which phases, have the greatest error associated with them.

Shown in Figures 20 and 21, the temperature profiles for Batches 1 & 3 illustrate some agreement in general shape between their observed and predicted temperature profiles. A large source of discrepancy in these two simulations is due to the fact that in both cases the physical system was not operating properly, and that Phase 2 was allowed to continue much longer than the prescribed 48 hours. In Batches 1 and 3, the second phases were 84 hours and 112 hours long, respectively. It can be seen from examination of the Figures 20 and 21, and from the MAE values reported for the 'shifted' temperature profiles, that excellent agreement is obtained between the profiles if the 'extension' of Phase 2 is discounted.

Examination of Figure 22 shows that the temperature profiles described by the model and the physical system are similar in that they both had difficulty maintaining the temperature setpoint in Phase 2. However, comparison of the rate of temperature changes in Phases 1 and 4 does not indicate good agreement for this batch. The differences between the predicted and observed temperature profiles appear to indicate more degradation activity in the model than in the physical system. This can be attributed to the fact that the model assumes that the system is uniformly mixed and each particle of substrate is equally available for breakdown. It is likely that the physical system still has areas or 'pockets' of substrate that are not degrading due to lack of oxygen, moisture or nutrients. Based on this, the model would seem to have more volatile solids available than the physical system, and would still be actively degrading and producing heat. This inhibits the cooling in the temperature profile predicted by the model, resulting in higher MAE values.

Examination of the temperature profile for Batch 38 also shows that there are differences between the observed and predicted temperatures for Phases 1 and 4. However, in Phase 2 the ideal conditions in the model result in very efficient degradation and therefore increased heat production. Although this is the case for all simulations, combined with less efficient aeration due to high ambient temperature, the difficulty in maintaining the setpoint in Phase 2 is not unexpected. Although the same response is expected in the physical system, both the temperature profile and the dry mass reduction data indicate that there was much less degradation activity in the physical system than in the simulated system, resulting in lower overall heat production.

It is apparent by looking at Figure 24 that the model has some difficulty reaching the setpoint temperature of 318K in Phase 1. It should be noted that the mass of substrate in Batch 47 is of the order of 35 tonnes. This much larger batch takes longer to warm to the setpoint temperature because of the assumption of uniformity used in this model. However, when higher temperatures are reached, the degradation proceeds rapidly. The production of CO₂ associated with this quantity of mass reduction is quite high. For this reason, aeration of the reactor is almost continual and setpoint temperatures are hard to maintain. Comparison of the model predicted data to the measured data for Batch 47 supports this trend. Recall that Batch 47 was removed from the reactor before the end of Phase 3, due to the fact that the reactor temperature never reaches the setpoint of 333K.

Examination of Figure 25 shows the best match between predicted and measured conditions. Batch 54 was processed in November, meaning that cool ambient air provided efficient cooling of the reactor when required. The processing of Batch 54 also was much later in the operation of the field system, when operations were much more stable and the reactor was operating as intended. So, it seems that when the control system in the field is operating most efficiently, there is much better correlation between predicted and observed results.

3.4.2 Comparison of Dry Mass Reduction

One of the most important measures of the performance of a composting system is dry matter reduction. The MAPE values for dry mass reduction, shown in Table 14, were 36.6% and 49.8%. This indicates that the model was not accurate in predicting the mass reduction over

the process. Unfortunately, output mass data is only available for two of the batches used for simulation. The batches for which output mass data is available are early in the operation of the system, when the process was not yet stable. The reason for selection of the later batches, even though none of them have output data available, is that the system was running fairly consistently as designed.

As shown in Table 13, in both cases the reduction predicted was much higher than was achieved in the field. As discussed previously in reference to the temperature profiles, this is a result of the fact that the model is based on a number of assumptions that result in optimum performance. The reactor itself was modeled as a CFSTR, meaning that it was assumed that all conditions within the reactor were uniform and all contents were uniformly mixed, including thermal energy, oxygen, moisture and nutrients. In reality, it is likely that the field system contains pockets of anaerobic conditions, thermal deactivation, clogging of pore space by excessive moisture or compaction, and dry of areas of biomass. In particular, the substrate in the Caledon system often had low moisture content and a great deal of clumping. These less than ideal conditions would result in a less efficient breakdown of the substrate, and were not accounted for in the model. For this reason, it is clear that the model will over-estimate both the mass reduction and the thermal energy production in the system.

3.4.3 Comparison of Final Moisture Content

As shown in Table 13, the final moisture content of the substrate is estimated to be higher than it was measured in the field. The MAPE values of 50% and 34.5% indicate that the

model was unable to reliably predict moisture content. This is a result of over-estimation of degradation by the model and of differences in the water balance over the field and simulated systems.

In both the field and simulated operation, condensate is collected from the aeration air during recycling. Both systems then return the condensate to the reactor, but the field system also collects leachate through the bottom of the reactor, and it is not entirely recycled. Originally it was intended that this leachate removal be recorded and taken into account in the water balance on the system. However, the flow meters that were installed to record this data were easily clogged by the suspended solids in the leachate and had to be removed.

Readings that were taken when the meters were operational indicate that a range 2-7 m³ of leachate accumulated over the cycle. Inclusion of this quantity of removed leachate in Batches 1 and 3, which included observed moisture content data, could account for 90% and 60% of the excess moisture predicted for batches 1 and 3, respectively.

3.4.4 Comparison of Process Duration

The results shown in Table 13 indicate that the process duration predicted by the model is not often in agreement with the observed values. In some cases, the observed duration is longer than the predicted, while in others it is shorter. Examination of Table 14 shows a variability in agreement between the physical system and the model, with MAPE values ranging from 4.2% to 38.1%. However, when examined closely it is apparent that this is

often due to the fact that the physical system did not consistently follow the control guidelines while the model did. As previously discussed, Batches 1 and 3 remain in Phase 2 of the process for well over the prescribed 48 hours. Inspection of the temperature profile for Batch 1, shown in Figure 20, illustrates that the trend of the predicted temperature profile is very similar to the measured data, with the exception of this shift of 36 hours. If we discount this extended time, it can be seen that the duration of the field system would be approximately 206 hours, which is much closer to the predicted length of 195 hours. Similarly, for Batch 3, comparing the temperature profiles shows that the profiles are very similar with the exception of the shift caused by the extension of phase 2. Again if we discount this extension of Phase 2, the measured duration would be approximately 202 hours, which compares much more favorably to the predicted duration of 210 hours.

The only other batch which has difficulty predicting process duration is Batch 47. It must be noted that Batch 47 was removed from the system at the end of Phase 2, thereby shortening its expected duration. If the process were allowed to go to completion, adding in Phase 3 and 4 the total duration would be approximately 246 hours which is closer to the predicted length of 223 hours.

When considering modelling results, it is important to consider the difficulty of simulating a full-scale MSW composting facility. The variability of the substrate between regions is significant as are the variations between batches of waste collected from the same location. The variability of within substrate pile is also significant, resulting in great difficulties in

establishing acceptable degradation rates and substrate composition for application in the model. For this reason, a model calibrated to a single data set that compares reasonably well to other data sets is significant.

3.5 Extreme Condition Simulations

The simulations of the extreme conditions as previously mentioned, are discussed individually below. The individual parameters used to in these simulations are outlined in Table 8.

3.5.1 High Ambient Temperature (305 K)

It is clearly illustrated in Figure 26 that when ambient temperatures reach 305 K, the reactor has difficulty maintaining setpoint temperatures. In fact, the typical “two-plateaus” that are expected with this control system are barely recognizable. The duration of the entire cycle becomes much shorter due to faster heating times.

The CO₂ and O₂ profiles shown in Figure 26 indicate that there is almost continual aeration through the system in an attempt to keep it cool. This is indicated by the fact that there are very few peaks or oscillations in these profiles. The high temperatures seen here indicate accelerated production of CO₂ and consumption of O₂, but continual aeration maintains these constituents at acceptable levels.

Comparison of these results with the observed data of batches 27 and 38, that were processed

in the summer, does not indicate the same temperature difficulties that the model exhibits. Batch 27 has some difficulty maintaining the setpoints, but batch 38 appears to have no difficulty, even though the ambient temperature was assumed to be 303K. This is another symptom of the fact that the model operates more efficiently than the physical system, resulting in increased degradation and therefore greater heat production. However, the results of the simulation indicates that this type of operating condition could have important implications for the use of Herhof Bioreactors in higher temperature climates. Hot, dry climates could provide increased cooling through evaporation of moisture, but operation of the Herhof system in hotter climates is likely to require additional cooling of aeration air and will result in excessive drying of the substrate.

3.5.2 Low Ambient Temperature (270 K)

The case of low ambient temperature is presented in Figure 27. It is clearly shown by the temperature profile presented that the model has difficulty attaining the setpoint temperature in Phase 3. In this phase, where the higher rate of degradation is taking place, the system is required to aerate solely to reduce the CO₂ concentration in the reactor. This results in cooling of the substrate, and the system *never* attains the 333K setpoint. Therefore the system should be closely monitored in cold weather to ensure that the important 333K setpoint is reached. If it is not attained, the system will not provide the necessary destruction of pathogens and some pre-heating of the aeration air may be required to ensure the quality of the end-product.

3.5.3 High Levels of Fast-Degrading Volatiles (100%)

This situation is akin to processing a batch of waste that is almost entirely food waste or grass clippings. The profile produced from this type of input is illustrated in Figure 28. The temperature profile shown here indicates that because of the readily available volatile solids source, degradation begins rapidly and the reactor is unable to maintain the Phase 2 setpoint because of all the thermal energy being generated as a result of degradation. Also shown in Figure 28 is a dry mass profile. It can be seen from this profile that the mass reduction begins immediately and the mass profile falls smoothly throughout the process.

3.5.4 Low Levels of Fast-Degrading Volatiles (100%)

Shown in Figure 29, the case of very low levels of fast-degrading volatiles could occur if the substrates were comprised mostly of lignins, such as papers and woody materials. The temperature profile shown in Figure 29 is almost entirely as expected. The reactor warms relatively slowly and has an extremely flat plateau in Phase 2 at 318K. Perhaps most surprising in this temperature profile is the slight over-shoot at the commencement of Stage 3. This is a result of the assumption in the model that the reaction adapts to the available sources so that slow-degraders degrade more quickly in Stage 3 than in Stages 1 and 2. Also contributing to the over-shoot is the fact that since there has been negligible mass reduction to this point in the process, the remaining mass of volatiles is relatively high. Since the degradation rate is also mass-dependent, this will contribute to a higher degradation rate. The dry mass profile shown in Figure 29 further illustrates this trend. The level of degradation in Phases 1, 2 and 4 are negligible, while an increased mass reduction is shown

in Phase 3.

Based on the preceding discussions, it is apparent that the model is able to simulate the system reasonably well, and provides the response that is expected in the physical system when used to simulate alternative or extreme conditions.

4.0 COMPOST QUALITY

The primary goal of a MSW composting facility is to transform waste into a useable soil amendment. For this reason, the quality of the end-product including nutrient value, metals and moisture content, is extremely important. To obtain the MOEE Certificate of Approval for the MSW composting facility located at Caledon Sanitary Landfill, a determination of compost quality was required.

Samples of inbound, outbound and mature compost were collected and analyzed in-house by the Caledon Sanitary Landfill and the results are summarized in Tables 16a and 16b. The inbound samples were collected for the entire day at less than one hour intervals at the end of the loading conveyor. These samples were then mixed and quartered to promote homogeneity. The outbound waste was sampled in the same manner. A total of ten samples were collected at regular intervals as the biocell was unloaded. The mature, screened compost samples were collected from the windrows using the composite sampling procedure developed by Otten and Halet (1995). Analysis was performed for heavy metals, nutrients, minerals and contaminants by Zenon Environmental Laboratories (October 3, 1995 - November 28, 1995); Novamann International (January 9, 1996 - November 14, 1996), and Canviro Analytical Laboratories (December 4, 1996 - January 28, 1997). Further detail regarding analytical methods and results can be found in the report authored by Otten (1998).

The results and findings of the report were submitted to the MOEE on June 24th 1995 and

are summarized here for completeness.

Table 16a - Statistical Summary of all samples submitted for analysis

COMPOSITION PARAMETERS	INBOUND			OUTBOUND			COMPOST	MOEE
	N	AVE	STD	N	AVE	STD		
METALS (ppm)								
Aluminum	16	3831	1745	8	4156	936		
Arsenic	49	3.5	1.7	47	3.9	2.1	2.7	< 10
Barium	16	45.6	8.5	9	49.4	8.8		
Beryllium	16	0.16	0.07	9	0.16	0.05		
Boron	16	15.4	4.9	9	17.6	4.1		
Cadmium	49	0.57	0.93	47	0.38	0.16	< 1	< 3
Chromium	49	12.7	9.3	47	11.7	3.4	8.9	< 50
Cobalt	49	4.1	1.3	47	4.0	1.1	< 5	< 25
Copper	49	24.6	10.6	47	24.1	8.2	17	< 60
Iron	16	7219	2632	9	7900	1301		
Lead	49	14.1	7.6	47	13.2	4.6	12	< 150
Manganese	16	241	60.7	9	252.2	28.6		
Mercury	48	0.06	0.04	47	0.08	0.09	0.04	< 0.15
Molybdenum	49	1.1	1.05	47	0.87	0.32	< 2	< 2
Nickel	49	7.6	5.1	47	7.4	2.1	6	< 60
Selenium	49	1.5	0.9	47	1.6	0.9	< 1	< 2
Silicon	16	120	55.3	9	158.1	105.3		
Silver	16	0.5	0	9	0.5	0		
Sodium	19	1753	1096	11	975	290.6	760	
Strontium	16	60.5	8.4	9	65.8	7.4		
Thallium	16	20	0	9	20	0		
Tin	16	5.6	2.2	9	5	0		
Titanium	16	97.9	42.0	9	104.7	20.1		
Vanadium	16	12.1	2.9	9	11.8	1.5		
Zinc	49	86.4	27.0	47	92.3	65.4	58	< 500
Zirconium	16	5	0	9	5	0		

N.D. Not detected at a method detection limit of 3.2 nanograms/gram

Table 16b - Statistical Summary of all samples submitted for analysis (cont.)

COMPOSITION PARAMETERS	INBOUND			OUTBOUND			COMPOST	MOEE
	N	AVE	STD	N	AVE	STD		
NUTRIENTS (% d.b.)								
Total Carbon	46	27.5	8.1	4e+34	20.8	5.5	11.2	> 0.60
Total Nitrogen	49	1.39	0.57		1.29	0.49	0.52	< 22
C/N Ratio	44	18.4	7.0		17.0	7.0	21.5	
MINERALS (% d.b.)								
Calcium	49	4.18	2.27		4.47	1.89	5.9	> 3.0
Magnesium	49	0.48	0.14		0.56	0.16	1.2	> 0.30
Phosphorus	49	0.26	0.10		0.25	0.08	0.18	> 0.25
Potassium	49	0.85	0.31		0.91	0.34	0.40	> 0.20
Sulphur	10	0.17	0.03		0.17	0.03		
SALINITY								
SAR (ppm)	48	3.32	2.94		3.70	3.57	3.7	< 5
Conductivity (mS/cm)	46	5.44	1.59		4.98	1.31	4.5	< 3.5
Chlorides (ppm)							1860	
Sulphates (ppm)							340	
OTHER								
Ash (% d.b.)	49	51.3	14.8		60.4	12.0	85	> 30
Organic Matter (% d.b.)	29	56.5	13.1		45.7	9.8	17	30 - 55
Moisture Content (% w.b.)	57	53.3	9.8		41.8	12.2		5.5 - 8.5
pH (20°C)	49	6.35	0.88		7.00	0.57	8.1	> 300
WHC (% d.b.)	8	413	36.7		198	60.7	61	
CONTAMINANTS								
Plastics (% d.b.)	29	0.1	0		0.1	0.09	< 1	< 1.0
Other Inert (% d.b.)	8	0.1	0		3.1	3.93	< 1	< 2.0
Total PCBs (ppm)	29	0.26	0.48		0.09	0.06	N.D.	< 0.5

N.D. Not detected at a method detection limit of 3.2 nanograms/gram

The findings of the report include the following:

- Heavy metal concentrations in the inbound and outbound waste were well within the acceptable guidelines given by the MOEE, with few exceptions
- Heavy metal concentrations in the cured compost, shown in the second last column of Table 16, were all well below MOEE guidelines
- C/N ratio and moisture content were typically in the optimum range for efficient high-rate degradation

Otten (1995) concludes that sampling and analysis should be undertaken every two months

as required by MOEE guidelines unless significant changes are observed in the inbound waste or the analytical results. It was also recommended that the matured, screened compost be sampled every 500 tonnes. These recommendations were approved by the MOEE and the Certificate of Approval was extended.

5.0 EMISSIONS MONITORING

An odour emission test program was developed to comply with Section 5 of the Certificate of Approval (Number 8-3386-94-006) issued for the MSW facility located at Caledon Sanitary Landfill.

The source testing program consisted of two techniques. The first involved the use of a qualified odour panel. These tests were conducted in November 1995 by Ortech Corporation and the report was submitted to the Region of Peel in January 1996. The second technique involved the analytical measurement of dimethyl sulphide (DMS) and dimethyl disulphide (DMDS) concentrations in the exhaust stream. The rationale for this test is the fact that these two compounds are always present in composting off-gases when odour problems are observed. Therefore it is thought that these compounds could be used as indicator compounds to measure potential odour problems. The major potential benefit of this method would be to allow continuous monitoring of the odour compounds by using an on-line chromatograph as part of the composting process control system, eliminating the need for expensive odour panel testing.

The objectives of the analytical monitoring program are as follows;

- (1) develop a protocol for sampling and analysis of the exhaust stream; and
- (2) determine if significant odours are being produced at the Caledon site

5.1 Methodology

For this study, a methodology was developed for sample collection and analysis. Some additional analyses were also performed to improve confidence in the results. These different aspects of the study are described below.

5.1.1 Sampling Protocol

Samples were to be collected and analyzed approximately monthly for one year. Samples were collected at the initiation of the fourth phase of the composting cycle. This particular time was selected because phase four is the transition from high-rate degradation to the cooling/drying phase prior to unloading of the digesters. It is the only phase during which there is any significant exhaust to the atmosphere, and it was determined that this part of the process presents the greatest risk of odour problems.

5.1.2 Sample Collection

The gas samples were taken from sample ports drilled in the stack of the biofilters. These ports are located 0.5m upstream of the nearest disturbance in accordance with Ministry of Environment and Energy (MOEE) regulations for air sampling. The sample, drawn by an AirCheck™ sample pump at a rate of 2.5 litres/minute, was bubbled through an impinger of phosphoric acid desiccant and a moisture trap before collection in a Tedlar™ bag. Two 5 L Tedlar bags were filled from each sample location, namely, after the biofilter, before the biofilter but after the condenser, and before the condenser. The bags were kept cool and in darkness while being transported to the laboratory at the University of Guelph for analysis.

5.1.3 Sample Analysis

The off-gas samples collected at the site were analyzed on an SRI™ Gas Chromatograph (GC) equipped with a Photo-Ionization Detector (PID) immediately upon return to the laboratory. The complete set of samples were analyzed within 6 hours of collection.

Chromatography is a method for separation of closely related compounds. Samples must either be in gaseous form, or vaporized before passing into the sample column. The sample is carried by an inert 'carrier gas' through a rigid packed column. The affinity of each of the compounds for the packing material varies and results in different rates of passage for each compound through the column. When the compound emerges from the column, it is detected in this case by a Photo-Ionization Detector (PID). The PID operates by ionization of the gas with ultraviolet radiation. The current flow between the two detection electrodes is caused by this ionization, and gives a 'peak' on the chromatograph whose area is related to the quantity of the compound vaporized. The GC-PID settings used in this study are detailed in Table 17.

Table 17 - GC-PID Settings

Parameter	Setting
Column Type	Supelco SPB-1, length: 15 m internal diameter: 0.53 mm
Column Flow Rate	5.0 mL/min
Column Temperature	323K for 0 - 2 minutes, Ramp to 353K at 20K/minute
Carrier Gas	Ultra High Purity Helium
Injector Temperature	373K
PID Lamp Current	85 amps
Run Time	5.0 minutes

Fresh gas standards were prepared for each sampling event. The standards were prepared by dissolution of known concentrations of liquid DMS and DMDS in liquid methanol. The appropriate quantity of this mixture was then injected into a 5.0 litre Tedlar bag filled with nitrogen to make target gas concentrations of 0.1, 0.5, 1, 5 and 10 ppm (by volume) of DMS and DMDS.

Calibration lines were constructed from the resulting peak areas from each of the standards. The typical calibration curve in Figure 30 shows that the relationship between the concentrations and peak areas are not linear over the entire range. For this reason, a regression analysis was applied to each of the linear segments to yield a more accurate relationship between peak area and concentration within each range. The ranges selected were 0-0.5 ppm, 0.5-1.0 ppm and 1-5 ppm. The regression results are found in Appendix D.

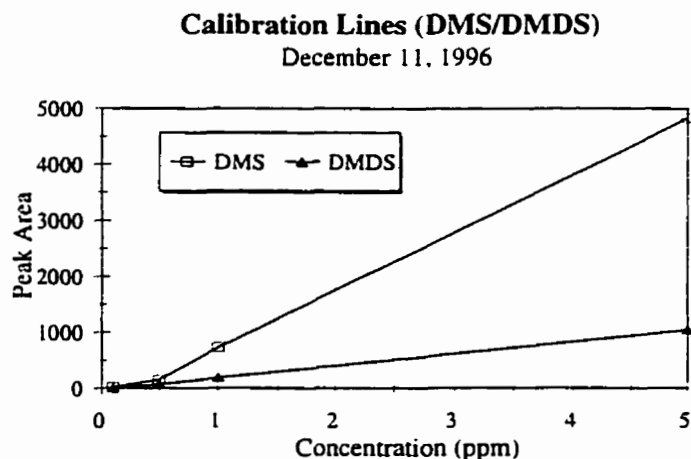


Figure 30 - Sample Calibration Lines

5.1.4 Limits of Detection/Limits of Quantification

Laboratory analysis is limited by the accuracy of the analytical equipment. For this reason, when reporting low concentration analysis data, it is also normal to report the limits of detection (LOD) and limits of quantification (LOQ). In essence, the LOD is the amount that is considered to be statistically different from a blank and is typically determined by the sensitivity of the analytical equipment, in this case the GC-PID. Often, the LOD is set at *three* times the standard deviation (SD) greater than the mean of the blank. Typically the background noise associated with a blank is normally distributed, and three SDs results in >99.8% confidence that a value measured above the LOD is not due to background noise. In the case where the noise in the blank is not normally distributed, the confidence is still >89% (Kuehl, 1994; Solomon, 1995).

The LOQ is the smallest concentration which can be assigned a numerical value with confidence. This value is greater than the LOD and depends on the precision of the analytical method. It is recommended that the LOQ is taken to be *ten* times the standard deviation greater than the mean of the blank.

Values below the LOD or LOQ are still included in reported results. In practice, responses below the LOD are reported as 'not detected' (ND). Values between the LOD and the LOQ can be reported as numerical values, but should be marked with LOD in parentheses. This will indicate that a response is observed and measurable, but confident quantification is not possible (Solomon, 1995).

5.1.5 Additional Analyses

Some additional analyses were performed to confirm that the results of the sampling and analysis were reliable. The first was the use of a Mass Spectrometer (MS) to determine if DMS and DMDS were actually present in the samples. The second was a simple test to determine that the desiccant used did not remove the contaminants from the sample before analysis.

Mass Spectral Analysis

Gas Chromatography is a useful method of determining the quantity of a particular compound that is known to be present in a sample. Constituents are separated in the GC based on their residence time in the column. Of concern is the possibility that two different compounds may have the same residence time. If this were to occur, there is the possibility that another compound in the sample will give a peak which is mistakenly assumed to be the compound of interest.

In order to confirm that DMS and DMDS were in fact present in the samples, a mass spectrometer (MS) was used. MS analysis is based upon the mass of the contaminant and the sequence in which the molecule breaks apart or fragments when energized. Each molecule, because of its individual structure and bonds, has a distinctive 'fragmentation pattern' which allows much more positive identification than GC analysis. Once the presence of the molecule of interest is confirmed, the GC results become more reliable.

Desiccant Tests

The use of a desiccant is common for removal of water vapour from sample streams. There are a number of liquid desiccants which are commonly used, including calcium chloride, diethylene glycol, glycerol, lithium chloride, phosphoric acid, sodium and potassium hydroxides, sulfuric acid and triethylene glycol (Lodge, 1988). In this case, phosphoric acid was chosen as the most appropriate desiccant due to its convenience, lower operating temperature range and ability to reduce moisture content to a relative humidity within 5-20%.

One of the concerns with the use of a desiccant is the possibility that the compounds of interest may be stripped when bubbling the gas stream through the desiccant. This was of particular concern in this study because of the affinity shown by DMS and DMDS for sorption to other materials. In order to ensure that this was not the case, a known concentration of 10 ppm was prepared in a Tedlar bag and passed through the phosphoric acid into a clean Tedlar bag. Both of these bags were then analyzed on the GC to determine the magnitude of losses.

5.2 Emissions Monitoring Results

The experimental LOD and LOQ values for DMS and DMDS are reported in Table 18. These are calculated from the standard deviation and the mean peak areas resulting from blank samples. The peak areas are converted to a concentration with the calibration equation, formulated from standard runs. It should be noted that since the LOD and LOQ concentration values are calculated using the calibration equations, they vary with each sampling event.

The values reported are the average for all sampling dates. Calculations are shown in Appendix D.

Table 18 - Analytical Limits

Compound	Peak Area		Concentrations (µg/L) ^a	
	LOD	LOQ	LOD	LOQ
Dimethyl Sulphide	9.6	22.3	0.178	0.406
Dimethyl Disulphide	7.86	27.9	0.127	0.462

^a Average values over all sampling events

5.2.1 Phase 4 Odour Sampling

The DMS and DMDS concentrations determined on each of the sampling dates are presented in Table 19. Sample calculations are provided in Appendix D and graphical representation of this data is provided in Appendix E.

Table 19 - Phase 4 Sampling Results

Sampling Date	Pre-Biofilter Concentration (µg/L)		Post-Biofilter Concentration (µg/L)	
	DMS	DMDS	DMS	DMDS
November 8, 1995	0.457	0.127*	0.356	ND
January 29, 1996	ND	ND	ND	ND
February 20, 1996	ND	ND	ND	ND
March 27, 1996	ND	ND	ND	ND
May 21, 1996	0.175*	ND	0.129*	ND
July 29, 1996	3.12	0.196*	0.734	0.058*
September 10, 1996	0.607	0.462	ND	0.308*
December 12, 1996	0.089*	0.058*	0.053*	0.112*

*Indicates values below LOD †Indicates below LOQ.

5.2.2 Distributed Sampling

In order to confirm the assumption that Phase 4 presents the greatest risk of odour problems, samples were taken from both phases 3 and 4 on December 9 to 12, 1996. Results of this sampling are shown in Table 20.

Table 20 - Distributed Sampling Results

Phase	Pre-Filter Concentration (µg/L)		Post-Filter Concentration (µg/L)	
	DMS	DMDS	DMS	DMDS
Initiation Stage 3	0.032 [*]	0.008 [*]	0	0
Middle Stage 3	0.212	0.177	0.14	0.001 [*]
Conclusion Stage 3	0.041 [*]	0.014 [*]	0.007 [*]	0.015 [*]
Initiation Stage 4	0.035 [*]	0.015 [*]	0.021 [*]	0.029 [*]

^{*}Indicates below LOQ

5.2.3 Mass Spectral Analysis

The mass spectral analysis confirmed the presence of approximately 27 distinct compound in both the pre- and post-filter samples taken September 10, 1996. The presence of DMDS was confirmed to 83% quality, but DMS was not identified in the sample.

5.2.4 Desiccant Test

The results of the desiccant test are shown in Table 21.

Table 21 - Results of Desiccant Tests

Source	Peak Area		Concentration (µg/L)		Percent Loss (Concentration)	
	DMS	DMDS	DMS	DMDS	DMS	DMDS
Known Standard	3469.48	9522.98	10	10	-	-
Desiccated	3079.3	8064.2	9.7	8.5	3.0%	15.0%

5.3 Discussion of Emissions Monitoring Results

The results of the MS analysis shows that DMDS was present in the exhaust gases. The lack of identification of DMS by the MS could be due to limits of the column used in the MS itself. It should be noted that the samples used for the MS tests were taken on September 10, 1996 when the GC-measured post-filter DMS concentrations were quite low. This, combined with the fact that the LOD is higher in GC analysis for DMS than DMDS, could readily explain why it was not detected by the MS analysis.

The mass losses of DMS and DMDS due to the phosphoric acid desiccant are 3% and 15%, respectively. Variations up to 20% are often observed in GC analysis, therefore it is still possible to say that the desiccant did not interfere with the results of the study.

The decision to sample consistently at the initiation of Phase 4 may appear to be in doubt when examining the distributed sampling results because the highest pre-filter concentrations of DMS and DMDS were observed approximately 25 hours into phase 3. However, it should be noted again that the release of exhaust gases to the atmosphere is very intermittent in Phase 3. Since this is a heating phase, the system may exhaust intermittently, for very

short periods, to decrease CO₂ concentration but the rate of exhaust is only of the order of 50 m³/h. At DMS and DMDS concentrations of this magnitude (< 0.5ppm), odour problems are unlikely. The reason for examining Phase 4 samples more closely is that the exhaust amounts to 1000-1500 m³/h for 36 hours. At this rate, the amount of DMS and DMDS emitted is of greater concern. It should also be noted that the Phase 4 samples were collected at the initiation of the phase, when the reactor first begins exhausting. It is realistic to assume that at this time, odours would be at their peak for this stage.

The results of Phase 4 sampling show that the concentrations of DMS and DMDS were in a number of cases below the quantification limit, and in other cases below the detection limit. To discern the potential for odour problems, it is necessary to compare these findings with published values for minimum requirements for human detection. This information is contained in Table 3 and shows that the odour thresholds for DMS and DMDS are 0.051 µg/L and 0.346 µg/L, respectively. Of the reported values from the Caledon facility, the values that are the most important are the post-filter values. The post-filter samples represent what is actually being released to the atmosphere. When considering the post-filter concentrations reported for this study, it is apparent that all of the post-filter reported values for DMDS are below the human detection limit. There were some instances where the post-filter DMS concentrations exceeded this limit, most notably on July 29, 1996 when the concentration reached 0.734 µg/L. This might initially appear to be cause for concern, however it should be noted that the samples were taken from the exhaust stack which is 0.23m in diameter. The rapid dilution achieved upon release from the stack would cause this

concentration to be reduced below the odour threshold of 0.05 µg/L long before the exhaust reached the nearest point of impingement.

The cases when the post-filter concentration of DMS was notably greater than the minimum detection limit occurred on July 29, 1996 and November 8, 1995. This is in line with expectations, as odours are typically more significant in the summer and fall months at composting facilities because of the higher proportion of grasses and leaves in the feedstock. (Haug, 1993). Comparison of these results to the odour panel tests supports this finding. The odour panel results, from testing of samples taken November 8, 1995, showed that nuisance odours were unlikely to occur. Also included in the report were dispersion calculations indicating that threshold dilution (ED_{50}) is likely to be reached within 45 metres of the source, after which there is unlikely to be occurrence of complaints.

6.0 CONCLUSIONS AND RECOMMENDATIONS

Based on the preceding studies, the following conclusions and recommendations arise.

6.1 System Modelling Study

The model developed and tested in this study shows potential to simulate actual field scale operations of the fully-automated Herhof Reactor System. When compared to the physical system in the field, the model usually exhibits the same trends and responses. For this reason, with some improvements, it will be a useful tool in approximating the response of the system to various inputs and conditions.

When tested with variable conditions such as extreme ambient temperatures and volatile solids availability, the model also exhibited the response expected. Based on the simulations performed, it is apparent that use of a Herhof System in particularly hot or cold climates could require cooling or warming of the aeration air, respectively.

The major limitations of the model include the exclusion of a pore-space correction factor and the lack of field data for determining appropriate degradation factors. The uncertainty of the degradation factors are illustrated by over-estimation of mass reduction exhibited by the model, which in turn results in overestimation of thermal energy, water and CO₂ production.

By incorporating air space, the response of the system to moisture saturation could be

observed. It should be noted that in this case leachate removal was not incorporated into the model and as a result, moisture contents predicted by the model are much higher than those observed in the field. Based on this, inclusion of a pore-space or moisture correction factor would also result in artificially low degradation rates that would not compare to the field data. So, if a pore space/moisture correction factor were included, the leachate removal would also have to be included to allow realistic comparison to field data.

For better comparison between the model and the physical system, more field data is required. Both input and exit masses and volatile solids analyses would allow more confident comparison of predicted to measured results. Data regarding the fractional components of different batches would allow the use of the multiple substrate capabilities of the model. This could account for faster and slower degrading fractions at a more complex level than can be included when the substrate is considered homogeneous.

6.2 Odour Emissions Study

Based on the analytical findings, odour problems are of little concern with the Herhof Biocells™ at the Caledon Sanitary Landfill. Measured concentrations of odour-causing DMDS are typically below human detection limits even before release from the exhaust stack. The DMS concentrations are higher than the detection limit in some cases, but atmospheric dilution would result in concentrations below the detection threshold before moving off-site. These findings are supported by the odour panel testing that was performed by Ortech Corporation.

It is noted that if odour problems occur, they are more likely to occur in the summer or fall months due to the change in feedstock. For this reason, it is recommended that the emissions be monitored more closely at these times. If odours problems are identified, manipulation of component proportions by inclusion of more slow-degrading components or second-run compost could be considered.

The results of this study are slightly limited by the detection capability of the equipment. The Limit of Quantification is below the odour detection threshold and therefore confidence in the accuracy of the *exact* value of measured concentrations is limited. For confidence in exact concentration values, more sensitive analytical equipment would be required. The findings presented here are an approximation of the potential odour problems associated with this facility.

The concentrations observed here are low enough that we can conclude that they would not be a problem off-site. However, knowledge of the dispersion characteristics of the site would also be helpful in determining what concentrations *would* cause off-site problems. It is conservative to assume that the concentration of the compounds will be diluted by an order of magnitude within 1000m of release (Heagy, 1998), but if an on-line monitoring system is used it is recommended that approximate dispersion calculations are used to determine the maximum acceptable concentration that can be released from the stack. The results provided here indicate that an on-line monitoring system would be a useful addition to the control system to provide warning of potential emissions problems.

7.0 REFERENCES

- Balling, R.C. and Reynolds, C.E. 1980. *Evaluating Odor Reduction Technologies: Model*. Journal of the Environmental Engineering Division, ASCE. Vol. 106(5): 901-906.
- Brinton, W.F. Jr., Evans, E., Droffner, M.L. and Brinton, R.B. 1995. *Standardized Test from Evaluation of Compost Self-Heating*. BioCycle. Vol 25(11): 64-69.
- Cardenas, R.R., and Wang, L.K. 1979. Composting Process. In Handbook of Environmental Engineering, Vol. 2. Ed. Wang, L.K and Pereira, N.C. The Humana Press. New Jersey. pp.269-325.
- Cho, K., Hirai, M. and Shoda, M. 1991a. *Degradation Characteristics of Hydrogen Sulphide, Methanethiol, Dimethyl Sulphide and Dimethyl Disulphide by Thiobacillus thiosparus DWSS Isolated from Peat Biofilter*. Journal of Fermentation and Bioengineering. Vol. 71(6): 384-389.
- Diaz, L., Savage, G.M., and Golueke, C.G. 1994. Composting of Municipal Solids Wastes. In Handbook of Solid Waste Management. Ed. Kreith, F. McGraw-Hill, Inc. U.S.A.
- Diaz-Raviña, M., Acea, M.J. and Carballas, T. 1989. *Microbiological Characterization of Four Composted Urban Refuses*. Biological Wastes. Vol. 30: 89-100.
- Falcón, M.A., Corominas, E., Pérez, M.L. and Perestelo, F. 1987. *Aerobic Bacterial Populations and Environmental Factors Involved in the Composting of Agricultural and Forest Wastes of the Canary Islands*. Biological Wastes. Vol. 20: 89-99.
- Finstein, M.S. 1980. *Composting Microbial Ecosystem: Implications for Process Design and Control*. Compost Science/Land Utilization. Vol. 21(4): 24-39.
- Finstein, M.S. 1992. *Composting in the Context of Municipal Solid Waste Management*. Environmental Microbiology: 355-374.
- Fricke, K. and Vogtmann, H. 1993. *Quality of Source Separated Compost*. BioCycle. Vol. 34(10): 64-71.
- García, C., Hernández, T. and Costa, F. 1990. *Color Changes of Organic Wastes during Composting and Maturation Processes*. Soils Science and Plant Nutrition. Vol. 36(2): 243-250.
- Gibson, M.J. 1995. *Biofiltration for Composting Odour Control: Laboratory Studies using Dimethyl Disulphide*. Master's Thesis, University of Guelph.

- Golueke, C.G. 1977. Biological Reclamation of Solid Wastes. Rodale Press. Pennsylvania.
- Gray, K.R., Sherman, K. and Biddelstone, A.J. 1971a. *Review of Composting, Part 1*. Process Biochemistry. Vol. 6(6): 32-36.
- Gray, K.R., Sherman, K. and Biddelstone, A.J. 1971b. *Review of Composting, Part 2 - The Practical Process*. Process Biochemistry. Vol. 6(10): 22-28.
- Hamamoto, I., Kajimoto, H., Kumagaya, T., Shiamda, T., Tamura, T. and Yoneda, M. 1979. Development of New High-Rate Composting Process of Municipal Refuse. Technical Review. (Mitsubishi Heavy Industries, Ltd.) p.136-146. (as cited in Wong, 1991).
- Harada, Y. and Inoko, A. 1980. *The Measurement of Cation-Exchange Capacity of Composts for the Estimation of the Degree of Maturity*. Soil Science and Plant Nutrition. Vol. 26(1): 127-134.
- Harada, Y., Inoko, A., Tadaki, M. and Izawa, T. 1981. *Maturing Process of City Refuse Compost During Piling*. Soils Science and Plant Nutrition. Vol. 27(3): 357-364.
- Haug, R.T. 1980. Compost Engineering: Principles and Practice. Ann Arbor Science Publishers Inc. Ann Arbor.
- Haug, R.T. 1993. The Practical Handbook of Compost Engineering. 2nd edition. Lewis Publishers, Boca Raton, Florida.
- Haug, R.T. and Ellsworth, W.F. 1991. *Measuring Compost Substrate Degradability*. BioCycle. Vol. 32(1): 56-62.
- Hay, J.C. and Kuchenrither, R.D. 1990. *Fundamentals and Application of Windrow Composting*. Journal of Environmental Engineering, ASCE. Vol. 116(4): 746-763.
- Heagy, W. University of Western Ontario, Department of Applied Mathematics. 1998. (Personal communication).
- Inoko, A. 1985. *Evaluation of Maturity of Various Composted Materials*. Journal of Environmental and Resource Quality. Vol. 18(2): 103-108.
- Jeris, J.S. and Regan, R.W. 1973a. *Controlling Environmental Parameters for Optimum Composting - I: Experimental Procedures and Temperature*. Compost Science. Vol. 14(1): 10-15.
- Jeris, J.S. and Regan, R.W. 1973a. *Controlling Environmental Parameters for Optimum Composting - II: Moisture, Free Air Space and Recycle*. Compost Science. Vol. 14(2): 8-

15.

Jiménez, E.I. & García, V.P. 1989. *Evaluation of City Refuse Compost Maturity: A Review*. Biological Wastes. Vol. 27: 115-139.

Jiménez, E.I. & García, V.P. 1991. *Composting of domestic refuse and sewage sludge. I. Evolution of temperature, pH, C/N ration and cation-exchange capacity*. Resources Conservation and Recycling, 6: 45-60.

Kubota, H. and Nakasaki, K. 1991. *Accelerated Thermophilic Composting of Garbage*. BioCycle. Vol. 32(6): 66-69.

MacGregor, S.T., Miller, F.C., Psarianos, K.M. and Finstein, M.S. *Composting Process Control Based on Interaction Between Microbial Heat Output and Temperature*. Applied Environmental Microbiology. Vol 41: 1321-1330.

MacDonald, L. 1995. Physical and Mathematical Modelling of the Composting Process. Master's Thesis, University of Guelph.

Miller, J.M. 1993. Minimizing Odor Generation. In Science and Engineering of Composting: Design, Environmental, Microbiological and Utilization Aspects: Proceedings of an International Composting Research Symposium. Ed. Hoitink, H.A., Keener, H.M. March 27-29, 1992. pp.219-240.

Nakasaki, K., Kato, J., Akiyama, T. and Kubota, H. 1987. *A New Composting Model and Assessment of Optimum Operation for Effective Drying of Composting Material*. Journal of Fermentation Technology. Vol. 65(4): 441-447.

Nobili, M.E. & Petrusi, F. 1988. *Humification Index (HI) as Evaluation of the Stabilization Degree during Composting*. Journal of Fermentation Technology. Vol. 66(5): 577-583.

Otten, L. 1998. Analysis of Inbound and Outbound Waste and Matured Compost: Caledon Composting Plant. Prepared for the Ministry of the Environment and Energy, Toronto, ON.

Otten, L. and Halet, G. 1995. Sampling of MSW Compost for Metal Analysis RAC Project 734G. Prepared for the Research and Technology Branch, Ontario Ministry of Environment and Energy, Toronto, ON.

Rix, M. 1990. Odour Emission Tests as Required by a Certificate of Approval. Report by Ortech Corporation., Mississauga, Ontario.

Strom, P.F. 1985a. *Effect of Temperature on Bacterial Species Diversity in Thermophilic Solid Waste Composting*. Applied and Environmental Microbiology. Vol. 50(4): 899-905.

Van Durme, G.P., McNamara, B.F. and McGinely, C.M. 1992. *Bench-scale removal of odor and volatile organic compounds at a Composting facility*. *Water Environment Resources*. Vol. 64(19): 19-27.

Walker, John M. 1993. Control of Composting Odors. In Science and Engineering of Composting: Design, Environmental, Microbiological and Utilization Aspects: Proceedings of an International Composting Research Symposium. Ed. Hoitink, H.A., Keener, H.M. March 27-29, 1992. pp.185-218

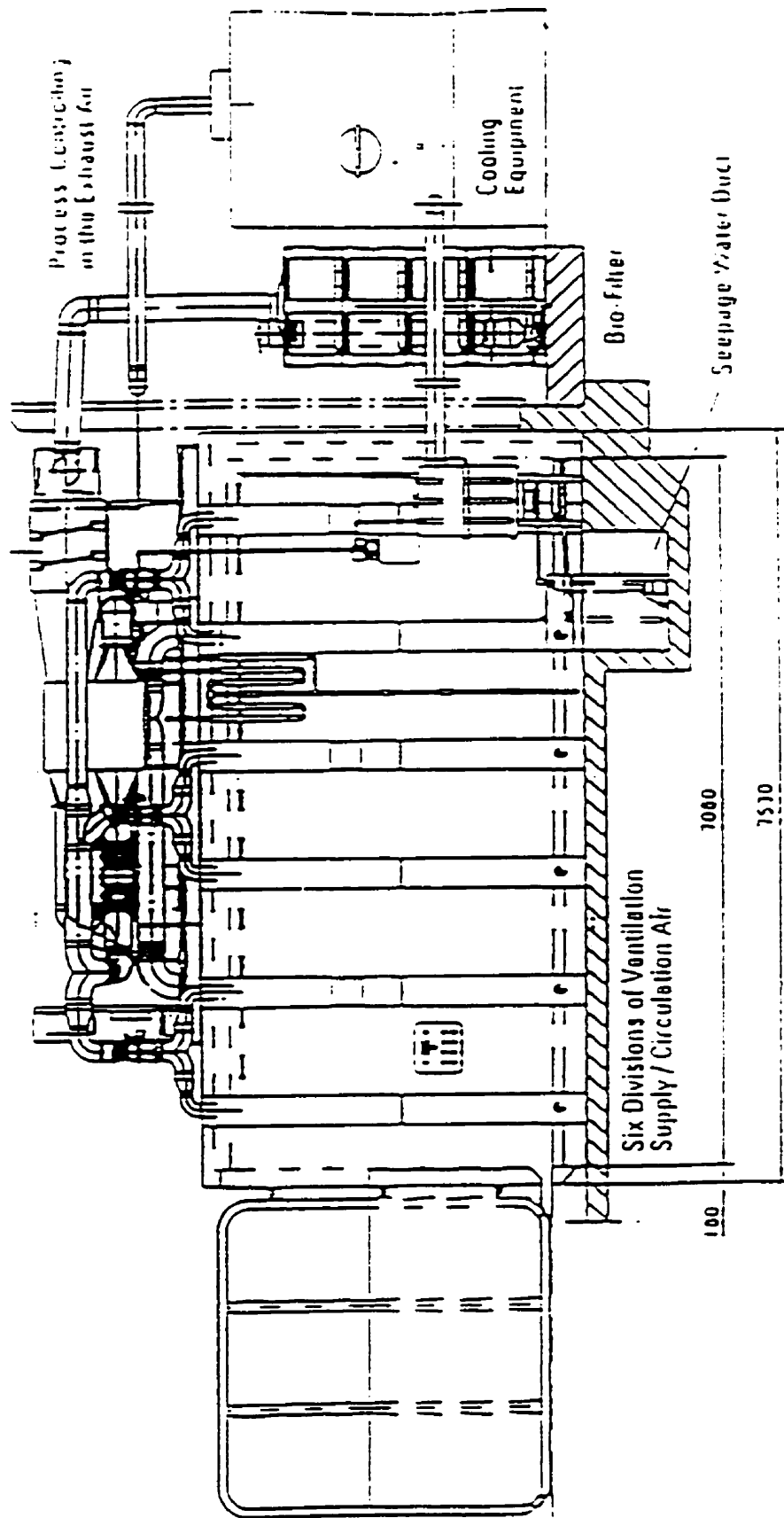
Whang, D.S. and Meenaghan, G.F. 1980. *Kinetic Model of the Composting Process*. *Compost Science and Land Utilization*, (May-June): 44-46.

Williams, T.O and Miller, F.C. Composting Facility Odor Control Using Biofilters. In Science and Engineering of Composting: Design, Environmental, Microbiological and Utilization Aspects: Proceedings of an International Composting Research Symposium. Ed. Hoitink, H.A., Keener, H.M. March 27-29, 1992. Pp. 262-281.

Wilson, G.E., Huang, J.Y.C. and Schroepfer, T.W. 1980. *Atmospheric Sublayer Transport and Odour Control*. *Journal of the Environmental Engineering Division, ASCE*. Vol. 106(2): 389-401.

Wong, William W.K. 1991. Monitoring and Composting of Source-Separated Municipal Solid Waste Using the City of Guelph's Pilot Facility. Master's Thesis, University of Guelph.

APPENDIX A - Schematic of a Herhof Biocell



- Diagram of the Herhof Biocell™

APPENDIX B - Sample Calculations: Degradation Model

SAMPLE DATA: BATCH 1

Field Data

Parameter	Input Value	Output Value
Date processed	October 5th, 1995	34988
Mass (kg)	25120	15330
Moisture Content (%)	62.68	44.19
Moisture (kg)	15745	6774

Model Input Data

*Substrate 1 Characteristics	Value
Mass (kg _{wet weight})	25120
Moisture Content (%)	62.68
Carbon Content (mole fraction)	18
Oxygen Content (mass fraction)	8
Nitrogen Content (mass fraction)	1.3
Hydrogen Content (mass fraction)	24
Rate Constant (h ⁻¹)	0.001
Specific Heat (solids) (kcal/kg-K)	1.04
Volatile Solids (mass fraction)	0.45
Fast Degrading volatiles (fraction of total volatiles)	0.3
Heat of Combustion of Substrate 1 (kJ/kg)	1500
System Parameters	
Condenser Outlet temperature (K)	333
Temperature Setpoint (phase 2) (K)	318
Temperature Setpoint (phase 3) (K)	333
CO ₂ setpoint (mass %)	0.5
Ambient Conditions	
Peak Daily Temperature (K)	288
Approximate Relative Humidity (%)	50

*Only one substrate is used to simulate the runs at Caledon Sanitary Landfill. The model currently can process up to three substrates, and is easily modified to handle more. For each additional substrate, the substrate characteristics must be provided as for Substrate 1.

SAMPLE CALCULATIONS

1. Calculate Molar Weight of Substrate:

$$MW_{\text{substrate1}} = MF_C * 12.01115 + MF_H * 1.00797 + MF_O * 15.994 + MF_N * 14.0067$$

$$MW_{\text{substrate1}} = 18 * 12.01115 + 24 * 1.00797 + 8 * 15.994 + 1.3 * 14.0067$$

$$MW_{\text{substrate1}} = 386.55269 \quad \frac{\text{kg}}{\text{kmol}}$$

2. Calculate Generation/Consumption Factors

$$G_{CO_2} = \frac{MF_C * 44.0095}{MW_{\text{substrate1}}}$$

$$G_{CO_2} = \frac{18 * 44.0095}{386.55269} = 2.04932 \quad \left[\frac{\text{kg}_{CO_2}}{\text{kg}_{\text{vs degraded}}} \right]$$

The other generation/consumption factors are calculated in the same manner:

$$G_{NH_3} = \frac{MF_N * 17.03061}{MW_{\text{substrate1}}} = 0.05727 \quad \left[\frac{\text{kg}_{NH_3}}{\text{kg}_{\text{vs degraded}}} \right]$$

$$G_{H_2O} = \frac{(MF_H - 3 * MF_N)}{2} * \frac{18.01534}{MW_{substrate}} = 0.4684 \left[\frac{kg_{H_2O}}{kg_{vs \text{ degraded}}} \right]$$

$$G_{O_2} = \frac{((2 * MF_C + ((MF_H - 3 * MF_N)/2) - MF_O)/2) * 31.9988}{MW_{substrate}} = 1.5748 \left[\frac{kg_{O_2 \text{ consumed}}}{kg_{vs \text{ degraded}}} \right]$$

$$G_{dry \text{ gases}} = G_{CO_2} + G_{NH_3} - G_{O_2}$$

$$G_{dry \text{ gases}} = \frac{2.04932 \text{ kg}_{CO_2} - 0.05727 \text{ kg}_{NH_3} - 1.5748 \text{ kg}_{O_2}}{kg_{vs \text{ degraded}}} = 0.53179 \left[\frac{kg_{dry \text{ gases}}}{kg_{vs \text{ degraded}}} \right]$$

Note: For multiple substrates, generation and consumption factors are calculated for each substrate based on its stoichiometric composition.

3. Calculate ambient conditions.

Saturated Vapour Pressure of Ambient Air is calculated from:

$$VP_s = \frac{101.325 * 0.01683}{10^{-2260.46 * ((1/288) - (1/T_{ambient}))}} \text{ [kPa]}$$

$$VP_s = \frac{101.325 * 0.01683}{10^{-2260.46 * ((1/288) - (1/288))}} = 1.7053 \text{ [kPa]}$$

Assuming standard atmospheric pressure, the humidity ratio of the ambient air can be calculated from (Treybal, 1980):

$$Y_{ambient} = \frac{0.622 * VP_s * RH_{ambient}}{101.325 - VP_s * RH_{ambient}} \left[\frac{kg_{water \text{ vapour}}}{kg_{dry \text{ air}}} \right]$$

$$Y_{ambient} = \frac{0.622 * 1.7053 * 0.5}{101.325 - 1.7053 * 0.5} = 0.010647 \left[\frac{kg_{water\ vapour}}{kg_{dry\ air}} \right]$$

The specific volume of water vapour in the air is also a function of temperature and is calculated by:

$$V_{wv} = (-1.06 * (T_{ambient} - 273.15) + 68.00081) \left[\frac{m^3}{kg} \right]$$

Calculate Enthalpy of removed condensate based on the condenser exit temperature of 333K.

$$\begin{aligned} h_w &= (7.183 * T_{cw}) + 0.180788 \left[\frac{kJ}{kg} \right] \\ &= (7.183 * 333) + 0.180788 = 1393.12 \left[\frac{kJ}{kg} \right] \end{aligned}$$

4. Set starting conditions for the simulation.

The inlet air conditions are set to the ambient conditions for the first time step. The outlet air conditions are calculated as above, using the reactor temperature instead of ambient. The mass flow rates are required for the dry air and water vapour portions of the aeration air. Initially, the aeration air is ambient, and the inlet mass flow rates are calculated by:

$$\begin{aligned} \dot{m}_{dry\ air} &= \frac{Q_{air}}{\frac{1}{\rho_{dry\ air}} + Y_{ambient} * V_{wv}} \\ \dot{m}_{dry\ air} &= \frac{1600}{\frac{1}{1.184} + 0.010647 * 52.26} = 1142.04 \frac{kg}{h} \end{aligned}$$

$$\dot{m}_{air} = (1 + Y_{ambient}) * \dot{m}_{dry\ air}$$

$$\dot{m}_{air} = (1 + 0.010647) * 1142.04 = 1154.19 \frac{kg_{air}}{h}$$

$$\dot{m}_{water\ vapour} = Y_{ambient} * \dot{m}_{dry\ air}$$

$$\dot{m}_{water\ vapour} = 0.010647 * 1142.4 = 12.16 \frac{kg_{water\ vapour}}{h}$$

5. Calculate substrate components

$$Mass\ of\ Dry\ Solids = M_{wet} * Solids\ content$$

$$= 25120 * 0.477 = 11982.24\ kg$$

$$Mass\ of\ Volatile\ Solids = M_{wet} * Solids\ content * Fraction_{vs}$$

$$= 25120 * 0.477 * 0.45 = 5392\ kg$$

$$Mass\ of\ Fast\ Degrading\ Solids = M_{wet} * Solids\ content * Fraction_{vs} * Fraction_{fast}$$

$$= 25120 * 0.477 * 0.45 * 0.3 = 1617.6\ kg$$

Calculate the approximate starting volume of each of the components (solid, water, air)

$$V_s = \frac{M_{wet}}{485.3} [m^3]$$

$$= \frac{25120}{485.3} = 51.76 [m^3]$$

$$V_w = \frac{M_{wet} * (1 - Solids\ content)}{1000} [m^3]$$

$$= \frac{25120 * (1 - 0.477)}{1000} = 13.14 [m^3]$$

$$V_{headspace} = 110 - 51.76 - 13.14 = 45.10 m^3$$

6. Calculations for each timestep*:

*note: a one-hour timestep is used here to simplify sample calculations.

i. Calculate degradation rate:

$$k_{adj_{fast}} = k * (1.066^{(T_r - 280)} - 1.21^{(T_r - 320)}) \left[\frac{1}{h} \right]$$

$$= 0.001 * (1.066^{(288 - 280)} - 1.21^{(288 - 320)}) = 0.0017$$

ii. Calculate Change in volatile solids

$$\Delta v s_{fast} = k_{adj} * (M_{fast}) * \Delta t$$

$$\Delta v s_{fast} = 0.0017 * 1617.6 = 2.75 \text{ kg}$$

$$k_{adj,slow} = k_{adj,fast} * 0.1 = 0.00017 \left[\frac{1}{h} \right]$$

$$\Delta v s_{slow} = 0.00017 * 3774.4 = 0.64 \text{ kg}$$

iii. Calculate mass of volatiles for next timestep*

$$M_{vs_{fast}}^{(t+1)} = M_{vs_{fast}} - \Delta v s_{fast}$$

$$= 1617.6 - 2.75 = 1614.9 \text{ kg}$$

$$M_{vs_{slow}}^{(t+1)} = M_{vs_{slow}} - \Delta v s_{slow}$$

$$= 3774.4 - 0.64 = 3773.76 \text{ kg}$$

iv. Calculate water balance

$$M_{water}^{(t+1)} = M_{water}^{(t)} + \Delta t (G_{H_2O} * (\Delta v s_{fast} + \Delta v s_{slow}) + \dot{m}_{dry\ air} (Y_i - Y_o))$$

$$= 13137.76 + (0.4684 * (2.75 + 0.64) + 1142.4(0.010647 - 0.010647)) = 13138.6 \text{ kg}$$

Note that for the first iteration the reactor temperature is considered to be ambient, therefore the humidity ratios are the same.

v. Calculate new reactor temperature

$$T_{avg}^{(t+1)} = T_{avg}^{(t)} + \left(\frac{\Delta t}{C_s M_s + C_w M_w + C_{rv} M_{rv}} \right) [m_a (C_g (T_i - T_{avg}^{(t-1)}) + \lambda_w (Y_i^{(t)} - Y_o^{(t)}) - (h_{ao}^{(t)} - h_{ai}^{(t)}) - h_w (Y_o^{(t)} + Y_i^{(t)})) + h_c (M_{vs}^{(t)} - M_{vs}^{(t)})]$$

$$= 288 + (1142.04 * 45 + 5085) = 288.835 \text{ K}$$

vi. Calculate new outlet humidity ratio:

Calculated in the same method as shown in (3) above, the outlet ratio is calculated to be:

Saturated Vapour Pressure of Ambient Air is calculated from:

$$VP_s = \frac{101.325 * 0.01683}{10^{-2260.46 \left(\frac{1}{288} - \frac{1}{288.835} \right)}} = 1.7968 \text{ [kPa]}$$

Assuming saturation and standard atmospheric pressure in the reactor, the humidity ratio of the reactor air can be calculated from (Treybal, 1980):

$$Y_{ambient} = \frac{0.622 * 1.7968}{101.325 - 1.7968} = 0.01123 \left[\frac{\text{kg}_{water \text{ vapour}}}{\text{kg}_{dry \text{ air}}} \right]$$

$$= 288 + \left(\frac{1}{1.04 * 11978.85 + 4.2 * 13138.6} \right) [1142.04(1.005(288 - 288)) + 2257.6(0.010647 - 0.010647) - (288 - 333) - 1393.12(0.010647 - 0.010647)) + 1500(3.39)]$$

vii. Calculate concentrations of CO₂, NH₃ and O₂ in the headspace:

First, calculate the partial pressure of CO₂ in the headspace for Henry's Law calculation.

Mass of CO₂ in the headspace at the beginning of the timestep:

$$\begin{aligned} \text{Mass of CO}_2 &= V_{\text{headspace}} * [\text{CO}_2] \\ &= 41.5 * (0.000501 \frac{\text{kg}_{\text{CO}_2}}{\text{kg}_{\text{air}}} * 1.184 \frac{\text{kg}_{\text{air}}}{\text{m}^3}) = 0.02462 \text{ kg} \end{aligned}$$

Calculate number of moles of CO₂

$$\begin{aligned} \text{Moles}_{\text{CO}_2} &= \frac{M_{\text{CO}_2}}{MM_{\text{CO}_2}} \\ &= \frac{0.02462}{44} = 5.6 * 10^{-4} \text{ kmol} \end{aligned}$$

Calculate Partial Pressure of CO₂

$$\begin{aligned} PP_{\text{CO}_2} &= \frac{101.325 * (\text{MOL}_{\text{CO}_2})}{\text{MOL}_{\text{CO}_2} + \text{MOL}_{\text{air}}} \\ &= \frac{101.325 * (5.6 * 10^{-4})}{(5.6 * 10^{-4}) + 41.5 * 0.041} = 0.033 \text{ kPa} \end{aligned}$$

Assuming equilibrium between the gas and aqueous phases, use Henry's Law to calculate

Aqueous Phase concentration of CO₂

$$[CO_2]_{aq} = PP_{CO_2} * H_c * 2444.640 \left[\frac{kg}{m^3} \right]$$

$$= 0.033 * 0.0000063 * 2444.640 = 5.08 * 10^{-4} \frac{kg}{m^3}$$

Calculate new concentration of CO₂ in the headspace.

$$M_{CO_2}^{(t+1)} = M_{CO_2}^{(t)} + ((G_{CO_2} * \Delta_{vs}) + Q_{air} * ([CO_2]_{inlet} - [CO_2]^{(t)})) * \Delta t - V_w ([CO_2]_{aq}^{(t+1)} - [CO_2]_{aq}^{(t)})$$

$$= 0.02462 + ((2.0493 * 3.39) + 1600 * (0.000593 - 0.000593)) - 13.14(5.08 * 10^{-4} - 0)$$

$$= 6.964 \text{ kg}$$

$$[CO_2]_{headspace}^{(t+1)} = 0.154 \frac{kg}{m^3}$$

⁴Note: The calculated values here are unrealistic due to the use of the 1 hour timestep for the sample calculation.

- viii. NH₃ generation and O₂ depletion are calculated in the same manner.
- ix. The concentration CO₂ in the headspace is calculated as a percent of the total mass of gases for the purpose of maintaining the setpoint.

Note: When the system is “recycling” aeration air, inlet concentrations are the same as outlet concentrations (with the exception of the recycled air, which is saturated at the condenser exit temperature). When the system is using ambient air, the inlet concentrations are set to ambient.

APPENDIX C - Degradation Model Computer Code

```

#include <c:\devstud\vc\include\math.h>
#include <c:\devstud\vc\include\stdio.h>
#include "vslam.h"
#define MAX_CHAR 100

//function declarations
void AERATE(double, double, double, double);
void RECYCLE(double, double);
void RATE_CALC();
void STAGE_CALC ();
void CALC_H ();
FILE *fp;

//declare variables from input arrays:

//input variables
double wwt1, wwt2, wwt3; //wet weight of substrates
double sc1, sc2, sc3; //solids content of substrates(fraction)
double vsf1, vsf2, vsf3; //volatile solids fraction
double fastfrac, slowfrac; //fast and slow degrading fractions
//constant parameters
double hvw; //heat of vapourization of water
double ddk; //degradation coefficient (25 degrees c)
double ht1,ht2,ht3; //heat of combustion for substrates
double Cs,Cw,Cg; //Specific heats for solid, water and dry gases
double Vr,Va, Vw, Vs, denswc; //volume of air, water and dry solids in system
double MOLAIR, Hc, WCO2a, wtotal; //moles of air, Henry's, total mass of gases
double TSET1, TSET3, CO2SET, Endtime;
double diam, area, V1; //diameter and area of recycle piping and vleocity of airflow into condenser - for
condloss calculation

//characteristics of substrate:
double MOLWT1, MOLWT2, MOLWT3; //molar mass of substrates
double O2FACT1, CO2FACT1, WATFACT1, NH3FACT1, DGASFACT1; //multiplication factors for
determining production of gaseous consituents
double O2FACT2, CO2FACT2, WATFACT2, NH3FACT2, DGASFACT2;
double O2FACT3, CO2FACT3, WATFACT3, NH3FACT3, DGASFACT3;
double DVS1, DVS2, DVS3; //change in volatile solids over time - substrate 1, 2, 3

//reactor conditions
double dTavg; //average temperature in reactor
double dVPCo2; //volume percent of CO2 in outlet air stream
double dQair; //volumetric flowrate of aeration air
double Yi,Yo, Yol, mdot_al; //influent and output absolute humidity and mass flowrate of the gas stream
double mdot_a, mdota_am, mdot_t; //mass flowrates of air, ambient air, water vapour and total gas flow
double Hw, H1, H2; //enthalpy of gas stream (H1 is into condenser and H2 is out of condenser)
double CONDLOSS; //condenser losses KJ/h
double Ti; //temperature of incoming aeration air
double Vpso, Vpsi; //saturated vapour pressure of outlet air
double MCO2, MOLCO2, PPCO2; //Mass, moles and partial pressure of CO2 in headspace
double wto2, wtco2, wtn2, CON2; //weight of O2, CO2, and N2

```



```

double volo2, volco2, voln2, volh2o, voltot; //volumes of gaseous constituents
double Stg1Time, Stg2Time, Stg3Time, Stg3wtime, Stg4Time, Stg3Phs; //time setpoints for stages

//static char setting[10] = "setting"; //setting indicator - is it aerating or recycling for this timestep??

//ambient conditions
double dTamb; //Ambient temperature
double dRHamb; //relative humidity of ambient air
double VspAMB, VpAMB; //saturated and unsaturated vapour pressure of ambient
double Yamb, Vv; //absolute humidity, and specific volume of water vapour at ambient conditions
double CO2IN, CO2OUT, O2IN, O2OUT, Tco; //inlet and outlet conc'n of CO2 and O2, temperature at
condenser outlet

BOOL SWFUNC INTLC(UINT uiRun)
//calculates initial conditions before each new simulation

{
    BOOL bContinue = TRUE;
    //declare variables that are only used for initial calcs.
    double dTs; //input temperature of substrate
    double dcc1, dcc2, dcc3; //carbon content of substrates
    double dnc1, dnc2, dnc3; //nitrogen content of substrates
    double doc1, doc2, doc3; //oxygen content of substrates
    double dhc1, dhc2, dhc3; //hydrogen content of substrates

    /* set experiment parameters */

    {
        /*defining which parameters are stored where. The values of each of these
        parameters are set in the control program */
        wwt1 = XX[1]; //wet weight of substrate 1 (Kg)
        sc1 = XX[2]; //solids content of substrate 1
        vsf1 = XX[3]; //volatile solids fraction of substrate 1
        dTs = XX[4];
        dcc1 = XX[5];
        doc1 = XX[6];
        dnc1 = XX[7];
        dhc1 = XX[8];
        dRHamb = XX[9]; //(-)
        dTamb = XX[10]; //(K)
        dQair = XX[11]; //(m3/h)
        ddk = XX[12]; //rate constant for substrate 1 (1/h)
        Cs = XX[13]; //kJ/kg-degC
        Cw = XX[14]; //kJ/kg-degC
        Cg = XX[15]; //kJ/kg-degC
        hvw = XX[16]; //kJ/kg
        ht1 = XX[17]; //kJ/Kg
        Vr = XX[18]; //volume of reactor (m3)
        Tco = XX[19]; //Outlet temperature form condenser
        TSET1 = XX[21]; //setpoint temperature for stage 1 & 2
        TSET3 = XX[22]; //setpoint temperature for stage 3
    }
}

```

```

CO2SET = XX[23]; //setpoint for CO2 concentration
fastfrac = XX[24]; //fast degrading fraction of vs for sub 1
wwt3 = XX[25]; //wet weight of substrate 3 (kg)
slowfrac = XX[28]; //slow degrading fraction of vs for sub 1
sc3 = XX[29]; //solids content of substrate 3
vsf2 = XX[30];
vsf3 = XX[31]; //volatile solids fraction of substrate 3
dcc2 = XX[32];
doc2 = XX[33];
dnc2 = XX[34];
dhc2 = XX[35];
dcc3 = XX[36];
doc3 = XX[37];
dnc3 = XX[38];
dhc3 = XX[39];
ht2 = XX[40]; //kJ/kg
ht3 = XX[41]; //kJ/kg

LL[1] = 1; //counter to keep track of stage number
LL[2] = 0; //counter to keep track of aeration calls
LL[3] = 0; //counter to keep track of recycle calls
LL[4] = 0; //tracking to follow aeration/recycle pattern
diam = 0.33; //diameter of piping (estimate - check this)
Stg3Time = 1000;

}

//Calculate multiplication factors for gas production
MOLWT1 = dcc1*12.01115 + dhc1*1.00797 + doc1*15.994 + dnc1*14.0067; //(kg/kmol)molar mass of
substrate 1
//MOLWT2 = dcc2*12.01115 + dhc2*1.00797 + doc2*15.994 + dnc2*14.0067; //(kg/kmol)molar mass of
substrate 2
MOLWT3 = dcc3*12.01115 + dhc3*1.00797 + doc3*15.994 + dnc3*14.0067; //(kg/kmol)molar mass of
substrate 3

//All gas production factors calculated below are (kg produced/ kg vs degraded)
O2FACT1 = ((2*dcc1 + ((dhc1-3*dnc1)/2)-doc1)/2)*31.9988/MOLWT1; //O2 production substr1
CO2FACT1 = dcc1*44.0095/MOLWT1; //CO2 production substr1
WATFACT1 = ((dhc1-3*dnc1)/2)*18.01534/MOLWT1; //H2O production substr1
NH3FACT1 = dnc1*17.03061/MOLWT1; //NH3 production substr1
DGASFACT1 = CO2FACT1 + NH3FACT1 - O2FACT1; //total gas production substr1
O2FACT3 = ((2*dcc3 + ((dhc3-3*dnc3)/2)-doc3)/2)*31.9988/MOLWT3; //O2 production substr3
CO2FACT3 = dcc3*44.0095/MOLWT3; //CO2 production substr3
WATFACT3 = ((dhc3-3*dnc3)/2)*18.01534/MOLWT3; //H2O production substr3
NH3FACT3 = dnc3*17.03061/MOLWT3; //NH3 production substr3
DGASFACT3 = CO2FACT3 + NH3FACT3 - O2FACT3; //total gas production substr3
Hc = 0.00000603; //(1/KPa)

/* calculate ambient conditions*/
VspAMB = 101.325*0.01683/(pow(10,(-2260.46*((1/288)-(1/XX[10]))))); //(Kpa) saturated vapour pressure

```

```

of ambient air
VpAMB = dRHamb*VspAMB;    //(Kpa) vapour pressure of ambient air
Yamb = 0.622*VpAMB/(101.325-VpAMB);    //(-) absolute humidity of ambient air (kgw/)
Vv = (-1.06*(dTamb-273.15) + 68.00081); //calculate specific volume of water vapour in ambient air

/*Calculate starting values */
SS[1] = dTs;    //(K) use substrate temperature to estimate the starting temp
Yi = Yamb;    //(-) initializing aeration variables (absolute humidity and mass flowrate) to ambient recycle
air
Vpso = 101.325*0.01683/(pow(10,(-2260.46*((1/288)-(1/SS[1]))))); //(KPa) saturated vapour pressure of
outlet air
Yo = 0.622*Vpso/(101.325 - Vpso);    //(-) absolute humidity of outlet air
mdota_am = dQair/((1/1.184)+(Yamb*Vv)); //mass flowrate of dry air in ambient
mdot_t = (1+Yi)*mdota_am;    //mass flowrate of air and water vapour
mdot_a = mdota_am;
Ti = dTamb;    //(K)
Hw = 4.183*Tco + 0.180788; //enthalpy of saturated water condensate KJ/Kg

/*calculate wet and dry solids mass - substrate 1*/
SS[2] = wwt1*sc1;    //(kg) Calculate mass of dry solids substrate 1(wwt1*sc1)
SS[3] = SS[2]*vsf1;    //(kg) mass of volatile solids substrate 1(Ms1*vsf1)
SS[11] = SS[3]*fastfrac; //fast degrading fraction of substrate 1
SS[12] = SS[3]*slowfrac; //slow degrading fraction of substrate 1
denswc = 288/sc3; //density of wodchips kg/m3
Vs = (wwt1/485.3) + wwt3/480; //volume of wet compost in m3
Vw = (wwt1*(1-sc1) + wwt3*(1-sc3))/1000; //volume of water in substrate based on density and water content
Va = Vr - Vs -Vw; //Volume of headspace (reactor volume - wet solids volume)
MOLAIR = (Va*0.041);    //(Kmol) the number of moles of air in headspace
SS[18] = Va;
SS[20] = Vw;

/*calculate wet and dry solids mass - substrate 3*/
SS[14] = wwt3*sc3;    //(kg) Calculate mass of dry solids substrate 2(wwt2*sc2)
SS[15] = SS[14]*vsf3;    //(kg) mass of volatile solids substrate 2(Ms2*vsf2)

SS[4] = (wwt1-SS[2]) + (wwt3-SS[14]);    //(kg) mass of water in solids all substrates (wwt-dry solids)
SS[5] = (0.000501*1.184); //(kg/m3) starting concentration of CO2 in air
SS[7] = 0.2134*1.184; //(kg/m3) starting concentration of O2 in air
SS[10] = 0;
CON2 = 0.7681*1.184; //(kg/m3) ambient concentration of N2
wttotal = (CON2 + SS[5]+ SS[7])*Va; //total mass of dry air
SS[8] = 0.05;//(SS[5]*Va/wttotal)*100; //mass percent of CO2 in headspace - starting
if ((fp = fopen("data", "w")) == NULL)
    printf ("\n Unable to create file.");
else
    {
    fprintf(fp, "\n Now entering stage 1. The time now is: %f The temperature is now %f The CO2 is at %f
%%%", TNOW, SS[1], SS[8]);
    fclose(fp);
    }

/*end of initial calculations*/

```

```

    return(bContinue);
}

void SWFUNC STATE(void)
/*state function includes those calculations that are performed each timestep*/

{ //start of calcs to repeat each timestep
SS[16] = dTamb + abs(5*sin(3.14*TNOW/24)); //tracking ambient temperature
switch (LL[1])
{

case 1: /* STAGE 1*/
{
if (SS[8] >= CO2SET) //if CO2 is above setpoint
{
AERATE (dTamb, VpAMB, Yamb, mdota_am); //call aeration subroutine
}
else
{
RECYCLE (Tco, dQair); //set to recycle air
}
if (SS[1] >= TSET1)
{
LL[1] = 2; //change to stage2
Stg2Time = TNOW + 48; //set end-time for stage2
if ((fp = fopen("data", "a")) == NULL)
printf ("\n Unable to create file.");
else
fprintf(fp, "\n\n Now entering stage 2. The time now is: %f The temperature is %f The CO2 is %f %% \n
Aeration called %6d times, Recycle called %6d times.", TNOW, SS[1], SS[8], LL[2], LL[3]);
fclose(fp);
}
RATE_CALC (); //calculate the rate constant for TNOW
STAGE_CALC(); //perform timestep calculations
}
break;

case 2: /*STAGE 2*/
{
if (SS[8] >= CO2SET) //if CO2 is above setpoint
{
AERATE (dTamb, VpAMB, Yamb, mdota_am); //calling aeration subroutine
}
else if (SS[1] > TSET1) //if temperature is above TSET1
{
AERATE (dTamb, VpAMB, Yamb, mdota_am); //calling aeration subroutine
}
else
{
RECYCLE (Tco, dQair); //set to recycle air
}
}
}

```

```

RATE_CALC(); //calculate the rate constant for TNOW
STAGE_CALC(); //perform timestep calculations
if (TNOW >= Stg2Time) //if TNOW equals end-time for stage2
{
  LL[1] = 3; //enter stage 3
  Stg3Phs = 1; //phase 1 - warming phase of stage 3
  Stg3wtime = TNOW + 24; //set time limit for warming phase of stage 3 (to 24hrs)
  if ((fp = fopen("data", "a")) == NULL)
    printf ("\n Unable to create file.");
  else
    fprintf(fp, "\n\n Now entering stage 3. The time now is: %f. The temperature is now %f The CO2 is at %f
    %% \n Aeration called %6d times, Recycle called %6d times.", TNOW, SS[1], SS[8], LL[2], LL[3]);
  fclose(fp);
}

}

break;

case 3: /*Stage 3*/
{
  if (SS[8] >= CO2SET) //if CO2 is above setpoint
  {
    AERATE (dTamb, VpAMB, Yamb, mdota_am); //calling aeration subroutine
  }
  else
  {
    RECYCLE (Tco, dQair); //set to recycle air
  }
  if ((TNOW >= Stg3wtime) || (SS[1] >= TSET3)) //if passed time limit for warming stage or passed tset for
  warming stage
  {
    if (Stg3Phs == 1) //if in the warming phase of stage 3 (phase 1) o
    {
      Stg3Phs = 2; //set to timed phase of stage 3 (phase 2)
      Stg3Time = TNOW + 72; //end warming phase, set end-time for stage 4
    }

    else //in timed phase of stage 3 - now cool to TSET3
    if (SS[1] >= TSET3)
    {
      AERATE (dTamb, VpAMB, Yamb, mdota_am); //calling aeration subroutine
    }
  }
  RATE_CALC (); //calculate the rate constant for TNOW
  STAGE_CALC(); //perform timestep calculations

  if (TNOW >= Stg3Time)
  {
    LL[1] = 4; //enter stage 4
    Stg4Time = TNOW + 36; //set stage 4 duration
    if ((fp = fopen("data", "a")) == NULL)
      printf ("\n Unable to create file.");
  }
}

```

```

else
    fprintf(fp, "\n\n Now entering stage 4. The time now is: %f. The temperature is now %f The CO2 is at %f
    %% \n Aeration called %6d times, Recycle called %6d times", TNOW, SS[1], SS[8], LL[2], LL[3]);
    fclose(fp);
}
}
break;

case 4: /*Stage 4*/
{

    if (TNOW >= Stg4Time) //end simulation
    {
        if ((fp = fopen("data", "a")) == NULL)
            printf ("\n Unable to create file.");
        else
            fprintf(fp, "\n End stage 4. The time now is: %f", TNOW);
            fprintf(fp, "\n Stage 4 is completed. Simulation Terminated");
MSTOP = -1;
fclose(fp);
}
else
{
    AERATE (dTamb, VpAMB, Yamb, mdota_am); //calling aeration subroutine
    RATE_CALC ();
    STAGE_CALC(S);
}
}
break;

}

return;

} /*end of calculations for each timestep*/

void AERATE (double dTamb,double VPamb,double Yamb,double Gamb)
{
    Ti = SS[16];
    Vpsi = VpAMB;
    Yi = Yamb;
    mdot_a = mdota_am;

    CO2IN = 1.184*0.000501; //Ambient concentration of CO2 as inlet concentration (kg/m3)
    O2IN = 1.184*0.2134; //Ambient O2 concentrations at inlet(kg/m3)
    CONDLOSS = 0; //no losses in condenser for aeration routine.
    LL[2] = LL[2]++;
    LL[4] = 1;
    return;
}

```

```

void RECYCLE (double Tco,double dQair)
{
  CALC_H();
  Ti = Tco;
  Vpsi = 101.325*0.01683/(pow(10,(-2260.46*((1/288)-(1/Ti)))));
  Yi = 0.622*Vpsi/(101.325-Vpsi);
  Vv = (-1.06*(Ti-273.15)) + 68.00081;
  mdot_a = dQair/((1/1.184)+(Yi*Vv)); //mass flowrate of dry air in
  CO2IN = SS[5]; //Reactor CO2 concentration as inlet concentration
  O2IN = SS[7]; //Reactor O2 concentrations at inlet
  LL[3] = LL[3]++;
  LL[4] = 0;
  return;
}

void RATE_CALC ()
{
  SS[6] = ddk*(pow(1.066,(SS[1]-280))-pow(1.21,(SS[1]-320))); // (1-pow(2.7128,(-TNOW/4)))
  {if (SS[6] < 0) /*the lagfactor is */
  SS[6] = 0;
  }
  SS[17] = 0.2*SS[6]; //rate constant for bulking agent 20% of rate for organics.
  SS[19] = 0.1*SS[6]; //rate constant for slowfrac degradation
  {if (LL[1] == 3)
  SS[19] = 0.75*SS[6];
  }
  return;
}

void CALC_H ()
{
  //calculate the enthalpys of dry air at inlet and outlet of condenser
  H2 = Tco; //regression gives 1:1??
  H1 = SS[1];
  /* fprintf(fp, "\n Enthalpys calculated. H1 equals %f, H2 equals %f", H1, H2);
  fclose(fp);*/
  return;
}

void STAGE_CALC ()
{
  DVS1 = (SS[6]*SS[11]); //((kg/h) change in volatile solids over time - fastfrac substrate 1
  DVS2 = (SS[19]*SS[12]); //((kg/h) change in volatile solids over time - slowfrac substrate 1
  DVS3 = (SS[17]*SS[15]); //change in Vol solids over time - substrate 3 (woodchips)
  SS[2] = SSL[2] - (DVS1+DVS2)*DTNOW; //((kg) new mass of dry solids substrate 1
  SS[3] = SSL[3] - (DVS1+DVS2)*DTNOW; //new mass of dry volatile solids substrate 1
  SS[11] = SSL[11] - DVS1*DTNOW; //new mass of fast degrading VS sub1
  SS[12] = SSL[12] - DVS2*DTNOW; //new mass of slow degrading VS sub1
  SS[14] = SSL[14] - DVS3*DTNOW; //new mass of dry solids substrate 3 (woodchips)
  SS[15] = SSL[15] - DVS3*DTNOW; //new mass of dry volatile solids substrate 3
  SS[4] = SSL[4] + DTNOW*(WATFACT1*(DVS1 + DVS2) + WATFACT3*DVS3 + (mdot_a*(Yi - Yo)));
}

```

```

//(kg) new Mw
SS[21] = SS[2]-SS[11]-SS[12] ; //estimated mass of ash
      S S [ 1 ] = S S L [ 1 ] +
(DTNOW/(Cs*(SS[2]+SS[14])+Cw*SS[4]))*(mdot_a*(Cg*(Ti-SSL[1])+hvw*(Yi-Yo)-(H1-H2)-Hw*(Yol
-Yi)))+(ht1*DVS1+ht2*DVS2)+(ht3*DVS3));
mdot_al = mdot_a; //save previous values for Go, Yo

Yol = Yo;
Vpso = 101.325*0.01683/(pow(10,(-2260.46*((1/288)-(1/SS[1]))))); //(KPa) saturated vapour pressure of
outlet air
Yo = 0.622*Vpso/(101.325 - Vpso); //(-) absolute humidity of outlet air

//calculate O2, CO2, NH3 production
//first calculate pp of CO2 in headspace for Henry's calcs
MCO2 = SS[5]*Va; //(Kg) mass of CO2 in headspace
MOLCO2 = MCO2/44; //(Kmol)number of moles of CO2 in headspace
PPCO2 = 101.325*MOLCO2/(MOLCO2+MOLAIR); //(KPa) partial pressure of CO2 in air
SS[10] = PPCO2*Hc*2444.640; //(kg/m3) aqueous phase concentration of co2

//calculate CO2 production
SS[5] = SSL[5] + ((CO2FACT1*(DVS1+DVS2))+CO2FACT3*DVS3) - dQair*SSL[5] +
CO2IN*dQair)*DTNOW/Va - Vw*(SS[10]-SSL[10])/Va;//(Kg/m3) calculate concentration of co2 headspace
SS[7] = SSL[7] + (O2IN*dQair - SSL[7]*dQair - (O2FACT1*(DVS1 + DVS2) +
O2FACT3*DVS3))*DTNOW/Va;
wttotal = (SS[5]+ SS[7]+CON2)*Va; //(kg) total mass of dry gases
SS[8] = (SS[5]*Va/wttotal)*100; //(%) mass percent of CO2 in headspace
SS[9] = (SS[7]*Va/wttotal)*100; //(%) mass percent of O2 in headspace
return;
}

```


APPENDIX D - Sample Calculations - Odour Emissions Study

December 11, 1996

Dimethyl Disulphide Calibration:

Compound	Residence time (min.)	Peak Height	Peak Area	Concentration (ppm)	Concentration (ug/L)
DMDS	4.060	3.686	24.86	0.10	0.0260
DMDS	4.060	3.549	24.20	0.10	0.0260
DMDS	4.076	27.277	156.61	0.50	0.1299
DMDS	4.070	30.345	155.09	0.50	0.1299
DMDS	4.041	128.403	698.23	1.00	0.2597
DMDS	2.028	19.594	768.20	1.00	0.2597
DMDS	4.065	774.700	4833.17	5.00	1.2987
DMDS	4.060	792.111	4836.77	5.00	1.2987
DMDS	4.040	1455.548	9522.98	10.00	2.5974

Because the calibration lines do not have a constant slope, an regression analysis is applied to line segments 0-0.5 ppm, 0.5-1.0 ppm and 1-10 ppm.

Regression Analysis:

Regression Output 0 to 0.5 ppm		Regression Output 0.5-1.0 ppm	
Constant	0	Constant	0
Std Err of Y Est	4.604011629	Std Err of Y Est	156.545
R Squared	0.996981634	R Squared	0.7810627
No. of Observations	3	No. of Observations	4
Degrees of Freedom	2	Degrees of Freedom	3
X Coefficient(s)	309.14615	X Coefficient(s)	648.912
Std Err of Coef.	9.0292097	Std Err of Coef.	99.0077530566841
Concentration = Peak Area/309.146		Concentration = Peak Area/648.912	

Regression Output 1.0 to 10 ppm	
Constant	0
Std Err of Y Est	60.02316442
R Squared	0.999508208
No. of Observations	3
Degrees of Freedom	2
X Coefficient(s)	957.19667
Std Err of Coef.	4.9008709
Concentration = Peak Area/957.197	

Dimethyl Sulphide Calibration:

Compound	Retention time (min.)	Peak Height	Peak Area	Concentration (ppm)	Concentration (ug/L)
DMS	1.946	1.260	11.37	0.10	0.0394
DMS	1.950	1.117	6.67	0.10	0.0394
DMS	1.953	10.576	96.43	0.50	0.1969
DMS	1.955	9.515	57.00	0.50	0.1969
DMS	1.951	28.260	245.96	1.00	0.3937
DMS	1.956	25.281	141.58	1.00	0.3937
DMS	1.955	168.407	1087.91	5.00	1.9685
DMS	1.956	173.675	1011.94	5.00	1.9685
DMS	1.960	330.639	3469.48	10.00	3.9370

Regression Output: 0 to 0.5 ppm		Regression Output: 0.5 to 1.0 ppm	
Constant	0	Constant	0
Std Err of Y Est	16.983253497	Std Err of Y Est	47.874422
R Squared	0.8388960344	R Squared	0.6549435
No. of Observations	4	No. of Observations	4
Degrees of Freedom	3	Degrees of Freedom	3
X Coefficient(s)	150.99808	X Coefficient(s)	185.702
Std Err of Coef.	23.551535	Std Err of Coef.	30.278443
Concentration = Peak Area/150.998		Concentration = Peak Area/185.702	
Regression Output: 1.0 to 10 ppm (245.96 < Peak Area < 3469.48)			
Constant	0		
Std Err of Y Est	405.10714333		
R Squared	0.9091867952		
No. of Observations	5		
Degrees of Freedom	4		
X Coefficient(s)	299.87888		
Std Err of Coef.	32.858523		
Concentration = Peak Area/299.88			

Calibration Equations:

DMDS	
(Peak Area < 156.61)	[DMDS] = Peak Area/309.1462
(156.61 < Peak Area < 173.675)	[DMDS] = Peak Area/648.912
(Peak Area > 173.675)	[DMDS] = Peak Area/951.197
DMS	
(Peak Area < 245.96)	[DMS] = Peak Area/150.9981
(245.96 < Peak Area < 1087.91)	[DMS] = Peak Area/185.702
(Peak Area > 1087.91)	[DMS] = Peak Area/299.88

Sample Analysis - December 11, 1996

Res. Ht			Height Area			Concentration			Res. Ht			Height Area			Concentration			
Bag	Res. Ht	Height Area	Concentration (ppm)	Res. Ht	Height Area	Concentration (ppm)	Bag	Res. Ht	Height Area	Concentration (ppm)	Res. Ht	Height Area	Concentration (ppm)	Bag	Res. Ht	Height Area	Concentration (ppm)	
Bag 1							Bag 1							Bag 2				
DMS	1.906	0.343	1.58	0.0105	0.001196	0.0000	DMS	3.900	0.000	0	0.0000	0.0000	0.0000	DMS	4.076	0.211	1.02	0.0033
DMS	1.896	0.229	2.12	0.0140	0.0055275	0.0000	DMS	3.918	0.551	6.87	0.0222	0.00664	0.0000	DMS	4.091	0.187	1.02	0.0033
DMS	1.776	0.286	1.04	0.0069	0.0027116	0.0000	DMS	3.863	0.101	10.58	0.0142	0.0099	0.0000	DMS	4	0	0	0.0000
				Bag avg	0.0041196						Bag avg	0.0054537						
				Std dev.	0.0011496						Std dev.	0.0041095						
Bag 2							Bag 2							Bag 3				
DMS	1.8	0.0	0	0.0000	0	0.0000	DMS	4	1.21	9.58	0.0310	0.0090	0.0000	DMS	4	0	0	0.0000
DMS	1.791	0.308	1.21	0.0080	0.0031549	0.0000	DMS	3.9	0.0	0	0.0000	0.0000	0.0000	DMS	4	0	0	0.0000
DMS	1.8	0.0	0	0.0000	0	0.0000	DMS	3.9	0.0	0	0.0000	0.0000	0.0000	DMS	4	0	0	0.0000
				Bag avg	0.0010516						Bag avg	0.0029941						
				Std dev.	0.0014872						Std dev.	0.0042342						
Bag 3							Bag 3							Bag 4				
DMS	1.938	1.067	5.26	0.0348	0.0137145	0.0000	DMS	4.231	0.295	1.13	0.0037	0.0011	0.0000	DMS	4	0	0	0.0000
DMS	1.955	0.492	4.85	0.0321	0.0126455	0.0000	DMS	3.970	0.340	3.29	0.0106	0.0031	0.0000	DMS	4.050	0.162	1.60	0.0052
DMS	1.913	0.399	3.95	0.0262	0.0102989	0.0000	DMS	4	0	0	0.0000	0.0000	0.0000	DMS	4.000	0.515	6.57	0.0213
				Bag avg	0.0122197						Bag avg	0.006176						
				Std dev.	0.0014266						Std dev.	0.0004508						
Bag 4							Bag 4							Bag 5				
DMS	1.946	0.307	2.53	0.0168	0.0065965	0.0000	DMS	4.231	0.295	1.13	0.0037	0.0011	0.0000	DMS	3.981	0.175	4.66	0.0151
DMS	1.955	0.339	3.12	0.0207	0.0081348	0.0000	DMS	4	0	0	0.0000	0.0000	0.0000	DMS	4.050	0.162	1.60	0.0052
DMS	1.951	0.491	4.79	0.0317	0.0124891	0.0000	DMS	3.970	0.340	3.29	0.0106	0.0031	0.0000	DMS	4.000	0.515	6.57	0.0213
				Bag avg	0.0090735						Bag avg	0.0013814						
				Std dev.	0.0024955						Std dev.	0.0012797						
Bag 5							Bag 5							Bag 6				
DMS	1.955	0.912	9.88	0.0654	0.0257603	0.0000	DMS	4.050	0.162	1.60	0.0052	0.0015	0.0000	DMS	3.858	0.246	3.48	0.0113
DMS	1.953	0.933	10.41	0.0689	0.0271422	0.0000	DMS	4.000	0.515	6.57	0.0213	0.0062	0.0000	DMS	3.945	0.544	5.76	0.0186
DMS	1.955	0.518	5.08	0.0336	0.0132452	0.0000	DMS	3.981	0.175	4.66	0.0151	0.0044	0.0000	DMS	4.273	0.614	4.95	0.0160
				Bag avg	0.0220493						Bag avg	0.0040098						
				Std dev.	0.0062509						Std dev.	0.0019193						
Bag 6							Bag 6							Bag 6				
DMS	1.950	0.398	3.54	0.0234	0.0092299	0.0000	DMS	3.858	0.246	3.48	0.0113	0.0033	0.0000	DMS	3.945	0.544	5.76	0.0186
DMS	1.953	0.484	4.51	0.0299	0.011759	0.0000	DMS	4.273	0.614	4.95	0.0160	0.0046	0.0000	DMS	4.273	0.614	4.95	0.0160
DMS	1.948	0.380	3.31	0.0219	0.0086302	0.0000	DMS	4.273	0.614	4.95	0.0160	0.0046	0.0000	DMS	4.273	0.614	4.95	0.0160
				Bag avg	0.0098731						Bag avg	0.0044348						
				Std dev.	0.0013559						Std dev.	0.0008848						

Concentration Averages by Location:		(ppm)	(ug/L)
Pre-Filter (post-condenser) (Bags 3 & 4):	DMS	0.0203	0.0082782
	DMDS	0.0026	0.0006785
Post-Filter (Bags 1 & 2):	DMS	0.0049	0.0020104
	DMDS	0.0109	0.0028388
Pre-Condenser (Bags 5&6)	DMS	0.0304	0.0124106
	DMDS	0.0109	0.0028377

Impinger Test Results

10 ppm Standard Analysis			Peak Area	(ppm)
DMS	1.960	330.64	3469.48	10
DMDS	4.040	1455.55	9522.98	10
Receiving Bag Analysis			Peak Area	(ppm)
DMS	1.960	280.03	3079.38	9.7
DMDS	4.076	1258.99	3064.2	3.5

DMDS	
(Peak Area *{DMDS}) = Peak Area/309.1462	
(Peak Area *{DMDS}) = Peak Area/953.475	
DMS	
(Peak Area *{DMS}) = Peak Area/150.9981	
(Peak Area *{DMS}) = Peak Area/318.5571	

*Concentrations are in ppm

Calculation of Percent Losses

(Peak Area Concentration)	
DMS	11.2%
DMDS	15.3%
DMS	3.0%
DMDS	15.0%

Calculation of Analytical Limits

	DMS Range		DMDS Range	
	Peak Ht.	Peak Area	Peak Ht.	Peak area
Blank 1	0.913	5.70	0.375	2.19
Blank 2	0.903	4.58	0.362	1.62
Blank 3	0.000	0.00	0.00	0.00
Blank 4	0.650	5.38	0.00	0.00
Blank 5	0.00	0.00	0.00	0.00
Blank 6	0.00	0.00	0.00	0.00
Blank 7	0.00	0.00	0.557	5.57
Blank 8	0.00	0.00	1.285	2.35
Blank 9	0.00	0.00	1.187	4.97
	mean	1.80	mean	1.86
	std dev	2.5	std dev	2.0

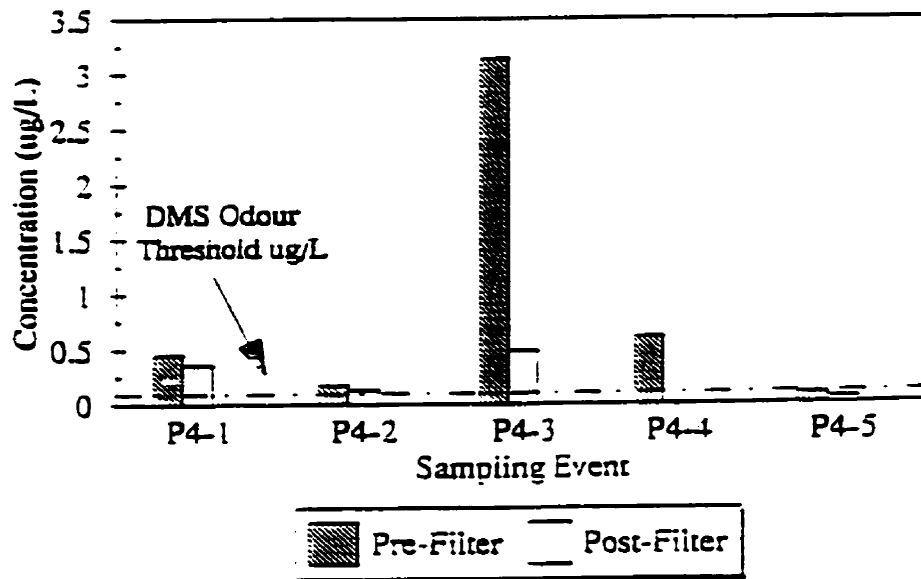
Limit of Detection (LOD) = 3*Standard Deviation+ Mean

Limit Quantification (LOQ) = 10*Standard Deviation + Mean

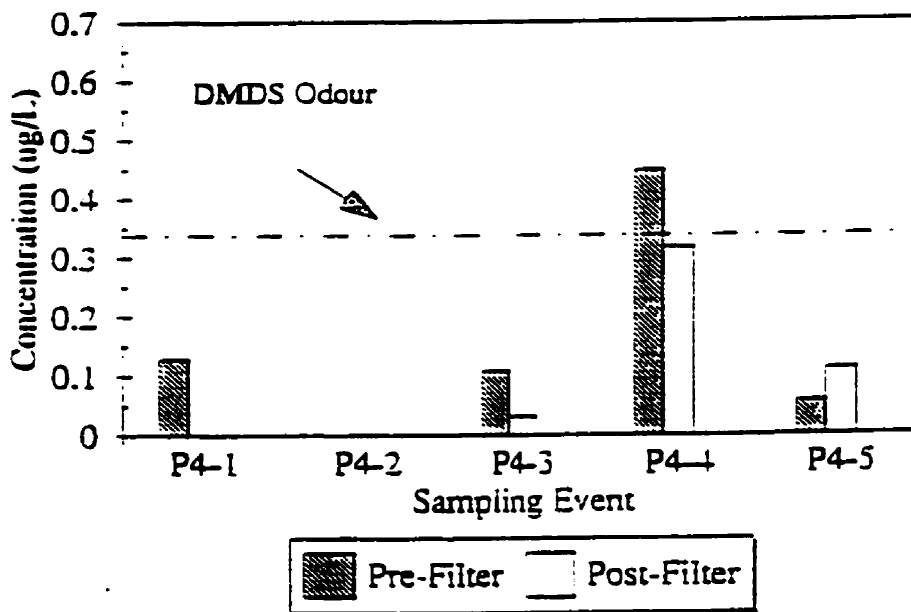
	Peak Area	
	LOD	LOQ
DMS	9.6	22.3
DMDS	7.36	27.9

APPENDIX E - Graphical Results - Odour Emissions Study

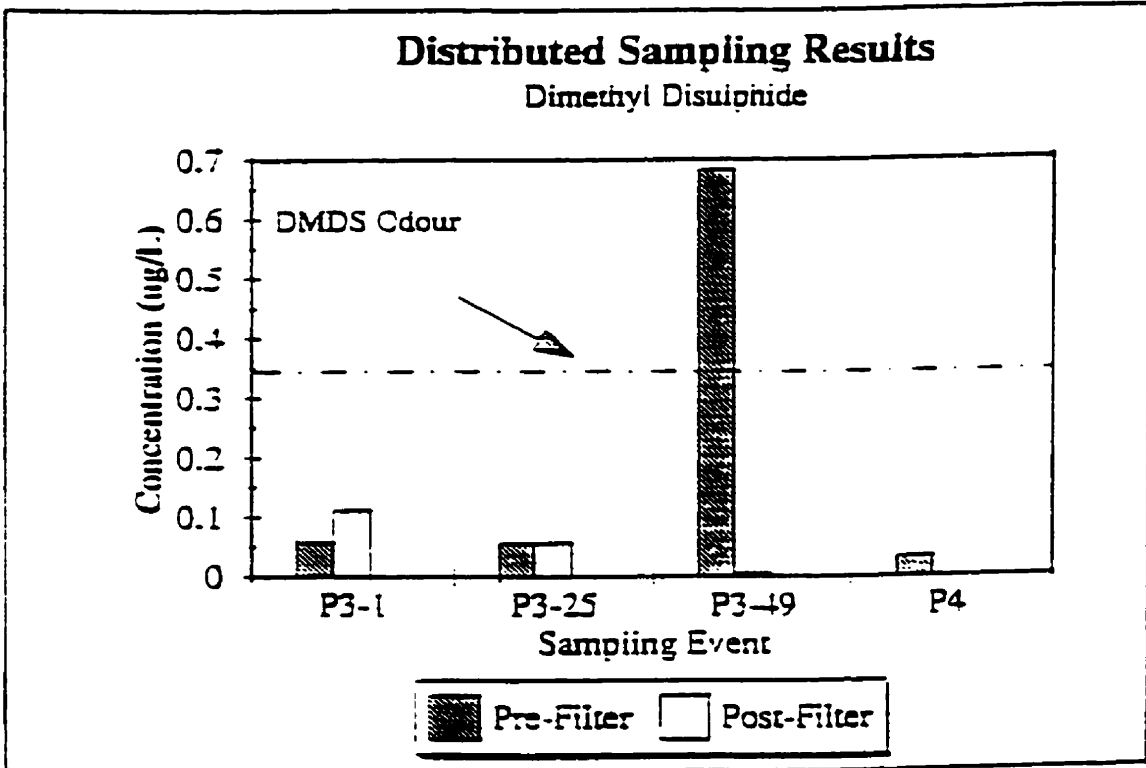
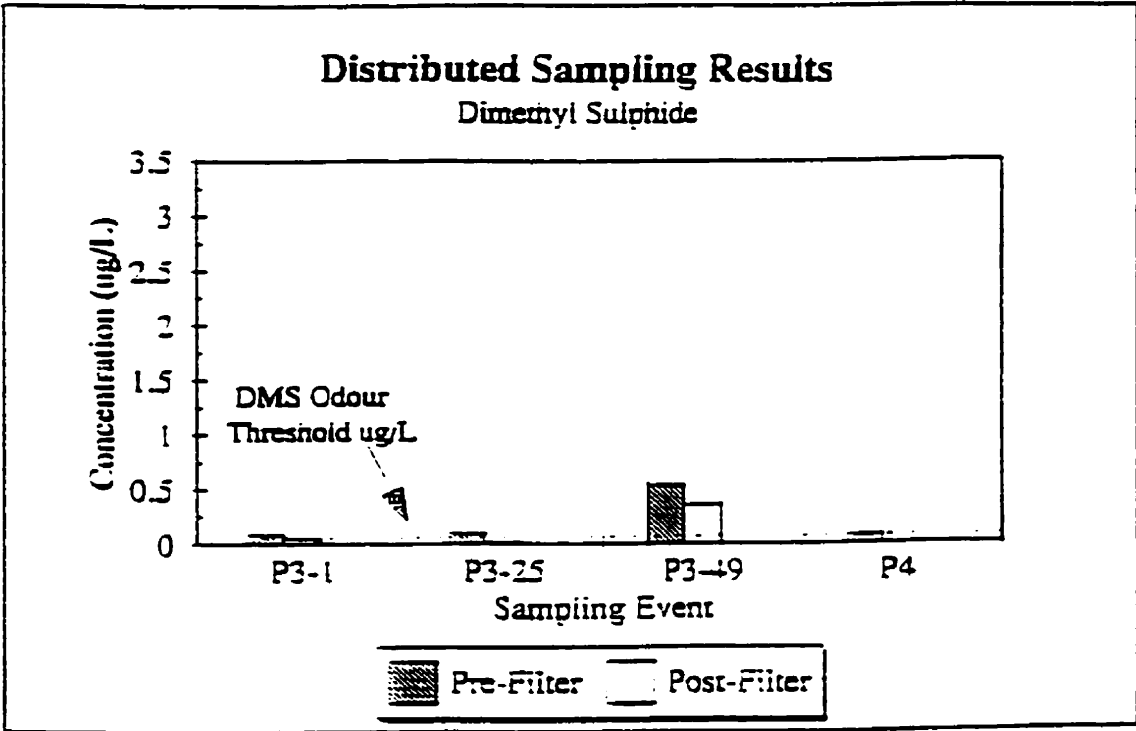
Phase 4 - Sampling Results Dimethyl Sulphide



Phase 4 Sampling Results Dimethyl Disulphide



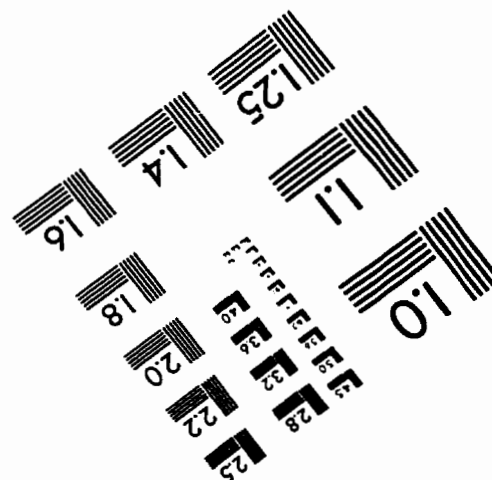
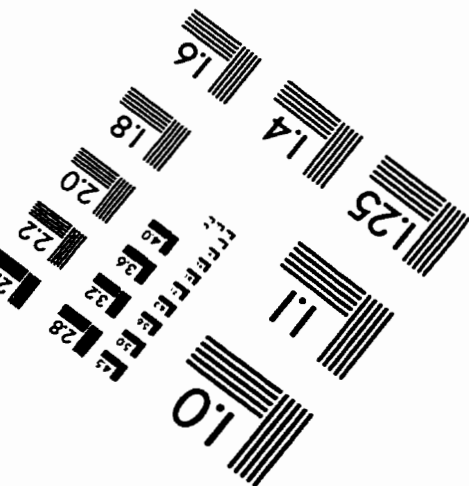
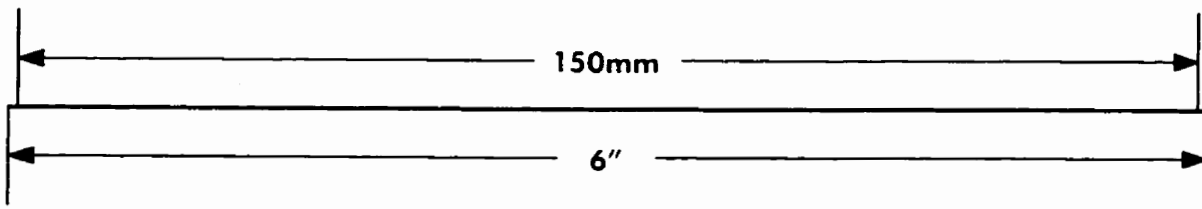
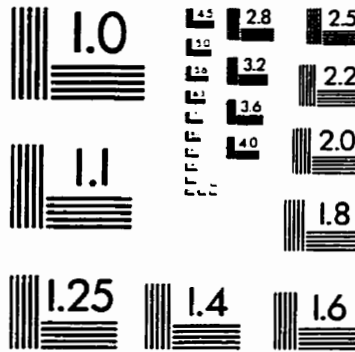
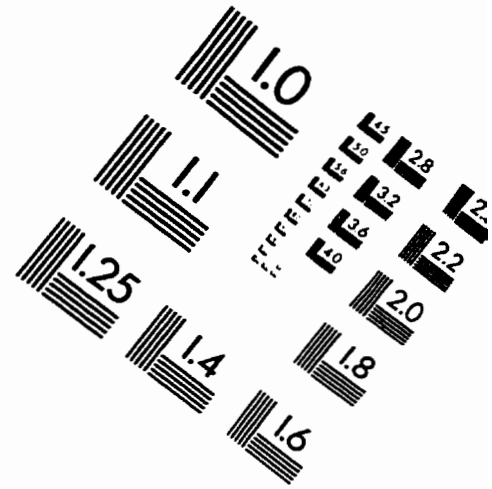
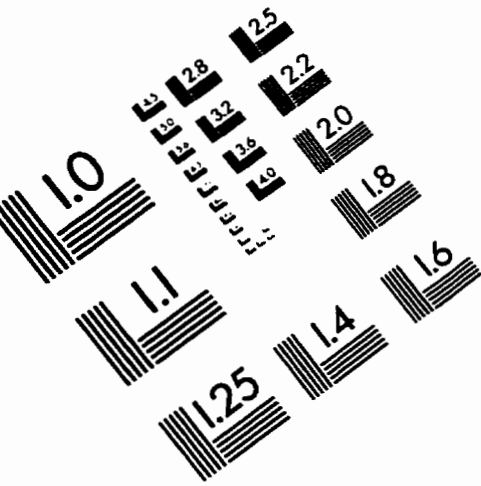
*Sampling Event notation is as follows:	
P4-1	November 8, 1995
P4-2	May 21, 1996
P4-3	July 29, 1996
P4-4	September 10, 1996
P4-5	December 12, 1996



****Sampling Event notation is as follows:**

P3-1	1 hour into Phase 3
P3-25	25 hours into Phase 3
P3-49	49 hours into Phase 3
P4	Initiation of Phase 4

IMAGE EVALUATION TEST TARGET (QA-3)



APPLIED IMAGE, Inc
1653 East Main Street
Rochester, NY 14609 USA
Phone: 716/482-0300
Fax: 716/288-5989

© 1993, Applied Image, Inc., All Rights Reserved